

การสังเคราะห์พอลิอิมิดแบบตอ่กิ่งสำหรับแผ่นเชื้อเพลิงเปลี่ยนโปรตอน

นางสาวณัฐณี ศรีเนตร

วิทยานิพนธ์นี้เป็นส่วนหนึ่งของการศึกษาตามหลักสูตรปริญญาวิทยาศาสตรดุษฎีบัณฑิต

สาขาวิชาวิศวกรรมเคมี ภาควิชาวิศวกรรมเคมี

คณะวิศวกรรมศาสตร์ จุฬาลงกรณ์มหาวิทยาลัย

ปีการศึกษา 2556

ลิขสิทธิ์ของจุฬาลงกรณ์มหาวิทยาลัย

บทคัดย่อและแฟ้มข้อมูลฉบับเต็มของวิทยานิพนธ์ตั้งแต่ปีการศึกษา 2554 ที่ให้บริการในคลังปัญญาจุฬาฯ (CUIR)

เป็นแฟ้มข้อมูลของนิสิตเจ้าของวิทยานิพนธ์ที่ส่งผ่านทางบัณฑิตวิทยาลัย

The abstract and full text of theses from the academic year 2011 in Chulalongkorn University Intellectual Repository (CUIR)

are the thesis authors' files submitted through the Graduate School.

SYNTHESIS OF GRAFT COPOLYIMIDE FOR PROTON EXCHANGE MEMBRANE

Miss Nathinee Srinate

A Dissertation Submitted in Partial Fulfillment of the Requirements  
for the Degree of Doctor of Engineering Program in Chemical Engineering

Department of Chemical Engineering

Faculty of Engineering

Chulalongkorn University

Academic Year 2013

Copyright of Chulalongkorn University

Thesis Title                   SYNTHESIS OF GRAFT COPOLYIMIDE FOR PROTON  
  EXCHANGE MEMBRANE  
By                               Miss Nathinee Srinate  
Field of Study                Chemical Engineering  
Thesis Advisor               Associate Professor ML. Supakanok Thongyai, Ph.D.

---

Accepted by the Faculty of Engineering, Chulalongkorn University in Partial Fulfillment of  
the Requirements for the Doctoral Degree

.....Dean of the Faculty of Engineering  
(Associate Professor Boonsom Lerdhirunwong, Dr.Ing.)

THESIS COMMITTEE

.....Chairman  
(Professor Piyasarn Praserdthham, Dr.Ing)

.....Thesis Advisor  
(Associate Professor ML. Supakanok Thongyai, Ph.D.)

.....Examiner  
(Associate Professor Bunjerd Jongsomjit, Ph.D.)

.....Examiner  
(Assistant Professor Anongnat Somwangthanaroj, Ph.D.)

.....External Examiner  
(Assistant Professor Sirirat Wacharawichanant, D.Eng.)

ณัฐินี ศรีเนตร : การสังเคราะห์พอลิอิมิด์แบบต่อกิ่งสำหรับแผ่นเยื่อแลกเปลี่ยนโปรตอน  
(SYNTHESIS OF GRAFT COPOLYIMIDE FOR PROTON EXCHANGE  
MEMBRANE) อ.ที่ปรึกษาวิทยานิพนธ์หลัก : รศ.ดร.มล.ศุภกนก ทองใหญ่, 116 หน้า

ในงานศึกษานี้ ได้ทำการสังเคราะห์พอลิอิมิด์แบบต่อกิ่งที่มีหมู่กรดฟอสฟอนิกแบบใหม่ที่เตรียมจากมอนอเมอร์ NTDA และ ODA ขึ้น สายโซ่กิ่งของฟอสฟอเนตพอลิอิมิด์นั้นสามารถสังเคราะห์ได้จากการใช้ปฏิกิริยาโบรมิเนชันร่วมกับปฏิกิริยาอีเอชเอ็น ขณะที่โครงสร้างกิ่งแบบใหม่นั้นสามารถเตรียมได้จากการใช้มอนอเมอร์ 3,3'-ไดอะมิโนเบนซีนซึ่งมีหมู่เอมีน 4 หมู่ วิธีการสังเคราะห์แบบใหม่นี้เป็นวิธีการที่ค่อนข้างง่าย และสามารถปรับเปลี่ยนค่ามวลโมเลกุล, ความยาวของสายโซ่หลัก (PI) และสายโซ่กิ่ง (paPI) รวมทั้งปริมาณหมู่กรดฟอสฟอนิก หรือกรดซัลโฟนิกได้ตามที่ต้องการ และด้วยลักษณะโครงสร้างแบบใหม่ของพอลิอิมิด์แบบต่อกิ่งในงานวิจัยนี้ พบว่าสามารถเพิ่มค่าการนำโปรตอนของแผ่นเยื่อแลกเปลี่ยนโปรตอน ขณะที่ยังคงสามารถรักษาเสถียรภาพทางความร้อนและไฮโดรไลติกได้ดี และในงานนี้ยังได้ศึกษาผลของโครงสร้างระดับไมโคร เช่น ปริมาณกรดฟอสฟอนิก และความยาวสายโซ่กิ่ง ที่มีผลต่อค่าการดูดซับน้ำ การบวมตัว และค่าการนำไฟฟ้า จากการเตรียมและขึ้นรูปเมมเบรนอิเล็กโทรดแอสเซมบลี (MEA) ด้วยเทคนิคสเปรย์แบบเดียวกัน พบว่าเมมเบรน FPBPI-3 ที่มีค่า IEC ประมาณ 1.43 meq/g แสดงค่าการนำโปรตอนสูงที่สุด (0.045 s/cm) และมีค่าใกล้เคียงกับแนฟฟิออน®117 โดยพบว่าสภาวะที่เหมาะสมที่สุดสำหรับการทดสอบการทำงานของเซลล์เชื้อเพลิงของเมมเบรน FPBPI ที่สังเคราะห์ได้ ในงานนี้คือ ที่อุณหภูมิ 90 องศาเซลเซียส และความชื้นสัมพัทธ์ 74% นอกจากนี้ เมมเบรน FPBPI ยังมีค่าการซึมผ่านของเมทานอลน้อยกว่าแนฟฟิออน®117 ประมาณ 5 เท่า ซึ่งคุณสมบัติดังกล่าวนี้เป็นโอกาสที่จะนำเมมเบรนนี้ไปใช้ในเซลล์เชื้อเพลิงแบบเมทานอลมากขึ้น

ภาควิชา.....วิศวกรรมเคมี.....ลายมือชื่อนิติติ.....  
สาขาวิชา.....วิศวกรรมเคมี.....ลายมือชื่อที่ปรึกษาวิทยานิพนธ์หลัก.....  
ปีการศึกษา.....2556.....

## 5171842221: MAJOR CHEMICAL ENGINEERING

KEYWORDS: PHOSPHONIC ACID / GRAFT COPOLYIMIDE / PROTON EXCHANGE  
MEMBRANE / FUEL CELL / PROTON CONDUCTIVITY

NATHINEE SRINATE: SYNTHESIS OF GRAFT COPOLYIMIDE FOR PROTON  
EXCHANGE MEMBRANE, ADVISOR: ASSOC. PROF. ML. SUPAKANOK  
THONGYAI, Ph.D., 116 pp.

In this study, the novel phosphonated graft copolyimide based on NTDA and ODA monomer was synthesized. The phosphonated polyimide side chain was obtained from the series of bromination and lithiation reaction while the graft structure was achieved by novel use of 3,3'-diaminobenzidine monomer with 4 reactive amine group. This synthesis route leads to relatively simple and easily adjustable of molecular weight, chain length of backbone (PI) or side chain (paPI) segment as well as phosphonation or sulfonation level, if preferred. This novel structure of graft copolyimide can improve proton conductivity while maintaining good thermal and hydrolytic stability. The effects of microstructure e.g. phosphonation level and side chain length on water uptake, swelling ratio and proton conductivity were studied. Based on spray techniques for MEAs fabrication, the fPBPI-3 membrane with IEC of 1.43 meq/g showed the highest proton conductivity (0.045 s/cm) which comparable to Nafion<sup>®</sup>117, moreover, this membrane also showed more stable proton conductivity at operating temperature of 80-100°C than Nafion<sup>®</sup>117. The optimal condition of fuel cell test for fPBPI membrane in this study was reported at 90°C and 74%RH. In addition, the methanol permeability of fPBPI membrane was 5 times lower than Nafion<sup>®</sup>117 which increased the feasibility of this membrane for DMFC application.

Department ..... Chemical Engineering ..... Student's signature .....

Field of study ..... Chemical Engineering ..... Advisor's signature .....

Academic Year ..... 2013 .....

## ACKNOWLEDGEMENTS

I would like to express my truly grateful and gratitude to my advisor, Associate Professor Dr. ML. Supakanok Thongyai, for warm welcoming to his research group. His assistance, support, guidance and encouragement throughout my research and study are greatly appreciated. I also would like to thank my co-advisor, Professor Robert A. Weiss at Department of polymer engineering, The University of Akron, USA, for his support and guidance during my research time in his group.

I am grateful to Professor Dr. Piyasarn Prasertthdham, Associate Professor Dr. Bunjerd Jongsomjit, Assistant Professor Dr. Anongnat Somwangthanaroj and Assistant Professor Dr. Sirirat Wacharawichanant for serving as chairman and thesis committees, respectively, whose comments were constructively and especially helpful.

Sincere thanks are made to the Thailand Research Fund through the Royal Golden Jubilee Ph.D. Program for financial support, Grant PHD/0292/2549, during my study, and partially supported by the Civil, Mechanical and Manufacturing Innovation of the National Science Foundation, Grant CMMI 1032201 during my work in Prof. Weiss research group. I also would like to thank MEKTEC Manufacturing Corporation (Thailand) Ltd. for supporting the materials and the characterization equipment.

Sincere thanks to all members in Prof. Supakanok and Weiss research groups for their assistances and friendly encouragement. I also would like to extend my sincerest thanks to Dr. Wongwit Wongwitwichote, Dr. Emmanuel Pitia and Dr. Nadzrina Armad Nazirm for spending their time teaching, commenting on my works and their kindly support.

Finally I thank my family for their love and support, for always cheering and believing in me, especially my parents. Thank you my mother and father for raising me to be happy, healthy, motivated person. I wouldn't pass my tough time without your guidance and encouragement.

## CONTENTS

	Page
ABSTRACT IN THAI .....	IV
ABSTRACT IN ENGLISH.....	V
ACKNOWLEDGEMENTS .....	VI
CONTENTS .....	VII
LIST OF FIGURE .....	IX
LIST OF SCHEME .....	XII
LIST OF TABLE.....	XIII
CHAPTER	
CHAPTER I INTRODUCTION.....	1
1.1 Overview .....	1
1.2 The Objective of This Thesis .....	5
1.3 The Scope of The Thesis .....	5
CHAPTER II THEORY .....	6
2.1 Polyimide.....	6
2.2 One-Step Method-High Temperature Solution Polymerization.....	7
2.3 Two-Step Method.....	7
2.4 Determination of The Degree of Imidization .....	8
2.5 Proton Exchange Membrane Fuel Cells .....	9
2.6 The Measurement of PEM Fuel Cell Performance .....	11
2.7 Electrochemical Impedance Spectroscopy (EIS) Analysis .....	15
2.8 Basic Property of Polymer Electrolyte Membrane.....	18
CHAPTER III LITERATURE REVIEWS.....	25
3.1 Current Perfluorinated Membranes .....	25

	Page
3.2 Alternative Polymer Electrolyte Membrane.....	29
CHAPTER IV EXPERIMENTS.....	50
4.1 Materials .....	50
4.2 Synthesis Method .....	51
4.3 Film Preparation .....	61
4.4 Characterization And Properties.....	61
4.5 Fabrication of Membrane Electrode Assembly (MEA) And Measurements of Fuel Cell Performance .....	66
CHAPTER V RESULTS AND DISCUSSION.....	68
5.1 The Characterization Results of 2,2'-Dibromo-4,4'-diaminophenyl ether Monomer .....	68
5.2 The Characterization Results of Obtained Polyimide Sample .....	69
5.3 The Properties of Phosphonated Graft Copolyimide Membranes.....	83
CHAPTER VI CONCLUSIONS AND RECOMMENDATIONS.....	102
6.1 Conclusions .....	102
6.2 Recommendations .....	104
REFERENCES .....	105
VITA.....	116



## LIST OF FIGURE

	Page
Figure 2-1	General structure of polyimide..... 6
Figure 2-2	General mechanism of aromatic imide formation reaction ..... 7
Figure 2-3	The concept of polymer electrolyte membrane fuel cell ..... 10
Figure 2-4	The single cell of polymer electrolyte membrane fuel cell composition that used in laboratory. .... 11
Figure 2-5	A typical polarization curves for a proton exchange membrane fuel cell (H <sub>2</sub> /O <sub>2</sub> cell) ..... 12
Figure 2-6	Typical Nyquist plots for fuel cell system..... 16
Figure 2-7	The common circuit of Randles Cell..... 17
Figure 2-8	Interpretation of graphical complex plane of impedance data for an equivalent circuit..... 18
Figure 2-9	The vehicular mechanism (up) and Grotthus mechanism (down) for proton transportation..... 19
Figure 2-10	Proximity of neighboring acid groups within an aqueous channel. Distance between acid groups in (a) is greater than in (b). .... 20
Figure 2-11	The Plot of Proton conductivity as a function of IEC value for ETFE-g-PSSA, BAM membrane, SPEEK and Nafion ..... 21
Figure 2-12	Graphic of microphase separation in Nafion and SPEEKK..... 22
Figure 2-13	Ratios of Methanol to Water uptakes for S-SEBS membranes as a function of sulfonation degree ..... 23
Figure 3-1	General structure and type of perfluorinated membrane ..... 25
Figure 3-2	Illustration of Cluster-network model for the morphology of hydrated Nafion..... 27
Figure 3-3	Schematic representation of Nafion under different water volume fraction..... 28
Figure 3-4	Illustration of micro-structure features of Nafion ..... 29
Figure 3-5	Chemical structure of SPEEK, SPEEKK and SPEKK..... 31
Figure 3-6	The structure of Sulfonated polystyrene graft copolymer ..... 32

	Page
Figure 3-7	General structure of sulfonated poly(arylene ether)s obtained from direct copolymerization ..... 35
Figure 3-8	Structure of sulfonated poly(arylene ether)s obtained from polycondensation of bisphenol A, DCDPS and SDCDPS ..... 36
Figure 3-9	Relationship between water uptake and degree of sulfonation of sulfonated poly(arylene ether)s ..... 37
Figure 3-10	Relative humidity dependence on proton conductivity for NTDA-BAPBDS based polyimide membrane at 50 °C ..... 42
Figure 3-12	Temperature dependence of methanol permeability for SPI and Nafion 112 membranes at methanol concentration in feed (X <sub>M</sub> ) of 30 or 10 wt.% respectively ..... 43
Figure 3-13	FTIR spectra of pure PI and PI·1·0H <sub>3</sub> PO <sub>4</sub> ..... 45
Figure 3-14	The proton conductivity data of phosphonated polydulfonemembrane with various degree of phosphonation and Nafion 117 under 100%RH ..... 48
Figure 3-15	Structure of BPA-based Poly(arylene ethers) containing phosphonic acid groups ..... 49
Figure 4-1	Structure of NTDA-4,4'-ODA-based polyimide – main chain (PI) where x is number of repeating unit ..... 52
Figure 4-2	Structure of phosphonated polyimide side-chain (paPI) where y is number of repeating unit and R <sub>2</sub> is P=O(OH) <sub>2</sub> unit ..... 52
Figure 4-3	Structure of all intermediated product that obtained from method A where y is repeating unit and R <sub>1</sub> represents -P=O(OEt) <sub>2</sub> ..... 55
Figure 4-4	Structure of all intermediated product that obtained from method B where y is repeating unit and R <sub>1</sub> represents -P=O(OEt) <sub>2</sub> ..... 56
Figure 4-5	Structure of phosphonated graft copolyimide (PBPI) where x, y is repeating unit in main-chain and side-chain respectively and R <sub>2</sub> represents -P=O(OH) <sub>2</sub> ..... 60
Figure 4-6	Carver compression press ..... 61
Figure 4-7	Nicolet 380 Fourier transform infrared ..... 62
Figure 4-8	Nuclear Magnetic Resonance Spectrometers ..... 62

	Page
Figure 4-9	PGSTAT, Autolab ..... 66
Figure 4-10	Scribner 850e Fuel Cell Station..... 67
Figure 5-1	The <sup>1</sup> H-NMR spectrum of 2,2'-dibromo-4,4'-diaminophenyl ether in CDCl <sub>3</sub> solvent..... 69
Figure 5-2	FTIR spectra of polyimide (A) PI, (B) S-B3 (Intermediated PI), (C) paPI and (D) PBPI samples ..... 72
Figure 5-3	(A) <sup>1</sup> H-NMR spectrum and chemical structure of polyimide, PI ..... 75
Figure 5-4	<sup>31</sup> P-NMR spectra of phosphoanted graft copolyimide; PBPI samples ..... 79
Figure 5-5	The example of TGA results of PI, paPI and PBPI samples ..... 83
Figure 5-6	The relation between side chain length and water uptake and swelling properties ..... 85
Figure 5-7	The relation between % phosphonation and water uptake and swelling properties ..... 85
Figure 5-8	The polarization curve of fPBPI-1 membrane at 90 °C and 100% RH under different equilibrate time. .... 87
Figure 5-9	The study of suitable relative humidity range for proton conductivity measurements ..... 88
Figure 5-10	Comparison of polarization curve between phosphonated graftcopolyimide (up) and Nafion membrane (down) ..... 90
Figure 5-11	Comparison of proton conductivity between phosphonated graft copolyimide membrane (blended with 20% PI) and Nafion®117 at 54%, 74% and 100% RH.... 93
Figure 5-12	Comparison of proton conductivity between phosphonated graft copolyimide membrane and Nafion®117 at 90°C ..... 94
Figure 5-13	A schematic of water drainage process of a model capillary system as water emerges from GDL surface ..... 95
Figure 5-14	The effect of side chain length on proton conductivity at 74% RH ..... 97
Figure 5-15	The effect of phosphonation level on proton conductivity at 74% RH..... 98

## LIST OF SCHEME

	Page
Scheme 3-1 The mechanism of directlithiation of the polysulfone main chain using n-butyllithium .....	33
Scheme 3-2 Bromination and lithiation of the polysulfone main chain .....	34
Scheme 3-3 Synthesis of 3,3'-disulfonate-4,4'-dichlorodiphenylsulfone .....	36
Scheme 3-4 Phosphonation of polysulfone via combination of chloromethylation and Michaelis-Arbuzov reaction .....	47
Scheme 3-5 Functionalization of difluoromonomers .....	48
Scheme 5-1 The synthetic pathway of phosphonated graft copolyimide .....	71

## LIST OF TABLE

	Page
Table 2-1	Summary of basic information for proton exchange membrane fuel cell (PMFC) and direct methanol fuel cell (DMFC) ..... 9
Table 2-2	Common circuit elements used in equivalent circuit models ..... 17
Table 3-1	Summary of commercial of poly(perfluorosulfonic acid) membranes ..... 26
Table 3-2	Comparison of physical properties of sulfonated polyimide with different sulfonation level and Nafion 117 ..... 38
Table 3-3	The starting materials for synthesis of naphthalenic polyimides ..... 39
Table 3-4	Summary of effective reactions for synthesis of phosphonated polymers ..... 46
Table 3-5	The degree of polymerization (DP) and % phosphonation of phosphonate polyimide; paPI samples ..... 60
Table 5-1	Solubility of the polyimide samples ..... 80
Table 5-2	Comparison of intrinsic viscosity and theoretical molecular weights of the polyimides ..... 81
Table 5-3	Comparison of IEC values between NMR calculation and Titration method ..... 82
Table 5-4	Comparison of phosphonate grafted copolyimide membrane and Nafion®117 properties. .... 84
Table 5-5	The methanol permeability and proton conductivity of phosphonate graft copolyimide membrane; fPBPI and Nafion®117 ..... 100

## **CHAPTER I**

### **INTRODUCTION**

#### **1.1 OVERVIEW**

Fuel cell is one of the new promising energy converters that directly transforming the chemical energy into electricity and offers many benefits including high performance efficiency, durability and clean energy power. They can operate on wide range of fuels from the gaseous fuels such as hydrogen and air etc. to the liquid fuels such as methanol etc., while emitting zero level of pollutants.[1, 2] Based on the type of electrolyte, fuel cells are classified into several types i.e. polymer electrolyte membrane fuel cell (PEMFC), direct methanol fuel cell (DMFC), alkaline fuel cell (AFC), phosphoric acid fuel cell (PAFC) etc., however they all consist of an anode (negative side), cathode (positive side) and electrolyte. Each fuel cell technology has different advantages and disadvantages, the suitable application need to be considered in various aspects i.e. operating condition, cost and stability etc.

Proton exchange membrane plays a major role in PEMFC and DMFC systems. Both systems are similar except that DMFC uses methanol as reactant and directly feed to the anode instead of hydrogen gas. The polymer membrane serves as electrolyte that provides proton and electron and also as separator for the two reactants at both electrodes.[3] The polymer membranes are the important units for producing electrical power. In order to efficiently produce electricity, the polymer electrolyte membrane of should has high proton conductivity, chemically and thermally stable, good mechanical property, non-electrically conductive, and inexpensive. Moreover, the PEM can be applied under the aggressive conditions; such as automobile operation, which includes hydrolysis, oxidation, reduction or hydrogenation that can lead to degradation of the polymer thereby reducing the lifetime of polymer electrolyte membrane.

Current commercial polymer membranes that utilized in PEMFC and DMFC application are perfluorinated sulfonic acid membranes such as Nafion (developed by Dupont de Nemours) and Dow membrane (developed by Dow Chemical Co.,Ltd), Flemion (developed by Asahi Glass Co.,Ltd) etc. These membranes showed high proton conductivity at temperature approximately 80°C and high relative humidity condition while poorly perform at higher temperature (above 80°C) and lower relative humidity due to the dehydration of membrane.

Many researchers studied and attempted to find the membrane material that endure the fuel cell operation and optimize the proton and water membrane transport properties while minimize the reactant permeability. Some of the most promising candidates for PEMs are based on high performance aromatic polymers, i.e. sulfonated polyimides (PI), poly(ether ether ketone)s (PEEK), polysulfones (PSU) or poly(ether sulfone)s (PES), poly(phenylene oxide) (PPO), poly(phenylene sulfide) (PPS), polyphosphazenes, polybenzimidazole (PBI) and others. Historically, the acid functionalities used in ionomers for PEMs had primarily contained carboxylic and sulfonic acids. Many sulfonated aromatic polymer systems have been investigated since they have high operating temperature, good processibility, improving water uptake and lower cost than perfluorinated membranes.

Sulfonated polyimides have excellent thermal, oxidative stability and mechanical properties. Many works reported the advantage and disadvantage of polyimide membrane. Normally, the five-membered ring phthalic polyimides showed poor hydrolytic stability under the strongly acidic conditions of fuel cell. The hydrolysis of the five-membered ring imide structure probably led to chain scission (decreased the molecular weight) and then caused the membranes to become brittle. In comparison, the six-membered ring naphthalic polyimides displayed better thermal and chemical stabilities; along with the improvement of mechanical strength than phthalic polyimides. Although their properties were excellent, the synthesis and film preparation of naphthalic polyimides were difficult due to their low solubility in common organic solvents.[4]

Moreover the optimization between the degree of sulfonation and swelling properties were challenging as well. Basically, to adjust the molar ratio of sulfonated diamine and non-sulfonated diamine in SPI copolymer could precisely control the degree of sulfonation in SPI copolymer. However, it was crucial to control the degree of sulfonation, because the high degree of sulfonation generally led to high swelling ratio.

In place of using sulfonic acid, phosphonic acid is an alternative functional group that may serve as proton-transporting group in PEMs. Organophosphonic acids ( $\text{RPO}_3\text{H}_2$ ) have two ionizable acid groups, that depended on the chemical groups, attached to the phosphorous atom, with having  $\text{pK}_{\text{a}1} \sim 1 - 4$  and  $\text{pK}_{\text{a}2} \sim 4 - 9$  respectively [4, 5]. The stronger acid P-OH group has the dissociation constant at the intermediate between those of sulfonic ( $\text{pK}_{\text{a}} \sim 1$ ) and carboxylic ( $\text{pK}_{\text{a}} \sim 4 - 5$ ) acids [6-8]. Although phosphonic acids are less acidic than sulfonic acids, they generally have higher thermal stability [9], which might make the phosphonic acids to be the attractive candidates for the higher temperature PEMs. [10-15]

Phosphonic acid-containing ionomers had been much less investigation than carboxylate and sulfonate ionomers [16]. Early works on phosphonate ionomers concerned chlorophosphonylation of polyolefins and using organolithium compounds to minimize the formation of side products from the reaction [17-21]. Lafitte and Jannasch [xx] had phosphonated polysulfone up to 50% by using direct lithiation in the presence of diphenyl or diethyl chlorophosphate. Souzy et al. [22] synthesized perfluorovinyl ether monomers containing phosphonic acid groups that incorporated into the polymer backbones by a free radical polymerization reaction or directly grafting onto an aromatic ring. Phosphonated polyphosphazenes have been prepared by using bromination and lithiation reaction in a presence of chlorophosphonic acid ester. [15, 23] Wu and Weiss [24] prepared phosphonated ionomers by copolymerization reactions of styrene and vinylphosphonate, followed by hydrolysis to the phosphonic acid derivative.



In addition to the type of acid groups, the microstructures of the polymer also affect the properties of PEMs. Various chain architectures and/or morphologies had been considered to design for PEM materials. These included different copolymer architectures, such as block, graft and random copolymers. Micro-phase separation between hydrophobic and hydrophilic phase usually occurs in block copolymers, the hydrophilic part can promote the proton transfer and sustain the water stability while the hydrophobic backbone can provide durability.[25, 26] Ding et al. reported that graft-block copolymers, e.g., poly(sodium styrene sulfonate) grafted to a polystyrene backbone, exhibited the higher proton conductivity than a random copolymer with the same composition[27]. Lee et al. [28] prepared sulfo-alkylated graft polyimides and found that the ionomers with the longest side chains had the best durability and chemical resistance. The SPIs series prepared from 4,4'-ketone dinaphthalene 1,1',8,8'-tetracarboxylic dianhydride (KDNTDA) showed the good solubility in aprotic solvent and their cross-linked membrane improved the mechanical properties and water swelling of PEMs.[29].

In this research, the study and synthesis of proton exchange membrane from phosphonated polyimide are interested. Since polyimide has excellent thermo-mechanical properties, and high chemical resistance. The graft copolyimide in this study consists of hydrophilic phosphonated polyimide and hydrophobic polyimide backbone. The new phosphonated graft copolyimide series with phosphonic acid units as proton transfer group are prepared by combination of one step polymerization and lithiation reaction. This method will enable the proton transfer while maintain high thermal stability of the membrane, while and the relations between the microstructures of polymer membrane, prepared from different chain length, the phosphonation level and the fuel cell performance were also investigated.

## **1.2 The Objective of This Thesis**

- To study and synthesis polyaromatic membrane from phosphonated polyimide and compare membrane properties to Nafion membrane.
- To develop novel high temperature membranes with low methanol crossover, while maintain proton conductivity
- To obtain new better membrane properties this utilizes in the proton exchange membrane applications.

## **1.3 The Scope of The Thesis**

1. Preparation of the phosphonated graft copolyimide series and developing effective synthesis methods.
2. Preparation of membrane from phosphonated graft copolyimide and characterizing the membrane properties by using different techniques.
3. Assemble the single cell of a PEM fuel cell using synthesized membrane, and evaluating its performance.

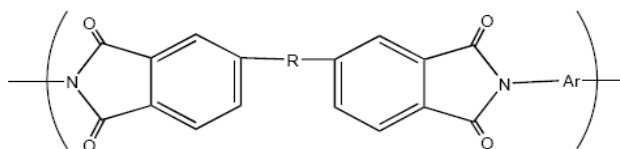
## CHAPTER II

### THEORY

This chapter will briefly review basic concepts that related to this study including polyimide and its basic property, proton exchange membrane fuel cell technology with some specific issues on factors controlling its performance i.e. irreversible losses (polarization curve characterization) and fundamental of electrochemical impedance data analysis etc. and mechanism of proton conductance in polymer electrolyte membrane.

#### 2.1 POLYIMIDE

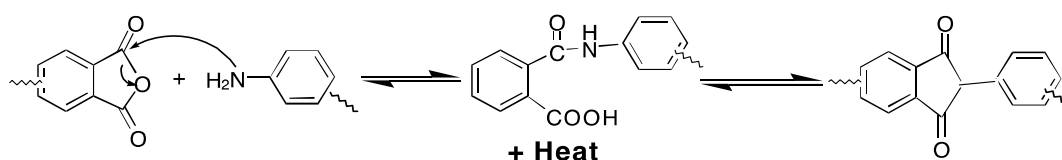
Polyimides are one of a step or condensation polymers that generally derived from the reaction of organic diamine and organic dianhydride or derivatives thereof and its general structure can be shown in Figure 3-1. [30] The variation in the structure of diamine and dianhydride monomers has magnificent effected to the final polyimide property. However, most of polyimides are thermally stable based on stiff aromatic backbones. Generally there are two methods for polyimide synthesis; two-step method and one-step method. Both methods are starting from poly(amic acid) formation and following by imidization process.



**Figure 2-1 General structure of polyimide**

## 2.2 ONE-STEP METHOD-HIGH TEMPERATURE SOLUTION POLYMERIZATION

The one step polymerization is employed for polyimides that are soluble in organic solvents especially in dipolar aprotic solvents i.e. NMP, *m*-cresol or nitrobenzene. [31] In this procedure, the stoichiometric mixture of dianhydride and diamine monomers in a high boiling point solvent are heated and homogeneous stirred at 180-220°C. [30, 31] Under these conditions, the imidization occurs rapidly at this temperature and the water generated from the reaction is distilled from reaction mixture along with azeotrope solvent i.e. toluene etc., which added during the synthesis step. The imidization mechanism of poly(amic acid) are shown in Figure 3-2.



**Figure 2-2 General mechanism of aromatic imide formation reaction [30]**

As shown in Figure 3-2, the amic acid are continuously converted to imide group or reverted back to diamine and dianhydride, however, this method is generally conducted in the presence of catalysts i.e. quinolone, triethyl amine or tertiary amine etc. This one step method is very useful for polymerization of unreactive dianhydride and diamine which cannot form high molecular weight poly(amic acid) by two-step method. In addition, this method is often yields polyimide with higher degree of crystallinity than two-step method as well, it was possibly due to an increase in solubility of monomer in the solvent at high temperature.

## 2.3 TWO-STEP METHOD [30]

The most common procedure of polyimides synthesis is two-step process. It involves the reaction of dianhydride and diamine at ambient temperature in dipolar aprotic solvent, such as N-

methylpyrrolidone (NMP), dimethylacetamide (DMAc) or dimethylsulfoxide (DMSO), to form a soluble, processable poly(amic) acid

The high molecular weight isomeric poly(amic)acid formation is completed within 24 hours or less, depending on monomer reactivity. Since it is fully soluble in the reaction solvent, the solution may be cast into a film on a suitable substrate. The second step in this synthetic method is imidization reaction that accomplished by thermal (heating to elevated temperatures), chemical (incorporating a chemical dehydration agent) or by azeotropic solution imidization.

This method was initiated since 1950's and continues to be the widely practical way to synthesize high performance polyimides. Most polyimides are insoluble and infusible due to their planar aromatic and hetero aromatic structure thus they are usually need to be processed from the solvent route. On the other hand, the soluble and processable poly(amic) acid intermediates that are heated to elevated temperatures also facilitate the generation of fully cyclized films via spin casting in coating procedures.

#### 2.4 DETERMINATION OF THE DEGREE OF IMIDIZATION[32]

The prominent procedure to assess the degree of imidization of polyimide is infrared spectroscopy technique. Although there are some overlap bands between chemical functional group of poly(amic acid) and polyimide, the investigation of the dominant peak of imide adsorption are still useful determination. The most band that frequently presented and related to polyimide bond are summarized as following;

- **Imide absorption band** : at  $1780\text{ cm}^{-1}$  (C=O asymmetric stretching),  $1720\text{ cm}^{-1}$  (C=O symmetric stretching),  $1380\text{ cm}^{-1}$  (C-N stretching), and  $725\text{ cm}^{-1}$  (C=O bending). [33]
- **Carboxylic acid band in poly(amic acid)** : at  $1700\text{ cm}^{-1}$  (C=O symmetric stretching) and  $2800\text{-}3200\text{ cm}^{-1}$  (O-H). [33]

- **Amide band in poly(amic acid)** : at  $1650-1680\text{ cm}^{-1}$  (C=O symmetric stretching), and  $1550\text{ cm}^{-1}$  (C-NH) and  $3200-3300\text{ cm}^{-1}$  (N-H)[33]

These absorption bands are important for qualitative assessment and confirmation of imide bond formation.

## 2.5 PROTON EXCHANGE MEMBRANE FUEL CELLS

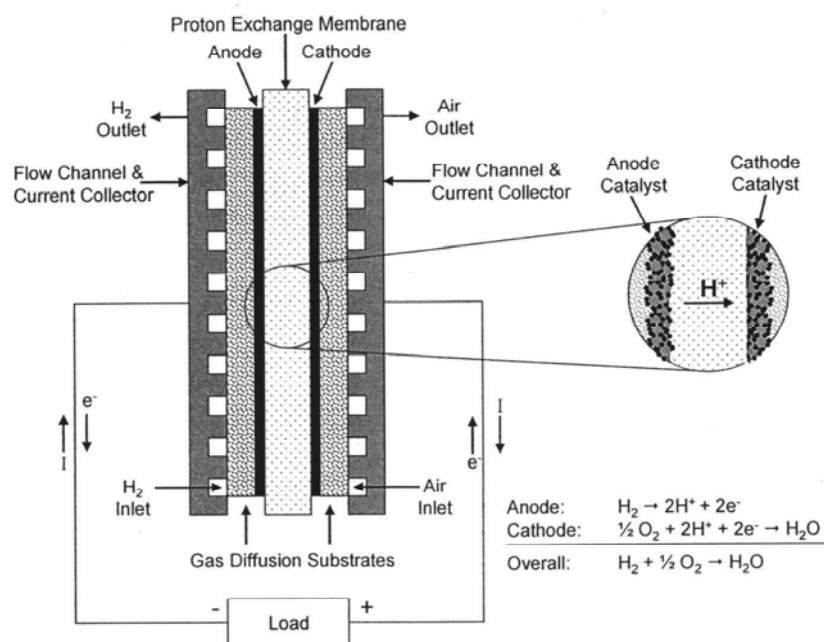
Fuel cell is currently developed for new power sources as alternative to fossil fuel because they have more efficient and environmental advantage including high power density, reliability, durability and pollution free. A fuel cell is an electrochemical device to convert the chemical energy to electricity. The polymer electrolyte membrane can be applied for both proton exchange membrane fuel cell (PEMFC) and direct methanol fuel cell (DMFC) systems. The basic information for both PEMFC and DMFC is summarized in Table 2-1. This PEMFC is currently used in automotive, stationary and portable power.[34]

**Table 2-1 Summary of basic information for proton exchange membrane fuel cell (PMFC) and direct methanol fuel cell (DMFC)**

Fuel cell Type	Operating Temperature	Efficiency	Electric Power	Electrochemical Reactions
Proton exchange membrane fuel cell (PEMFC)	60-130	40-60	$\leq 250\text{ kW}$	Anode: $\text{H}_2 \rightarrow 2\text{H}^+ + 2\text{e}^-$ Cathode: $\text{O}_2 + 4\text{H}^+ + 4\text{e}^- \rightarrow 2\text{H}_2\text{O}$ Cell: $2\text{H}_2 + \text{O}_2 \rightarrow 2\text{H}_2\text{O}$
Direct methanol fuel cell (DMFC)	60-130	40	$< 10\text{ kW}$	Anode: $\text{CH}_3\text{OH} + \text{H}_2\text{O} \rightarrow \text{CO}_2 + 6\text{H}^+ + 6\text{e}^-$ Cathode: $3\text{O}_2 + 12\text{H}^+ + 12\text{e}^- \rightarrow 6\text{H}_2\text{O}$ Cell: $2\text{CH}_3\text{OH} + 2\text{H}_2\text{O} + 3\text{O}_2 \rightarrow 2\text{H}_2\text{O} + \text{CO}_2$

The proton exchange membrane fuel cell (PEMFC) is sometime called as polymer electrolyte membrane and solid polymer electrolyte membrane. The cross-section of a proton

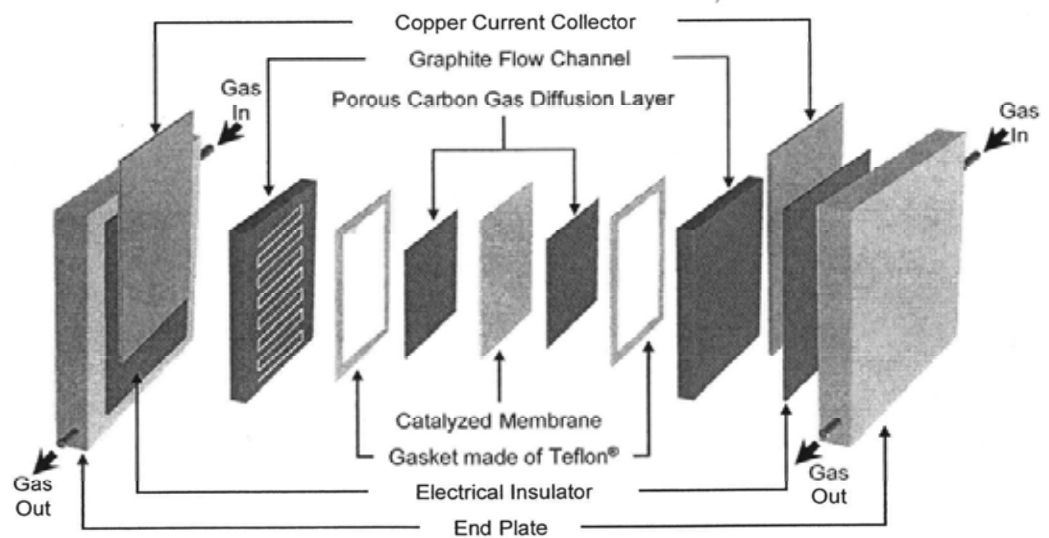
exchange membrane fuel cell is shown in Figure 2-3. The membrane plays as a major role for proton conducting function. On both sides of membrane surface, the catalyst layers are coated by various techniques including printing and spraying method. Then the membrane is fabricated to contact with gas diffusion layers (GDL) on both sides as well and this composition is named as membrane electrode assembly (MEA) which will be applied for set up single fuel cell component as shown in Figure 2-4.



**Figure 2-3 The concept of polymer electrolyte membrane fuel cell [2]**

The hydrogen gas is fed into anode side of the system while the oxygen, either in air or pure oxygen gas, is fed into cathode side. Both reactant gases flow through gas channel inlet (Graphite flow channel) and pass through the gas diffusion layers to the catalyst surface on their respective sides of membrane. When the hydrogen gas contacts to the noble metal catalyst layer i.e. platinum (Pt), ruthenium (Ru) etc., the hydrogen is oxidized to form protons and electrons. The protons pass through the polymer electrolyte membrane and electrons transfer through external circuit to the cathode side, thereby producing an electric current. At catalyst layer of

cathode side, oxygen combines with the protons that pass through membrane and electrons from external circuit to produce water and heat.



**Figure 2-4 The single cell of polymer electrolyte membrane fuel cell composition that used in laboratory. [2]**

## 2.6 THE MEASUREMENT OF PEM FUEL CELL PERFORMANCE

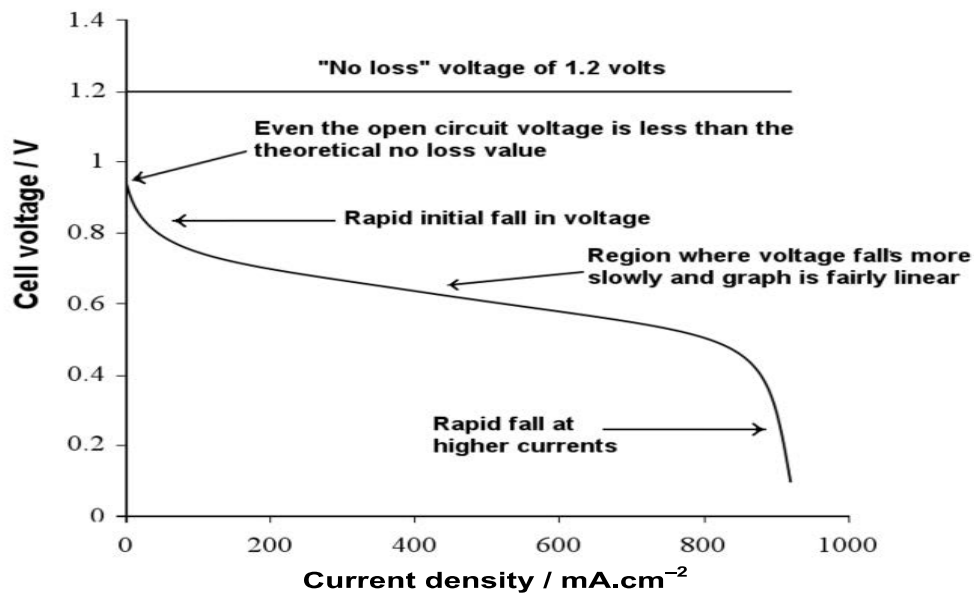
The performance of single cell fuel cell can be determined from;

- Relationship between voltage and current density (or polarization curve)
- Reactant utilization (calculation for gas consumption)

### 2.6.1 POLARIZATION CURVE–RELATIONSHIP OF VOLTAGE AND CURRENT DENSITY[35]

Polarization means the difference between voltages of both electrodes that shifts away from equilibrium value, leading to an electrochemical reaction. Polarization curves showed relationship between the voltage changes with current density, which is important data for depicting fuel cell performance. A fuel cell with good performance should have long current density range at high cell voltage, which indicating high power output.





**Figure 2-5 A typical polarization curves for a proton exchange membrane fuel cell (H<sub>2</sub>/O<sub>2</sub> cell) [36]**

As shown in Figure 2-5, the polarization curve presents three regions, which called as kinetic limitation (or Activation polarization), ohmic limitation and transport limitation. In the kinetic part; the cell voltage drops because of the charge-transfer kinetics (O<sub>2</sub> reduction and H<sub>2</sub> oxidation) rate at the electrode surface. In the ohmic part; the cell voltage drop is mainly due to the internal resistance of the fuel cell, including electrolyte membrane resistance, catalyst layer resistance, and contact resistance. In the mass transfer part; the voltage drop is due to the transfer speed of H<sub>2</sub> and O<sub>2</sub> to the electrode surface. [36]

- Open circuit voltage (OCV)

Open circuit voltage (OCV) is the cell voltage at condition of zero current (no load and no power output). In real operation, at an electric current of 0, the cell voltage is less than the standard theoretical potential ( $E_{\text{theory}}^{\circ}$ ) of approximately 1.2 V. This ideal value is calculated from the change of Gibbs free energy ( $\Delta G^{\circ}$ ) for overall reaction (both hydrogen oxidation reaction or HOR and oxygen reduction reaction or ORR) based on standard condition at 25°C and 1 atm. The

change of Gibbs free energy is  $-237$  kJ/mol (if liquid water is produced) and  $-228.1$  kJ/mol (if vapor water is produced), the corresponding  $E_{\text{theory}}^{\circ}$  values are 1.23 and 1.18 V, respectively. These ideal values are never observed in the reality since some reactant gases permeate across the electrode, for example;  $\text{H}_2$  permeates from anode to cathode while  $\text{O}_2$  permeates from cathode to anode, where it is oxidized and this can cause the overpotential at each electrode and results in lower open circuit voltage.

- Kinetic limitation period

Activation polarization is primarily function of temperature, pressure, concentration and electrode properties. As shown in Figure 2-5, the kinetic loss at cathode ( $\text{O}_2$  reduction reaction) is much greater than kinetic loss at anode because the oxygen reduction reaction on Pt catalyst is slower when comparing to the relative facile hydrogen oxidation reaction. The voltage loss in this period is dominated for resistance of reaction at electrode.

- Ohmic limitation period

At the mid-range of the polarization curve, the cell voltage drop is dominantly associated to internal resistance. This internal resistance is also called ohmic resistance and related to the electronic resistance and ion transport resistance of membrane and catalyst layer. The electronic resistance includes the resistance at cell electrode, gas diffusion layer, and contact resistance at each component interface. However, the losses due to electronic resistance are really smaller than the losses from resistance to ion transport. In PEMFCs case, the proton ( $\text{H}^+$ ) conductance in membrane and catalyst layer is contributed to the total ohmic resistance.

- Transport limitation period

The transport limitation period are also called as concentration polarization. Electrochemical reactions at electrode surface involve many steps including mass transfer and

electrode kinetics. If the mass transfer step is faster, while the adsorption and charge transfer are slower, the total reaction rate is dominantly determined by the electrochemical reaction kinetics. However, in the case of slower mass transfer and faster electrochemical kinetics, the mass transfer rate limits the whole reaction. In other word, the concentration gradient between the bulk and electrode surface is arisen when the reaction rate at electrode exceeds the rate at which reactant can be delivered to the active reaction site so the reactant that can reach the electrode surface is consumed immediately, and the insufficient reactant on the electrode surface can cause the voltage loss.

### 2.6.2 REACTANT UTILIZATION (U)

Reactant utilization and gas consumption have a significantly effected to fuel cell efficiency. Reactant utilization (U) is defined as the ratio between amount of consumed reactant to amount of supplied reactant while the stoichiometric ratio (S) is the inverse of the reactant utilization as shown in Equation 2-1 and Equation 2-2 respectively.

$$U = \frac{V_{react,consumed}}{V_{react,total}} \quad \text{Equation 2-1}$$

$$S = \frac{1}{U} \quad \text{Equation 2-2}$$

where V is the volumetric flow rate of reactant gas (L/min).

The total required flow rate of reactant gas can be calculated based on Faraday's Law (Equation 2-3) since the amount of consumed reactant is directly proportional to the electric current that generated from the fuel cell system. However, under typically fuel cell operation, the excess amount of required reactant will be fed to the system in order to keep the utilization value less than 1.

$$N = \frac{1}{nF}$$

Equation 3-3

where  $N$  is reactant consumption or product generation rate, mole/s

$I$  is current, A (coulomb/s)

$n$  is mole of electron exchanged per mole of species (equivalent/mole)

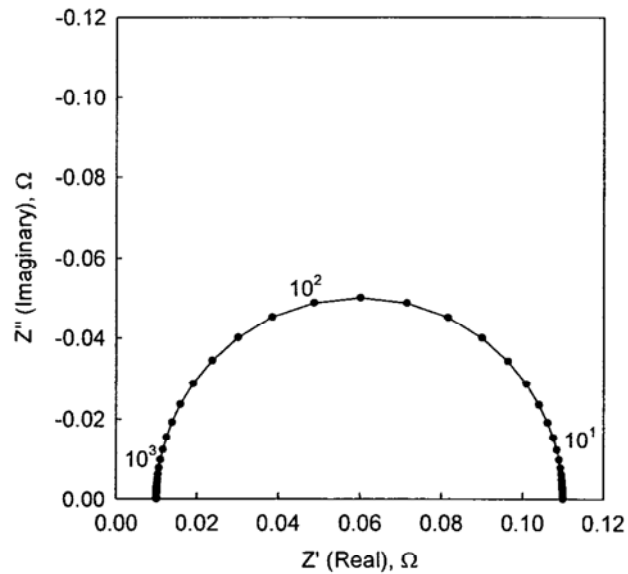
$F$  is Faraday constant, 96485 coulomb/equivalent

Remark : The  $n$  value of  $H_2$  and  $O_2$  gas is 2 and 4 eq./mole respectively

## 2.7 ELECTROCHEMICAL IMPEDANCE SPECTROSCOPY (EIS) ANALYSIS

An electrochemical system in fuel cell exhibits complex behaviors. Many factors effected to the fuel cell performance, some factors are directly related while others are dependent. In addition, some processes that occurring in the cell responded to when cell condition is changed over a broad frequency range. For example, diffusion processes and charge transfer process occurs at different time scale (sub-seconds to seconds for diffusion and sub-milliseconds for charge transfer), their effects are revealed at different frequency range.

In brief, electrochemical impedance spectroscopy is an experimental technique that measures the AC impedance of circuit element or an electric circuit. For actual electrochemical system, impedance is applied instead of resistance. Generally, the impedance spectrum of electrochemical system will be presented in Nyquist and Bode plots which represented the impedance data as a function of frequency. Some typical Nyquist plots for a fuel cell system are shown in Figure 2-6. The normal result is presented in a semi-circle shape, with the high frequency part giving the membrane resistance and the width of semicircle giving the charge-transfer resistance.



**Figure 2-6 Typical Nyquist plots for fuel cell system [36]**

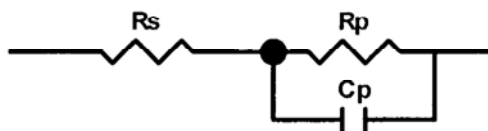
EIS data analysis is generally determined by fitting it to an equivalent electric circuit model. An equivalent circuit model consists of resistance, capacitances and/or inductances as well as a few specialized electrochemical elements (i.e. Warburg diffusion element), which produces the same response as the electrochemical system does when the same excitation signal is imposed. In the empirical model, each circuit component represents the physical process in electrochemical cell. The shape of model's impedance spectrum is controlled by the combination (parallel or series) and interconnection between electrical elements. The available Z-view software is a powerful program to fit the spectra and give the best values for equivalent circuit parameters.

The equivalent circuit contains at least electrolyte resistance, double layer capacity and impedance of Faradic or non-Faradic process. Some common equivalent circuit elements for electrochemical system are listed in Table 2-2.

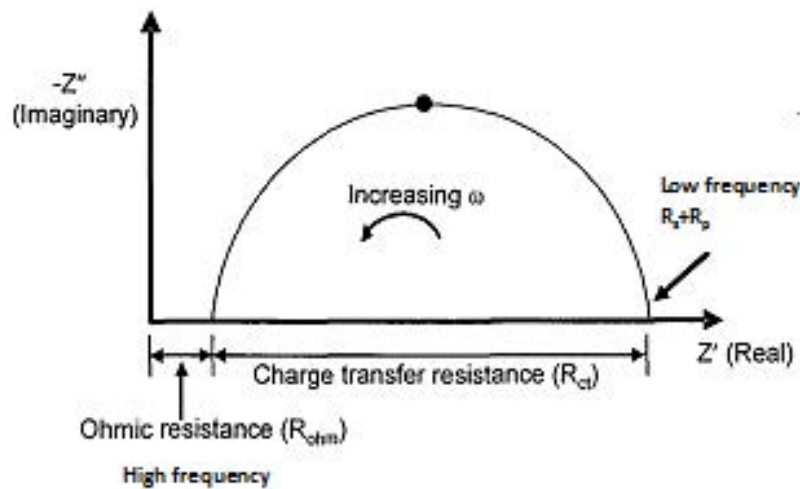
**Table 2-2 Common circuit elements used in equivalent circuit models**

Equivalent element	Name
R	Resistance
C	Capacitance
L	Inductance
W	Warburge

The Randles Cell is a simplest and most common model of electrochemical interface model. The equivalent circuit and Nyquist plots for Randles cell are shown in Figure 3-7. The circuit includes an electrolyte resistance, a double layer capacitance and charge transfer resistance. As shown in Figure 3-7,  $R_p$  is the charge transfer resistance of the electrolyte/electrode interface process,  $C_p$  is capacitance of double layer at interface, and  $R_s$  is the resistance of the electrolyte or called as ohmic resistance ( $R_{ohm}$ ). The double layer capacitance is in parallel with the charge transfer resistance.

**Figure 2-7 The common circuit of Randles Cell [36]**

The Nyquist plot of a Randles cell is commonly presented in a semicircle. At high frequency, the impedance of  $C_p$  is very low, so the measured impedance tends to  $R_s$  or  $R_{ohm}$ . At very low frequency, the impedance of  $C_p$  becomes extremely high, and thus, the measured impedance tends to  $R_p + R_s$ . Accordingly, the high-frequency intercept is corresponded to the electrolyte resistance ( $R_s$  or  $R_{ohm}$ ), while the low-frequency intercept corresponds to the sum of the charge-transfer resistance and the electrolyte resistance. The diameter of the semicircle is equal to the charge-transfer resistance.



**Figure 2-8 Interpretation of graphical complex plane of impedance data for an equivalent circuit**

## 2.8 BASIC PROPERTY OF POLYMER ELECTROLYTE MEMBRANE [3]

In order to get effective PEM fuel cell performance, the polymer electrolyte membrane should have these following characteristics.

- High proton conductivity
- Low gas (specially oxygen) and fuel (methanol) crossover
- Balanced water transport
- High chemical and water stability

Ideally, membrane should have excellent performance in all of these aspects. However, it is often found that PEMs will generally perform well in some of these areas while performing only adequately or even poorly in others.

### 2.8.1 PROTON CONDUCTIVITY[34,37]

The ability to conduct protons through membrane is key parameters of a PEM. This parameter is intimately associated to acid and water content in the membrane and also affected by

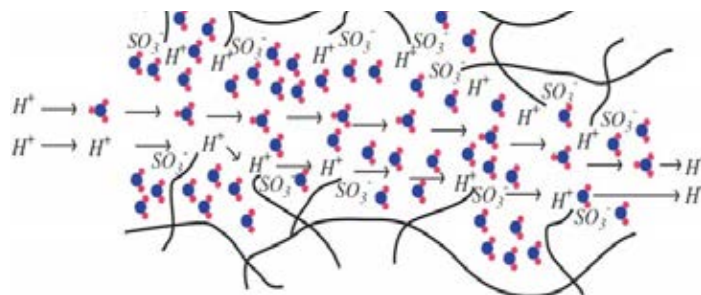
the strength of the acid, the chemical structure and morphology of the membrane, and temperature. The proton conductivity is calculated from Equation 2-4.

$$\sigma = \frac{L}{RA}$$

Equation 2-4

Where  $\sigma$  is conductivity (S/cm), L is membrane thickness (cm), A is electrode area ( $\text{cm}^2$ ), and R is resistance ( $\Omega$ ).

Water is a good proton conductor. Transport of proton or cation in solution usually consists of a solvated cation diffusing through a solution. In addition to the vehicular transport (Figure 3-9) of larger solvated cations, protons also move through solution via structural diffusion. This can be visualized as a chain mechanism in which protons are passed from one water molecule to its neighbor so that it appears the protons are migrating through the solution. This structural diffusion has also been called the Grotthuss mechanism (Figure 2-9).

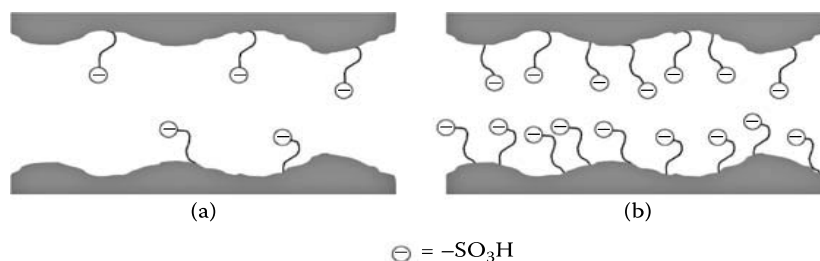


**Figure 2-9 The vehicular mechanism (up) and Grotthuss mechanism (down) for proton transportation. [38]**

In addition, the distance between acid groups may effect to proton mobility. With protons mediated via positively charge species between acid groups, it is expected that larger distances between these tethered counter-ions will require greater energy in comparison to shorter distances, thus leading to lower mobility in the former case. This is schematically represented in



Figure 2-10. Furthermore, the mobility of the proton is also affected by the degree of dissociation and its relationship to water content in membrane.

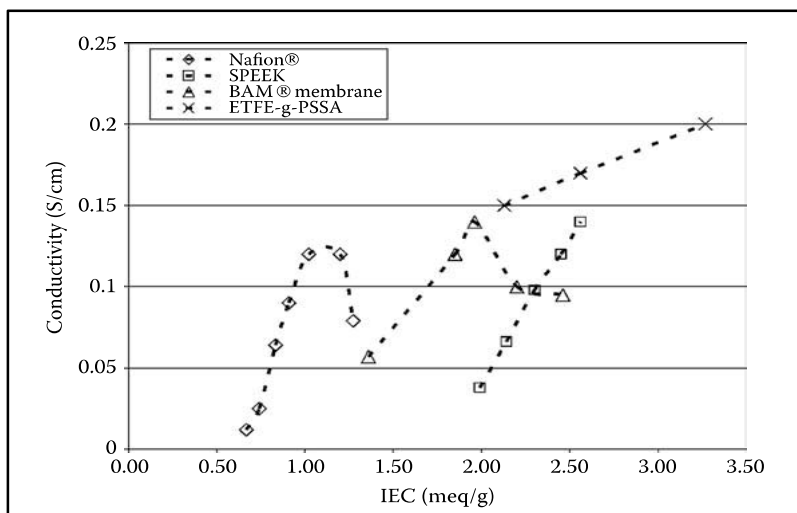


**Figure 2-10 Proximity of neighboring acid groups within an aqueous channel. Distance between acid groups in (a) is greater than in (b). [39]**

Other important factors that control the proton conductivity are polymer microstructure and morphology. The formation of hydrophobic and hydrophilic domains in membrane strongly relates to proton transport as expectation.

### 2.8.2 ION EXCHANGE CAPACITY AND WATER UPTAKE

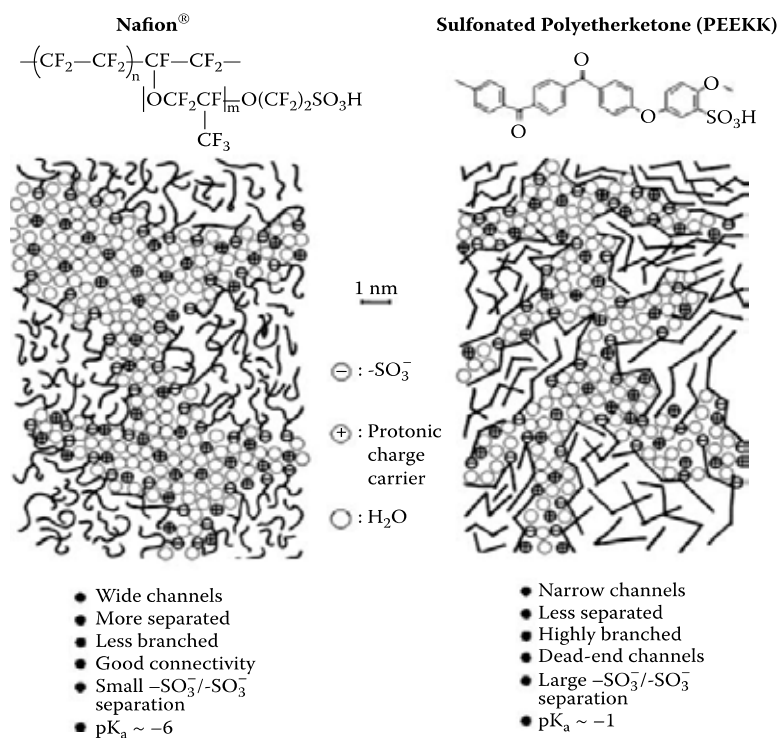
The ion exchange capacity value can tell the content of acid group in polymer chain. The effect of acid content on conductivity is normally plotted as Figure 2-11. The proton conductivity strongly depends on acid content for all PEM especially in sulfonic acid containing polymer membrane; It is not surprisingly found that the conductivity is dependent upon proton content. For example, as shown in Figure 2-11, the proton conductivity increases with increasing of IEC value for all membranes.



**Figure 2-11 The Plot of Proton conductivity as a function of IEC value for ETFE-g-PSSA, BAM membrane, SPEEK and Nafion [39, 40]**

In general polymer electrolyte membrane, the hydrophobic segment of the polymer is incompatible with the hydrophilic segment of acid group and results in phase separation. When the membrane is exposed to the water, the hydrophilic domains swell and yield proton transport channel. For example, the graphic of micro-phase separation and water channel in Nafion and SPEEKK was reported as shown in Figure 2-12.

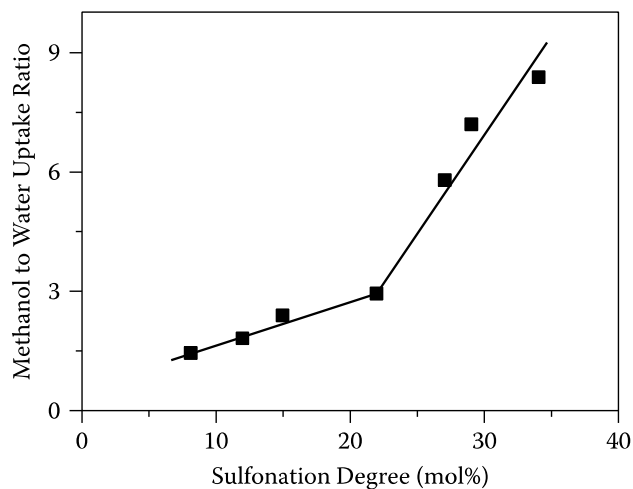
A smaller characteristic separation length with a wider distribution and a larger internal interface between the separated hydrophilic and hydrophobic micro-domains is corresponding to a larger average separation between neighboring acid sites. In general, it can be seen that the water-filled channels through SPEEKK membrane, which proton transport is thought to occur, are narrower than those in Nafion, as well as exhibiting greater degrees of branching and dead ends and less separation between the channels. This leads to a more complex pathway for proton conduction in SPEEKK versus Nafion.



**Figure 2-12 Graphic of microphase separation in Nafion and SPEEK. [41]**

### 2.8.3 METHANOL PERMEABILITY

Generally, methanol crossover is a major problem in direct methanol fuel cell (DMFC), MeOH permeating from the anode compartment through the membrane to the cathode compartment. The decrease of the cell efficiency due to the reactions and depolarization of permeated MeOH with oxygen at the cathode are issued. The relationship between %sulfonation and IEC value were reported as shown in Figure 2-13.



**Figure 2-13 Ratios of Methanol to Water uptakes for S-SEBS membranes as a function of sulfonation degree. [42]**

It was reported that the MeOH uptake of the membrane increased with increasing of %sulfonation. Chemical structure and morphology of membranes significantly affects the solvent absorption. For grafted or branched polymers, the phase separation exists due to the hydrophobic segment in polymer; however, a regular clustered structure, has not been proposed for these materials.

The MeOH crossover rate is closely related to several factors, including membrane structure and morphology, membrane thickness, membrane acid content, and the cell operating parameters, such as temperature and MeOH feed concentration. The MeOH crossover rate decreases with an increase in the thickness and can be reduced greatly by using a membrane with sufficiently high equivalent weight (EW). [42, 43] Therefore, it may be advantageous to use either thicker or higher EW membranes to reduce the MeOH crossover rate.

However, the disadvantage is the penalty of higher voltage losses due to higher specific resistance as a result of thicker and higher EW membranes. The voltage loss is particularly severe at higher current density operation. Moreover, a thicker membrane means increasing material

cost. Ideal membranes for DMFC would have no MeOH crossover, but would have some water transport to the cathode to prevent drying of the cathode catalyst layer.

## CHAPTER III

### LITERATURE REVIEWS

Fuel cells can be classified into two major groups depending on their operating temperature: (A) low temperature fuel cells (<200 °C) and (B) high temperature fuel cells (>450 °C). The proton exchange membrane fuel cell (PEMFC) and direct methanol fuel cell (DMFC) are one of the low temperature fuel cell that have operating temperature around 60-90°C. In this chapter, all polymer membrane types that used in polymer electrolyte membrane fuel cell and direct methanol are reviewed and detailed as following:

#### 3.1 Current Perfluorinated Membranes

Among the protonconducting membranes, the perfluorinated membranes, which have been developed as ion separators for fuel cells and have showed the characteristic features of super selectivity, very high thermal stability, and chemical resistance, which cannot be obtained by the other classes of polymeric membranes. This section provided the literature on perfluorinated membranes including their historical development, synthesis, and their structural and proton conductivity characteristics.

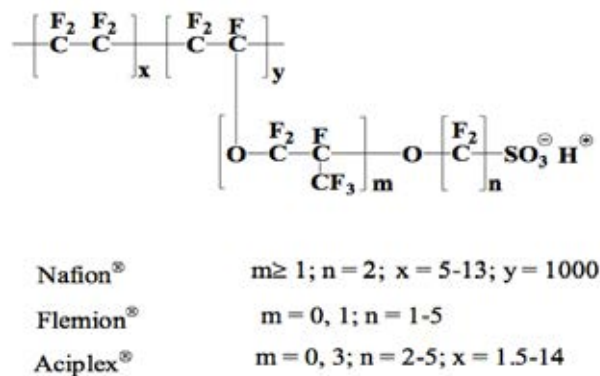


Figure 3-1 General structure and type of perfluorinated membrane [44]

The perfluorinated polymers or poly(perfluorosulfonic acid) have sulfonic acid groups which are attached to the polymer backbone as shown in Figure 2-1. These polymers have high proton conductivity up to  $10^{-2} - 10^{-1} \text{ S/cm}^{-1}$  under fully hydrated state and lifetime up to 60,000 hours at 80°C. [44]

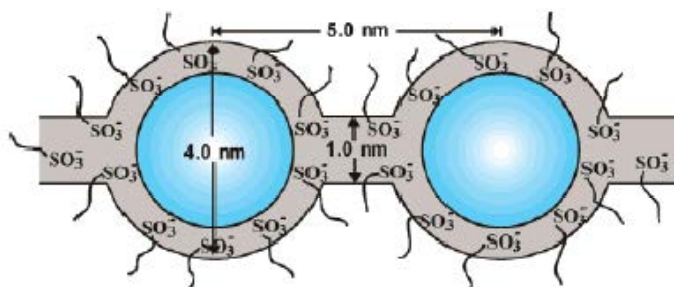
The commercial of poly(perfluorosulfonic acid) membranes have been developed in various series, equivalent weight (EW) and thickness by different company as summarized in Table 3-1.

**Table 3-1 Summary of commercial of poly(perfluorosulfonic acid) membranes [26,45]**

Membrane	Series	Equivalent weight (EW)	Thickness ( $\mu\text{m}$ )	Company
Nafion	112	1100	51	Dupont
	115	1100	127	
	117	1100	178	
	1110	1100	254	
	120	1200	260	
Flemion	R	1000	50	Asahi Glass
	S	1000	80	
	T	1000	120	
Aciplex	S	1000-1200	25-100	Asahi Chemicals

Among these membranes, the Nafion with 1100 EW are most currently used since this EW provides high proton conductivity, moderate swelling ratio, good chemical resistance and mechanical properties. Generally, the thinner membranes are suitable for proton exchange membrane fuel cells since the reduction in ohmic loss can increase stability, while thicker

membranes (e.g. Nafion 120) are usually applied for direct methanol fuel cells to reduce methanol crossover.

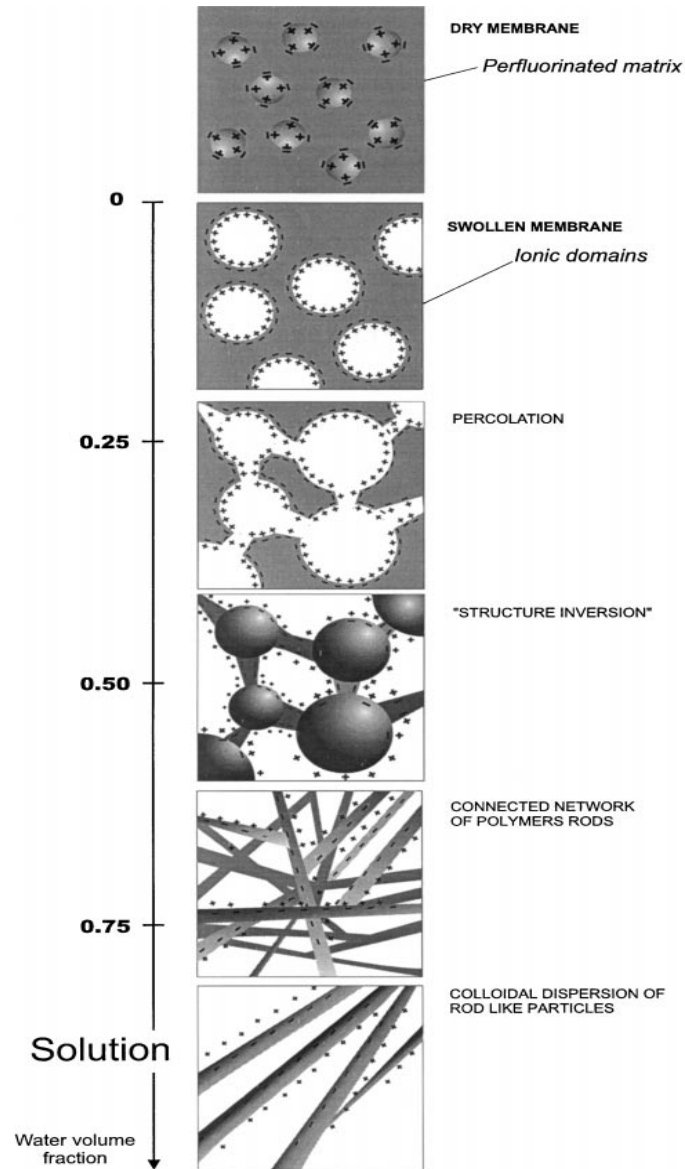


**Figure 3-2 Illustration of Cluster-network model for the morphology of hydrated Nafion. [31]**

Water is a major carrier for proton conduction in Nafion. Many researchers studied and proposed the Nafion network model. The fully hydrated membranes presented micro-phase separation between hydrophobic (fluorocarbon rich) and hydrophilic (sulfonic acid rich) in domain. The widely accepted “reverse-micelle-like” cluster network model as shown in Figure 3-2 was proposed since year 1982. All fluorinated membranes in their fully hydrated state, including Nafion have water uptakes above 15  $\text{H}_2\text{O}/\text{SO}_3\text{H}$  and proton conductivities of  $10^{-2}$ - $10^{-1}$  S/cm. However, their conductivity decreases dramatically above 80°C due to the loss of the absorbed water, which promotes a decrease of interconnection between neighboring sulfonic acid rich domains within the polymer membrane.

The small-angle neutron and X-ray scattering (SANS and XAXS) techniques were applied to study the swelling characteristics of Nafion membrane with different water content as presented in Figure 3-3. [46] The spherical ionic clusters in a dry membrane had original diameter approximately of 15 Å. By increasing the water volume fraction, each spherical cluster were swelled and started to connect to neighboring clusters by forming cylinder path when the volume fraction ranged between 0.3 - 0.5. At the volume fraction larger than 0.5, a structure inversion occurred and became a “rod-like” polymer network.

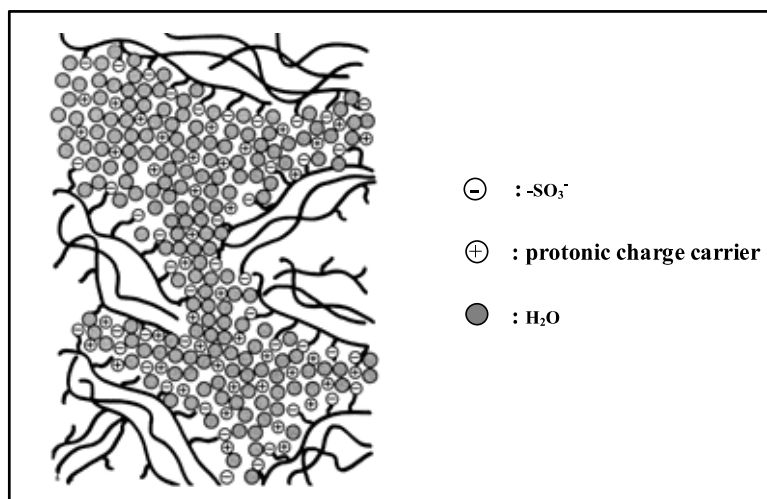




**Figure 3-3 Schematic representation of Nafion under different water volume fraction.[47]**

In the presence of water, the hydrophilic domain in Nafion is well-connected whereas the hydrophobic domain serves as a boundary. Water is required to transport protons as illustrated in Figure 3-4. The proton conductivity of Nafion 115 membrane has reached the maximum value at approximately 80°C and dropped at higher temperatures because the water is evaporated, the

temperature of 80 °C is then known as the best operating condition of poly(perfluorosulfonic acid) membrane. [41, 48]



**Figure 3-4 Illustration of micro-structure features of Nafion.[49]**

From overall disadvantages of poly(perfluorosulfonic acid) like Nafion such as expensive (600-800 \$US/m<sup>2</sup>), poor proton conductivity at low humidity or elevated temperature and high methanol crossover[50], these lead many researchers try to improve and study the alternative polymer membrane for fuel cell application.

### 3.2 Alternative Polymer Electrolyte Membrane

Due to shortcoming of Nafion membrane at high temperature, various types of polymeric materials were studied as alternative membrane for fuel cell application. In the past, there were many researches on new polymer membranes including modification of Nafion [51] acid-base polymer blends [52], synthesis of new condensation polymers such as polyimide and other aromatic polymer materials.

Presently, some of the most promising candidates for PEMs are based on high performance aromatic polymers, i.e. polyimides, poly(ether ketone)s, poly(arylene ether sulfone)s, polybenzimidazoles, etc.[1] Advantages of using these materials include;

- Lower cost than perfluorinated membranes
- Composing of polar groups to improve water uptake
- High operating temperature and good chemical stability

This section focused on the research of sulfonation and phosphonation of polymer materials by gathered all approaches for modification and functionalize of polymer materials. In addition, the basic properties of sulfonated and phosphonated aromatic membrane especially the polyimide membrane in fuel cell application were reviewed in this section as well.

### **3.2.1 Sulfonated polymer membrane**

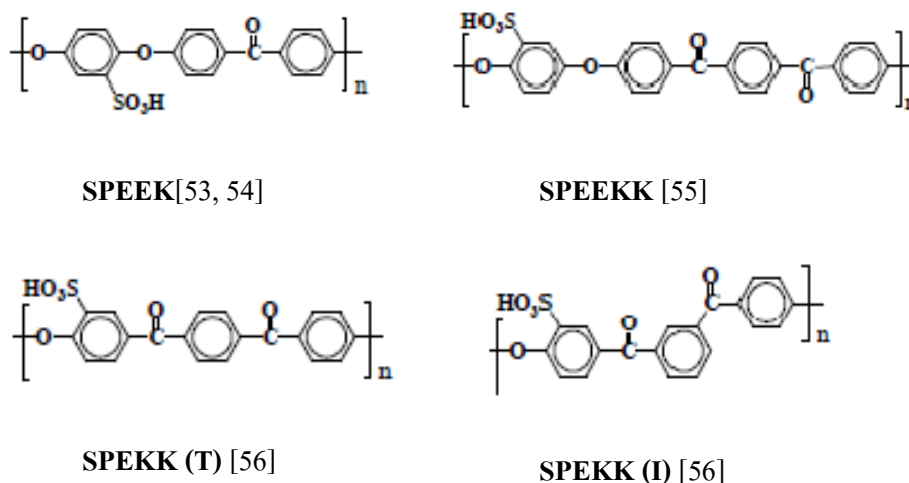
This section described the researches on sulfonated polymer membrane including method for preparing the sulfonated polymer; (A) Post-sulfonation and (B) Direct copolymerization of sulfonated monomer, and some basic membrane properties in fuel cell application.

#### **3.2.1.1 Post-Sulfonation**

One approach to obtain sulfonated polymer materials is the chemical modification of available polymers by treatment with different types of sulfonation agents, which namely as “**Post-sulfonation**”. In the beginning, the sulfonation was done by dissolving polymer powder in concentrated sulfuric acid solution and then participated it into water, however the degree of sulfonation could not be controlled.

Many reports attempted to find the proper method to control the degree of sulfonation while maintain their basic properties. Treatment of sulfonating agents was used for introducing the proton transfer sites into existing polymer backbone i.e. sulfonated poly(ether ether ketone) or SPEEK[53], sulfonated poly (ether ketone ketone) or PEKK, polysulfone. The sulfonation is an electrophilic substitution reaction which generally occurs at the aromatic ring between the two ether linkages in PEEK. However, a strong sulfonating agent such as chlorosulfuric acid could

cause the degradation of polymer materials. The SPEEK with 30-100% sulfonation level were obtained by controlling the reaction time and concentration of sulfuric acid [54]. The proton conductivity of SPEEK (structure in Figure 3-5) with 65% sulfonation level was reported about  $10^{-4}$  S/cm and start falling at temperature above 60 °C under 100% RH.

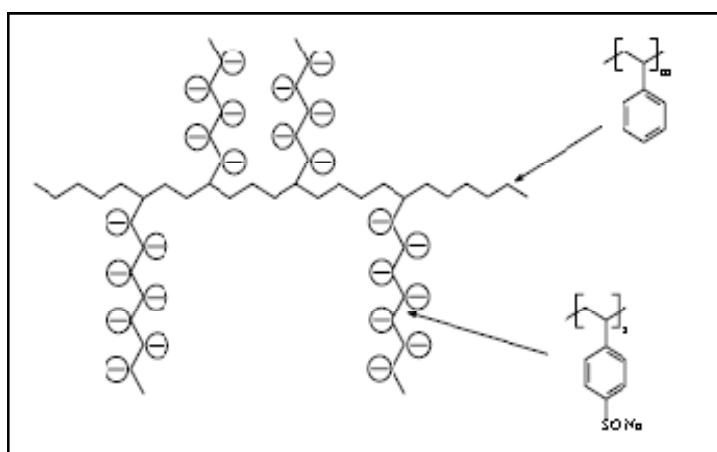


**Figure 3-5 Chemical structure of SPEEK, SPEEKK and SPEKK**

Post-sulfonation of poly(arylene ether)s which have less ether linkages like PEKK were more difficult than others such as PEK, PEEK and PEKEKK due to the increase of ketone/ether ratio of repeating unit. The ketone groups in polymer chain have withdrawn the electron from aromatic ring and results in less reactive toward sulfonation. The stronger sulfonating reagents such as mixture of concentrated and fuming sulfuric acid are required for these systems. The conductivity of SPEKK membrane prepared from mixed sulfuric acid at 80°C is about 0.05 S/cm and comparable to Nafion 112 (0.06 S/cm). In addition, the methanol permeability in SPEKK membrane is much lower than Nafion 112.[57]

Exclude the treatment of reagents in sulfuric acid group, the SEBS block copolymer with 28% wt of styrene content was sulfonated by using acetyl sulfate in 1-2 dichloroethane solution. The degree of sulfonation was controlled by the amount of sulfonating agent.[43] The proton conductivity and methanol crossover of the sulfonated SEBS membrane sharply increased when

the degree of sulfonation exceeded 15%mol. In addition, the conductivity of this membrane with 34% sulfonation level was closed to Nafion 117 at the same temperature. Holdcroft and co-workers developed a synthetic methodology to produce a series of sulfonated polystyrene graft copolymer by grafting the sulfonated graft chains of PS-g-PSSNa as shown in Figure 3-6 to polystyrene chain. [27]

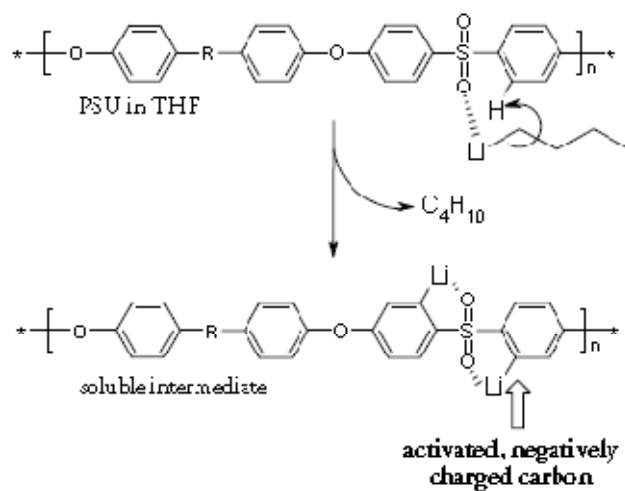


**Figure 3-6 The structure of Sulfonated polystyrene graft copolymer[27]**

The idea of direct functionalizes of polysulfone(PSU) main chain using metalation or lithiation techniques were investigated by many researchers.[7,8,58] In year 1986, the PSU was metalated and carboxylated by reaction with *n*-butyllithium (1.6 M *n*-BuLi in hexanes) and carbon dioxide at room temperature in dry tetrahydrofuran (THF). It was reported that the lithiated PSU precipitated from the reaction mixture at relatively low levels, and that an uneven carboxylation occurred. The mechanism of the of the lithiation of polysulfones was explained by Guiverand co-workers. Based on their reports, the lithiation of PSU was carried out at low temperature, typically at -78 °C in THF and maintain the low temperature by using a 2-propanol / dry-ice bath which in contrast of Beihoffer *et al* since the higher temperatures resulted in the precipitation of the polymer which caused by the intramolecular rearrangements.

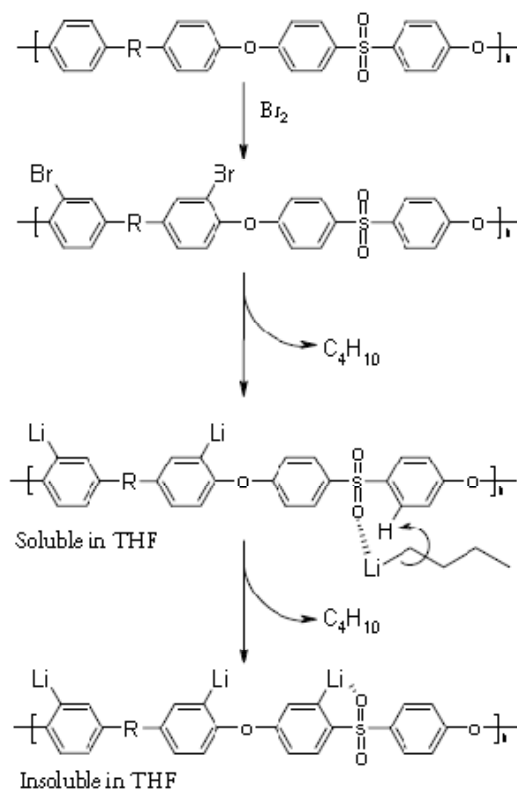
The direct lithiation of polysulfones using organolithium reagents such as *n*-BuLi is possible since the electron withdrawing power of the sulfone group gives an acidic character to

the *ortho*-to-sulfonehydrogens and allowing their replacement by strong organic bases. In addition, the lone electron pairs of the sulfone groups stabilize the lithium cations in the form of complexes (see Scheme 3-1).



**Scheme 3-1 The mechanism of directlithiation of the polysulfone main chain using n-butyllithium[7]**

In another works, Guiver and co-workers [59] reported that lithiated sites of *ortho*-to-ether could be accessed via a two-step bromination-lithiation reaction. This bromination pathway could increase the sulfonated active sites since the reactive substitution positions are located *ortho*-to-ether as for the direct sulfonation reactions. Notably, high degree of lithiation (DL) values can be obtained since *ortho*-to-sulfone positions may be lithiated when all the bromine atoms had been consumed (see Scheme 3-2).



**Scheme 3-2 Bromination and lithiation of the polysulfone main chain.[7]**

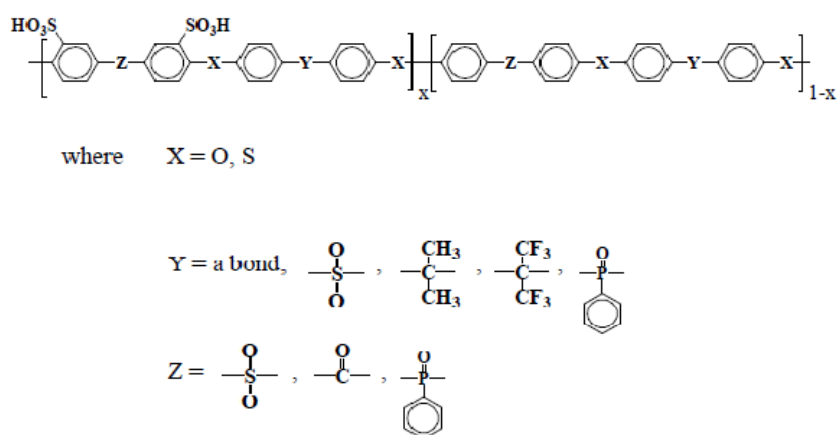
The introduction of sulfonic acid groups into aromatic polymer chain as described above seems to be unmanageable since the degree of sulfonation and location of acid site could not be controlled and this post-sulfonation procedure could lead the side reactions. In addition, the use of inappropriate sulfonating agents can cause the degradation of polymer materials. The sulfonic acid group presented in the phenyl ring could lead higher chemical stability; however, the desulfonation process might occur at elevated temperatures and under acidic condition. Another complication is that directly sulfonated polymers exhibited extensive swelling and lose their mechanical stability when reached critical degree of sulfonation, or temperature. For example, directly sulfonated polysulfones with a degree of sulfonation of 80% have been found to be water-soluble at room temperature, therefore the ion exchange capacity (*IEC*) of the polymers should be optimized for PEMFC application[6-8]

### 3.2.1.2 Direct copolymerization of sulfonated monomers

The direct copolymerization of sulfonated monomers is an alternative interesting procedure. Degree of sulfonation can be easily controlled by varying the ratio of sulfonated monomer and non-sulfonated monomer. Many sulfonated polymers were investigated and prepared by “**Direct copolymerization of sulfonated monomers**” procedure especially polyimide and poly(arylene ether)s.

- **Sulfonatedpoly(arylene ether)s copolymer**

The possible structure of sulfonatedpoly(arylene ether)s that obtained from direct copolymerization procedure are shown in Figure 3-7 and the polymer chain contains both hydrophilic and hydrophobic domain.

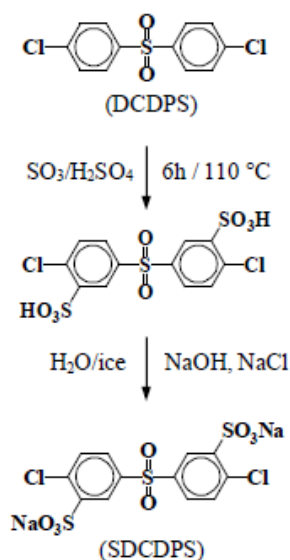


**Figure 3-7 General structure of sulfonated poly(arylene ether)s obtained from direct copolymerization [26]**

The 3,3'-disulfonate-4,4'-dichlorodiphenylsulfone(SDCDPS) is the most common sulfonated monomer applied for preparation of sulfonated poly(arylene ether)s. This monomer obtained by sulfonation of dichlorodiphenylsulfone (DCDPS) via 30%

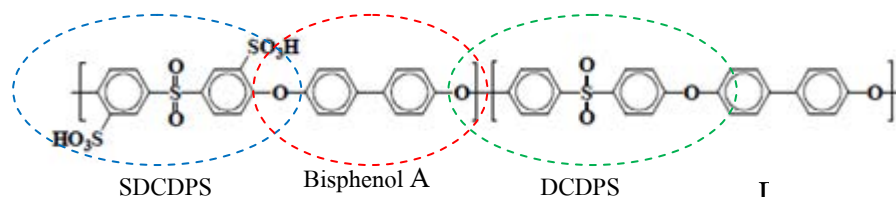


fuming sulfuric acid and precipitation it in mixture of ice water and diluted NaOH or NaCl solution as shown in scheme 2-4.[60]



**Scheme 3-3** Synthesis of 3,3'-disulfonate-4,4'-dichlorodiphenylsulfone[60]

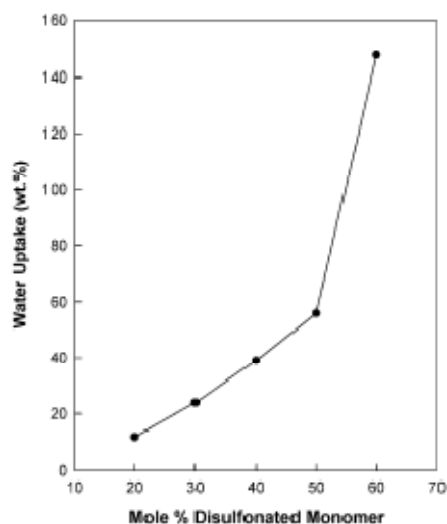
The accurate functional group stoichiometric ratio (between sulfonated monomer and non-sulfonated monomer) is required for direct copolymerization of poly(arylene ether) copolymers which known as step growth polymerization. The polymer structure shown in Figure 3-8



**Figure 3-8** Structure of sulfonated poly(arylene ether)s obtained from polycondensation of bisphenol A, DCDPS and SDCDPS[61]

The sulfonated poly(arylene ether)s were obtained in salt form and converted to acid via hydrolysis process after being cast into film and different degree of sulfonation can be controlled by varying amount of SDCDPS (disulfonated unit). However, the membrane prepared from 60%

mole of disulfonated monomer had dramatically increased in water uptake (up to 150%wt) as shown in Figure 3-9.[61]



**Figure 3-9 Relationship between water uptake and degree of sulfonation of sulfonated poly(arylene ether)s [61]**

The synthesis of polyarylene thioethersulfone has been reported by Dai et al. [62]The membrane prepared from polyarylene thioethersulfone with 40% sulfonation level were proven to apply in PEMFC application at medium temperature operation. Their mechanical properties were better than Nafion 112 in both dry and hydrated states. They also showed significantly lower H<sub>2</sub> crossover than Nafion 112 at 80°C under 100%RH.

- **Sulfonated polyimides**

Most polyimide membranes in fuel cell application were mainly focused on sulfonic acid as proton transfer group. Presently, the sulfonated polyimide copolymers have been synthesized by a direct copolymerization procedure. As mention earlier, the step growth polymerization requires the accurate stoichiometric amount of dianhydride, sulfonated diamine and non-sulfonated diamine to control sulfonation level. The copolymerizations are always carried out at high temperature; as one-step polycondensation in aprotic solvent such as NMR, DMAC and m-

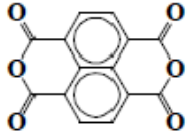
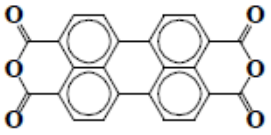
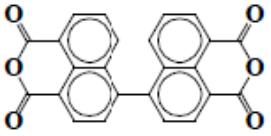
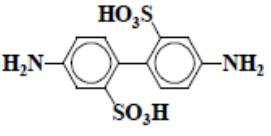
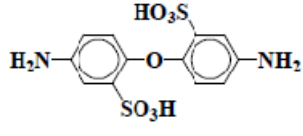
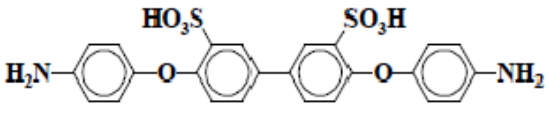
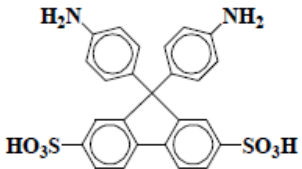
Cresol etc. The catalysts i.e. benzoic acid or isoquinoline, employed in this system have been varied while triethylamine is used for converting sulfonated diamine to salt form; this can increase the solubility of sulfonated diamine in reaction media like m-cresol and yield high molecular weight polyimides. In this section, the study on sulfonated polyimides including the essential properties in fuel cell application, which are described as following:

**Table 3-2 Comparison of physical properties of sulfonated polyimide with different sulfonation level and Nafion 117 [63]**

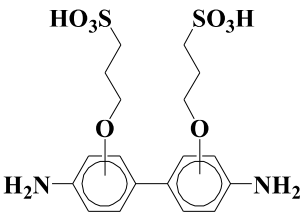
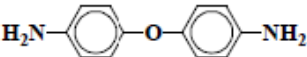
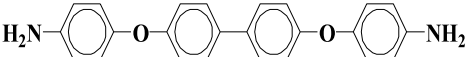
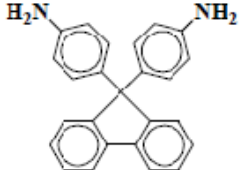
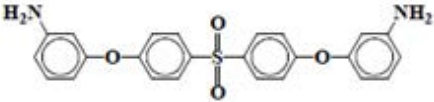
Sample	IEC (mmol/g)	Water Uptake (%wt)	Proton conductivity (S/cm)
Nafion 117	0.091	34.21	0.10
SPI 00	-	2.41	1.72 x 10 <sup>-3</sup>
SPI 07	0.250	3.24	2.26 x 10 <sup>-3</sup>
SPI 16	0.562	4.32	3.52 x 10 <sup>-3</sup>
SPI 25	0.844	5.99	3.64 x 10 <sup>-3</sup>
SPI 36	1.125	12.65	3.62 x 10 <sup>-3</sup>
SPI 46	1.375	14.74	1.11 x 10 <sup>-3</sup>
SPI 57	1.625	15.35	3.77 x 10 <sup>-3</sup>
SPI 63	1.750	15.89	4.10 x 10 <sup>-3</sup>

Woo and co-workers studied the physical properties of SPI membrane with different sulfonation level and reported in Table 3-2. The SPI membranes based on 3,3',4,4'-benzophenonetetracarboxylic dianhydride (BTDA), 4,4'-oxydianiline (ODA) and 2,2'-benzidinedisulfonic acid (BDSA) as starting materials have lower water uptake and lower proton conductivity than Nafion 117 even at higher IEC value. However, they exhibited significantly low methanol permeability. [63]

Table 3-3 The starting materials for synthesis of naphthalenic polyimides

Monomer Types	Chemical structures
Dianhydride	 <p>3.2.2 NTDA [29, 64-67]</p>
	 <p>PTDA [29]</p>
	 <p>BTDA [29]</p>
SulfonatedDiamine	 <p>BDSA (rigid) [66,68,69]</p>
	 <p>ODADS (flexible) [66]</p>
	 <p>BAPBDS(flexible)[29]</p>
	 <p>BAPFDS (rigid,bulky) [29]</p>

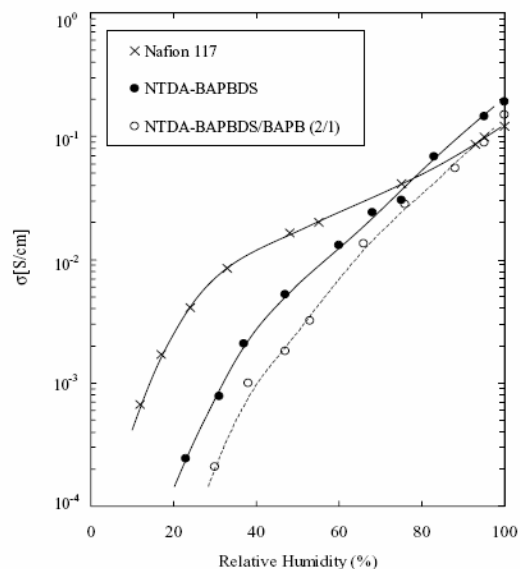
**Table 3-3 The starting materials for synthesis of naphthalenic polyimides**

Monomer Types	Chemical structures
	 <p style="text-align: right;">BSPB (flexible, bulky)</p>
Non-sulfonatedDiamine	 <p style="text-align: right;">ODA [64-67]</p>  <p style="text-align: right;">BABP</p>  <p style="text-align: right;">FDA [66,70]</p>  <p style="text-align: right;">BAPPS [64,65,70]</p>

The hydrolytic stability of phthalic (5-membered ring) and naphthalenic (6-membered ring) sulfonated polyimide was investigated. [64,65,68,69] It was reported that the 6-membered ring polyimides showed a better hydrolytic stability in PEMFC application than 5-membered ring polyimides. Therefore this section focused mainly on naphthalenic polyimides. The naphthalenic-

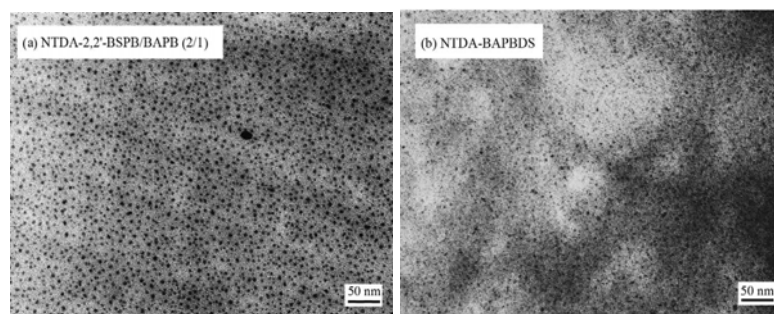
based polyimides are generally prepared by one-step polycondensation process at high temperature from various naphthalenic-based dianhydride, sulfonated diamine and non-sulfonated diamine as shown in Table 3-3.

Sulfonated diamines are important units for proton conducting polymer since protons transferred via sulfonic acid sites. BDSA and ODADS monomers were widely used for synthesis of sulfonated polyimides. When compared between these two sulfonated diamines, that ODADS-based polyimide membrane exhibited better water stability than BDSA-based polyimide, however both membranes had similar proton conductivity value. Since ODADS has a flexible ether linkage which results in good water stability. Besides the flexibility of polymer chain, the water stability also depends on the basicity of sulfonated diamine as reported by Okamoto and coworkers. [67, 71] Okamoto and coworkers studied and classified sulfonated diamine based on their chemical structures. The sulfonated diamine monomer that has sulfonic acid located at the same amino-phenyl ring, i.e. BDSA and ODADS, have weaker basicity than other types i.e. BPABDS, BAPFDS etc. (see structure in Table 2-3) since the electron density of amino-phenyl ring is reduced by stronger electron-withdrawing sulfonic acid groups. When compared the water stability of sulfonated polyimide membrane synthesized from different sulfonated diamines, the BAPBDS-based polyimide exhibited better stability than others and the proton conductivities of NTDA-BAPBDS based polyimide membranes was comparable to Nafion 117 at lower temperature (<80°C). However, it had been reported that NTDA-BAPBDS polyimide and NTDA-BAPBDS/BAPB copolyimide showed higher proton conductivity than Nafion 117 at 50 °C under fully hydrated condition as shown in Figure 3-10.



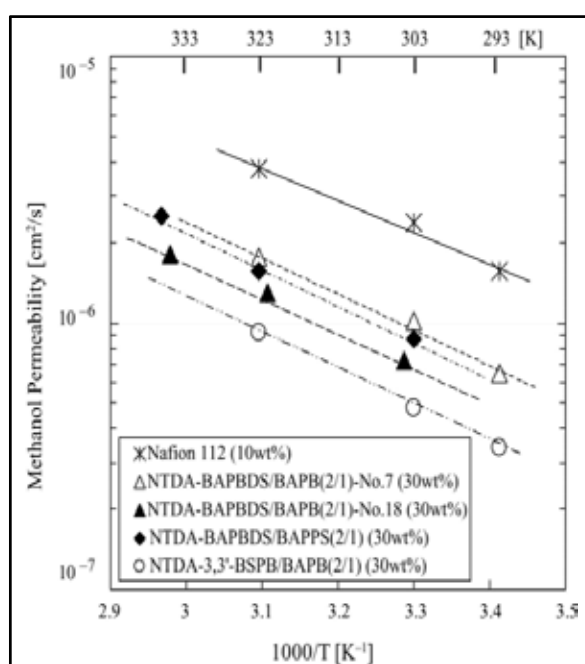
**Figure 3-10 Relative humidity dependence on proton conductivity for NTDA-BAPBDS based polyimide membrane at 50 °C [67, 71]**

NTDA-Based polyimides containing sulfoalkoxy groups have been investigated,[14, 72, 73] Okamoto and co-workers have synthesized and further studied on the NTDA-BSPB-based and NTDA-BAPBDS-based SPI membrane. Transmission electron microscopy (TEM) revealed clearly microphase-separation between hydrophilic (dark region) and hydrophobic (lighter region) domains and poor connection between hydrophilic parts of BSPB-based SPI membranes as shown in Figure 3-11. However, it was not clearly observed in BAPBDS-based SPI membranes.



**Figure 3-11 TEM Image of SPI membrane (Cross section in Ag<sup>+</sup> salt form)[71]**

Furthermore, this group has reported their proton conductivities and methanol permeability of the NTDA-based membrane series. The proton conductivities of SPI membrane were smaller than Nafion 117 at low RH whereas they were comparable to Nafion 117 at higher relative humidity (>80 %RH). The Arrhenius-type temperature dependence was found in methanol permeability measurement as shown in Figure 3-12 and SPI membrane exhibited much lower methanol permeability than Nafion 117.



**Figure 3-12 Temperature dependence of methanol permeability for SPI and Nafion 112 membranes at methanol concentration in feed (XM) of 30 or 10 wt.% respectively. [71]**

The effect of polymer microstructure on proton conductivity has been investigated.[28] The membrane prepared from SPI based on DSDSA/FDA/ODA (70/10/20) displayed higher proton conductivity than Nafion 115 at 140 °C. This was probably due to the flexibility of linear structure of ODA and the bulky structure of FDA. The bulky structure increased interchain spacing where the water could be trapped and difficult to evaporate at elevated temperature. Lee and co-workers confirmed this study by synthesis of grafted sulfonated polyimide membrane with had different alkyl chain length. The grafted SPI membrane with long side chains exhibited lower



IEC value than one with short side chains. However, the SPI grafted with long side chain displayed a large number of water molecules per  $-\text{SO}_3\text{H}$  group, which resulted in higher proton conductivity.

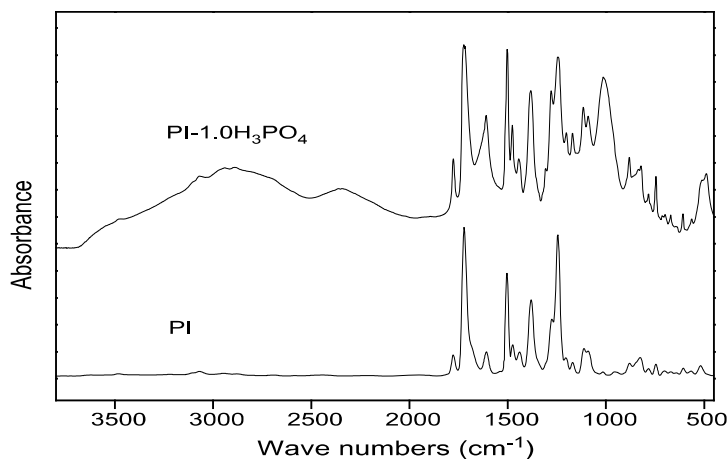
Even though many publications had reported about sulfonated polymer membrane, the optimization between sulfonation level and the basic properties such as water uptake swelling ratio and methanol permeability has been challenged, as well as maintain the proton conductivity at higher temperature or low relative humidity condition.

### **3.2.3 Phosphonated polymer membrane**

The search for alternative proton-conducting membranes, which are capable at high operating temperatures, has been widened and increased in the investigation of new alternative acidic or proton transfer groups that have the ability to facilitate proton conductivity under low-humidity conditions. These groups include the phosphonic acid and various heterocycles i.e. imidazole and benzimidazole group. Considerably, polymers carrying these groups have quite different properties than sulfonated polymers. For example, phosphonated polymers generally show a higher degree of hydrogen bonding and lower water uptake than their sulfonated moieties at comparable ion exchange capacity value. Moreover, phosphonated membrane have recently been the attractive candidates for the higher temperature PEMs due to their higher thermal stability.[12,74] Because the information of phosphonated membranes for fuel cells is less than sulfonated membrane, this section will focus on some phosphonation reactions, key characteristics of the phosphonic acid containing polymer and the possibility of phosphonated polymers for proton exchange membrane fuel cell applications.

Like as sulfonation process described earlier, the phosphonic acid was introduced to polymer chain by various methodologies; (A) post-phosphonation i.e. acid doping[75], metalation reaction [8] and chloromethylation [76] etc. and (B) direct copolymerization of phosphonated


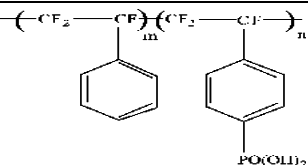

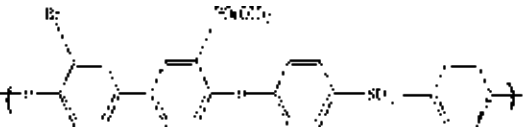

monomers. However, these methods had been less investigated especially in polyimide membranes.



**Figure 3-13 FTIR spectra of pure PI and PI-1.0H<sub>3</sub>PO<sub>4</sub> [77]**

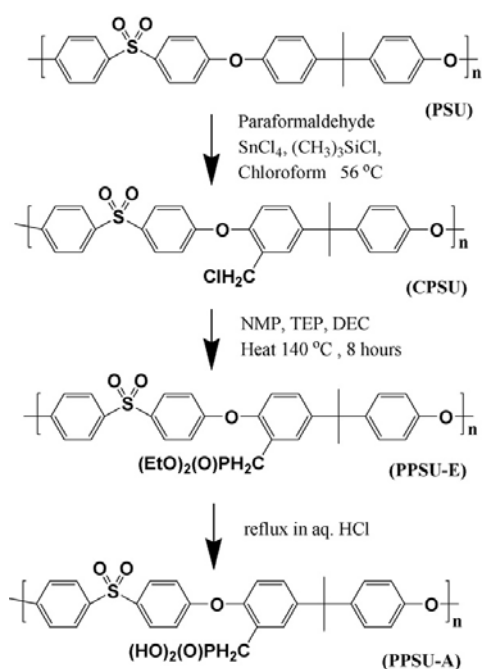
The phosphoric acid doped in polyimide solution and casted into the membrane was a basic method. The FTIR of the ODPA-DDE polyimide membranes revealed the hydrogen bonding interaction between  $\text{-OH}$  group in  $\text{H}_3\text{PO}_4$  and  $\text{-C=O}$  group in polyimide chain as shown in Figure 3-13. It was reported that the hydrogen bond played a major role on proton transportation in this system, which was different from proton exchange between Bronsted acid ( $\text{H}_2\text{PO}_4^-$ ) and a Bronsted base ( $\text{HPO}_4^{2-}$ ). [75] In addition, the temperature dependence of methanol permeability was found in this PI- $x\text{H}_3\text{PO}_4$  membrane system ( $E_a \approx 10.9\text{-}17.7$  kJ/mol), however, they were less sensitive to temperature than Nafion membranes ( $E_a \approx 18.0$  kJ/mol). Parcero and co-workers gathered all effective reactions that applied for introduction of phosphonic acid to monomers or polymer chains as summarized in Table 3-4. [74]

**Table 3-4 Summary of effective reactions for synthesis of phosphonated polymers**

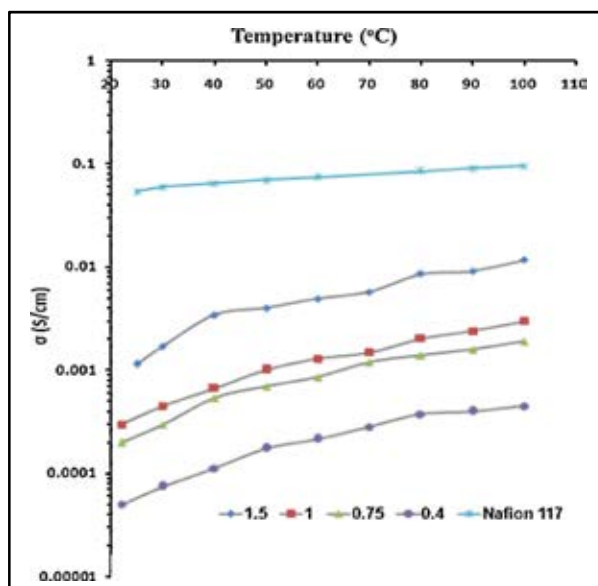
Polymer	Reaction or Reactant	Reference
	Michaelis–Arbuzov	M. Sander (1968) [78]
$\left( \text{CF}_2\text{CF}_2 \right)_m \left( \text{CF}_2\text{CF} \left( \text{O}(\text{CF}_2)_3\text{P}(\text{O})(\text{OEt})_2 \right) \right)_n$	Copolymerization of phosphonated fluorinated vinyl ethers	S.V.Kotov (1997) [5]
	Polymerization of phosphonated vinylstyrene	C.Stone (2000) [79] and R. Souzy (2005) [80]
	Michaelis–Arbuzov	S. Yanagimachi (2003) [81]
	Pd catalyst/HP(O)(OEt) <sub>2</sub>	K. Jakoby (2003) [82, 83]
	BuLi/CIP(O)(OEt) <sub>2</sub>	B.Laffite (2005) [8]

It was reported that for phosphonation of polyphenylsulfone, the method like a Michaelis-Arbuzov reaction was an ineffective whereas an effective one was a system with presence of Pd catalyst, which yielded 90% phosphonation level of polyphenylsulfone.

[82,83] Laffite and his co-workers proposed a non-catalytic route for phosphonation of polysulfone. By direct lithiation of polysulfone with diphenyl or diethyl chlorophosphate, the biphenyl sulfone segment was functionalized. While the lithiation lead by the bromination can achieve the phosphonation of the bisphenol A segment in polymer chain. The polysulfone with up to 50% phosphonation level was obtained from this procedure and the prepared membrane reached proton conductivity of 0.005 S/cm at 100°C.[8] The high content of phosphonic acid containing polysulfone are synthesized by the development of post-phosphonation method via chloromethylation followed by Michaelis-Arbuzov reaction as shown in Scheme 3-4. By this method, the obtained polysulfone had phosphonation level up to 150% per repeating unit, which resulted that their membrane had higher water uptake (52%) than other phosphonate polymer membrane, and reached the maximum proton conductivity of 0.012 S/cm at 100°C under fully hydrated condition. [76] However, it was about 8 times lower than Nafion 117 as shown in Figure 3-14.

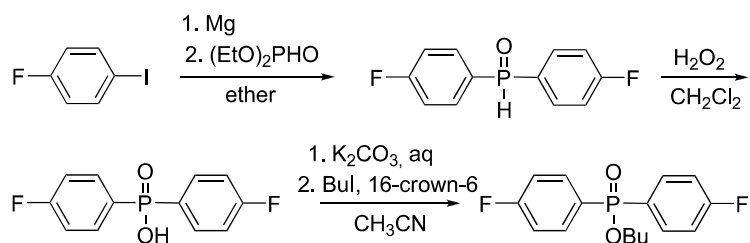


**Scheme 3-4 Phosphonation of polysulfone via combination of chloromethylation and Michaelis-Arbuzov reaction [76]**



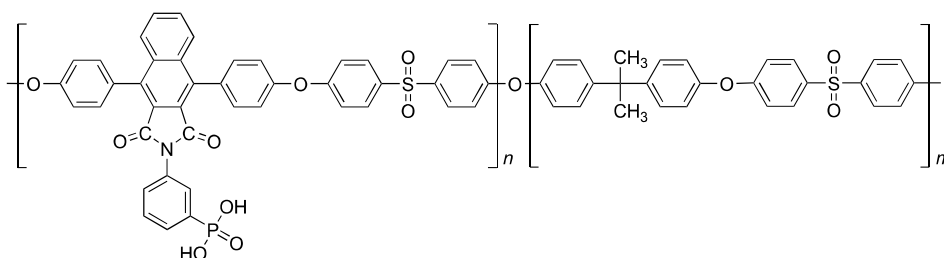
**Figure 3-14** The proton conductivity data of phosphonated polydulfone membrane with various degree of phosphonation and Nafion 117 under 100%RH [76]

The polycondensation of phosphonic acid containing monomers was an alternative way to produce the phosphonated polymer materials. In general, only few articles can be found. Miyatake and co-workers functionalized the monomer as described in scheme 3-5 and prepared the phosphonic acid containing polymers and copolymers from obtained monomers and bisphenol A.



**Scheme 3-5** Functionalization of difluoro monomers [14]

Poly(arylene ethers) containing phosphonic acid groups were prepared from the bis-phenol (mixed with bis-phenol A) and 4,4'-difluorodiphenyl sulfone and their structure was shown in Figure 3-15.



**Figure 3-15 Structure of BPA-based Poly(arylene ethers) containing phosphonic acid groups [9, 37]**

The proton conductivity of phosphonated BPA-based poly(arylene ethers) was determined about  $2.96 \times 10^{-5}$  S/cm which magnitude lower than Nafion. Surprisingly, when the phosphonic acid moiety was larger than 50%, the proton conductivity were not changed or increased.

From the literature reviews, the sulfonated polyimide has been reported on some limitations especially in the optimization between the sulfonation level and water stability or swelling problem. Furthermore, most of polymer membranes have started to lose water above 100°C. These initiated the idea to study the new proton transfer sites like phosphonic acid group due to its high thermal stability. In addition, it was reported that phosphonic acid could keep more water than sulfonic acid [84,85] therefore phosphonic acid containing polymer membrane was expected to retain water and able to transport proton at higher temperature. This motivation leads to synthesis of new phosphonated polyimide, which shows possible application as proton exchange membrane in  $H_2/O_2$  or direct methanol fuel cells, and their basic properties will be discussed in the chapter 5.

## CHAPTER IV

### EXPERIMENTS

#### 4.1 MATERIALS

The starting materials that used in this study are listed as following;

- Aniline (Acros Organics)
- n-Butyllithium (1.6 M in Hexane) (Acros Organics)
- Bromine (Br<sub>2</sub>) (Acros Organics)
- Bromotrimethylsilane (TMSBr) (Acros Organics)
- 3,3'-diaminobenzidine (Acros Organics)
- 4,4'-diaminodiphenylether (4,4'-ODA) (Acros Organics)
- Diethyl-chlorophosphate (DECP) (Acros Organics)
- Hydrochloric acid (HCl) (Acros Organics)
- 1,4,5,8-naphthalenetetracarboxylic dianhydride (NTDA) (Sigma-Aldrich)
- Sodium Chloride (NaCl) (Acros Organics)
- Sodium Hydroxide (NaOH) (Acros Organics)
- Triethylamine (Et<sub>3</sub>N) (Acros Organics)
- Acetone (Fisher Scientific)
- Chloroform (Fisher Scientific)
- *m*-cresol (Sigma-Aldrich)
- *N,N'*-Dimethylacetamide (DMAC) (Merck)
- *N,N'*-Dimethylformamide (DMF) (Merck)
- Dimethyl sulfoxide (DMSO) (Merck)
- Methanol (Fisher Scientific)
- *N*-Methyl-2-pyrrolidone (NMP) (Merck)

- 2-Propanol (Acros Organics)
- Tetrahydrofuran (THF) (Acros Organics)
- 40 wt% Pt/C catalyst (Alfa Aesar)
- Nafion™ solution (Alfa Aesar)
- Segracet® Graphite sheet (Ion power)

Most of reagents were used as received except some solvents such as m-cresol and tetrahydrofuran (THF), which were purified before use. The m-cresol was pre-dried over magnesium sulfate (MgSO<sub>4</sub>) and distilled under vacuum to remove all stabilizers and impurities, and tetrahydrofuran (THF) was pre-dried over calcium hydride and distilled under inert gas.

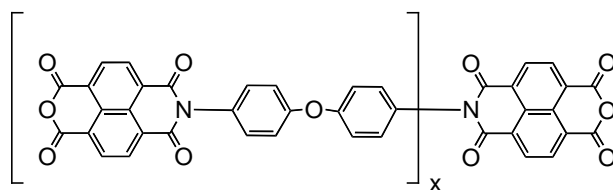
## 4.2 SYNTHESIS METHOD

In this work, the main chain and side chain polyimide were prepared separately and then both polyimide parts were connected together under basic condition and elevated temperature to produce graft copolyimide. The synthesis method in each step will be described as follows;

### 4.2.1 Synthesis of the NTDA -4,4'-ODA-based polyimide main-chain

To a 250 mL three-neck flask, equipped with a Dean-Stark trap and a N<sub>2</sub> inlet and outlet, 6.01 g (30 mmol) of 4,4'-ODA and 100 mL of m-cresol were added. After the 4,4'-ODA completely dissolved, 8.15 g (30.4 mmol) of NTDA, and 1.46 g (14.4 mmol) of triethylamine were added and then stirred at 80°C for 4 h, then at 180°C for 16 h and finally at 200°C for 4 h. The 50 mL of toluene was added during the thermal imidization step. When the reaction was complete, the reaction mixture was precipitated with 2-propanol, filtered, washed with acetone and dried at 80°C in a vacuum oven overnight (13.10 g, 92% yield). The polyimide product was here denoted after as "PI" and its structure was shown in Figure 4-1.



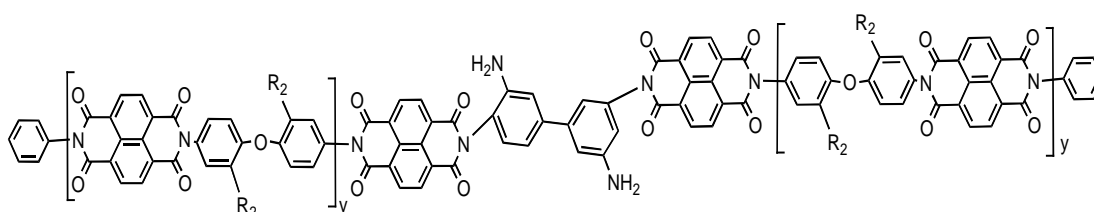


**Figure 4-1 Structure of NTDA-4,4'-ODA-based polyimide – main chain (PI)**

where  $x$  is number of repeating unit.

#### 4.2.2 Synthesis of the phosphonated polyimides side-chain

The target structure of phosphonated polyimide side-chain was shown in Figure 4-2 and this side chain was named as “paPI”



**Figure 4-2 Structure of phosphonated polyimide side-chain (paPI)**

where  $y$  is number of repeating unit and  $R_2$  is  $P=O(OH)_2$  unit.

In this step, we studied the two different methods to produce phosphonic acid containing polyimide or “paPI” by using post-phosphonation method (named as “method A”) and direct copolymerization of phosphonated monomer method (named as “method B”). Since there are many reaction steps and intermediate products in this synthesis part, all intermediates were simply denoted as;

- S-A-Series will be used for all intermediate that obtained from post-phosphonation method.
- S-B-Series will be used for all intermediate that obtained from direct copolymerization of phosphonated monomer method.

However, the final product that obtained from both methods was expected to have the same structure as shown in Figure 4-2.

#### 4.2.2.1 Method A – Post-phosphonation method

- Step 1 :Synthesis of intermediate-polyimide 1 (S-A1)

The first step was a polycondensation reaction. To a 125 mL three-neck flask, equipped with a dean stark trap and a N<sub>2</sub> inlet and outlet, 2 g (10 mmol) of 4,4'-ODA and 30 mL of m-cresol were added. After the 4,4'-ODA had completely dissolved, 2.79 g (10.4 mmol) of NTDA, and 0.88 g (8.6 mol) of triethylamine were added and the solution was stirred at 80°C for 2 h. Then 0.02 g (0.2 mmol) of aniline was added and the solution was stirred for another 2 h. The polymer was imidized at high temperature by heating the reaction mixture to 180°C for 16 h and then 200°C for 4 h. The 30 ml of toluene was added during the thermal imidization step. When the reaction was complete, the polymer was precipitated with 2-propanol (100 mL), filtered, washed with acetone and dried overnight at 80°C in a vacuum oven. The polyimide product (S-A1) was a brown powder (4.53 g, 95% yield) and its structure was shown in Figure 4-3 (A).

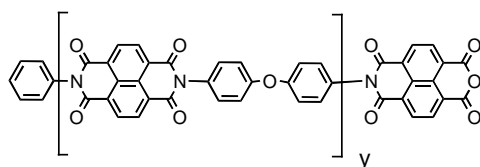
- Step 2 : Synthesis of intermediate-polyimide 2 (S-A2)

S-A1 chains were extended by using 3, 3'-diaminobenzidine, which had 4 reactive amine groups to selectively react with the one group of anhydride end-group of the S-A1, to produce S-A2 (Figure 4-3 (B)). The aniline provided the amine non-functional end-group to the S-B1, so that only a dimer needed to be formed. A stoichiometric molar ratio of 3,3'-diaminobenzidine to S-A1 and the steric hindrance of S-A1 would restrict the reaction to occur at only 2 amine groups of the 3,3'-diaminobenzidine. To a 100 mL three-neck flask, equipped with a N<sub>2</sub> inlet and outlet, 0.04 g (0.18 mmol) 3,3'-diaminobenzidine and 5 mL of m-cresol were added. After the diaminobenzidine was completely dissolved, 2 g (0.36 mmol) of S-A1 in 25 mL m-cresol was slowly dropped to solution and stirred at 150°C for 6 h. When the reaction was completed, the

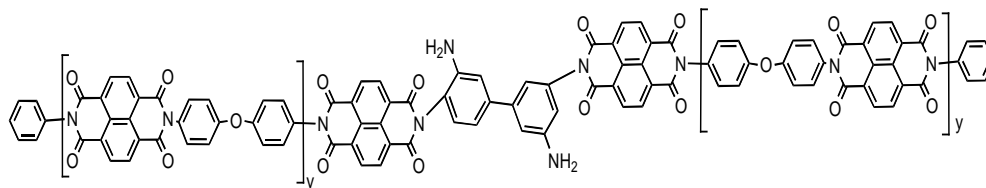
product (S-A2) was precipitated with 2-propanol (100 mL), filtered, washed with acetone and dried overnight at 80°C in a vacuum oven. S-B2 was a dark brown powder (1.53 g, 75% yield).

- Step 3 : Synthesis of intermediate-polyimide 3 (S-A3)

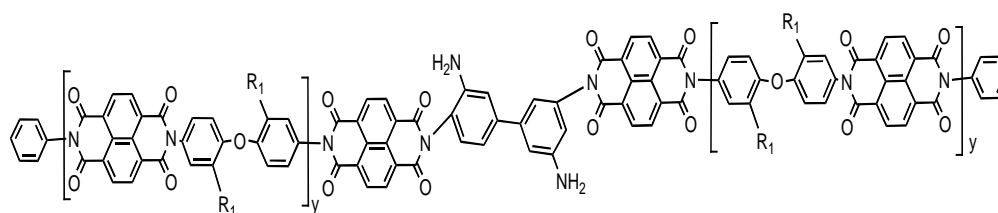
S-A2 was phosphonated by using a 100 mL three-neck flask, equipped with a N<sub>2</sub> inlet and outlet. The 1% of suspended S-A2 (1 g, 8.824 μmol) in THF was cooled to -78°C using a dry ice/2-propanol mixture. Excess amount of n-BuLi was slowly added and stirred for 30 min. Then, a 200% molar of excess amount of diethylchlorophosphate was quickly added and stirred for 3 h. The reaction was terminated with 2 mL of 2-propanol and the product (S-A3) was precipitated in 2-propanol (100 mL), filtered, washed with acetone and dried overnight at 80°C in a vacuum oven (0.67 g, 67% yield). The expected structure of S-A3 was presented in **Figure 4-3 (C)**, but the desired product cannot be obtained. *Consequently, it can be summarized that the phosphonated polyimide cannot be prepared via post-phosphonation method even though all reagent concentration and reaction time were adjusted.*



intermediated-polyimide 1 (S-A1)

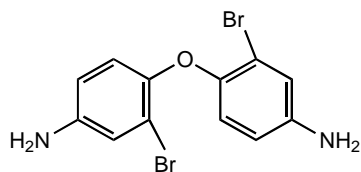


intermediated-polyimide 2 (S-A2)

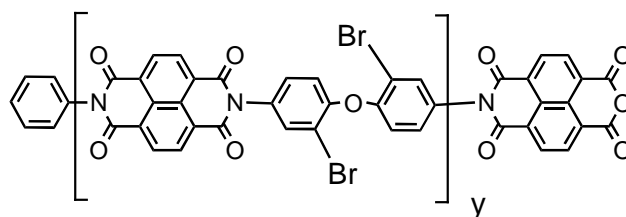


intermediated-polyimide 3 (S-A3) –No desired product

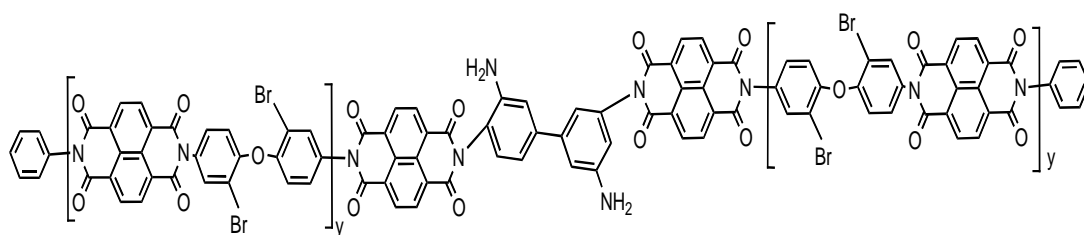
**Figure 4-3 Structure of all intermediated product that obtained from method A where  $y$  is repeating unit and  $R_1$  represents  $-P=O(OEt)_2$**



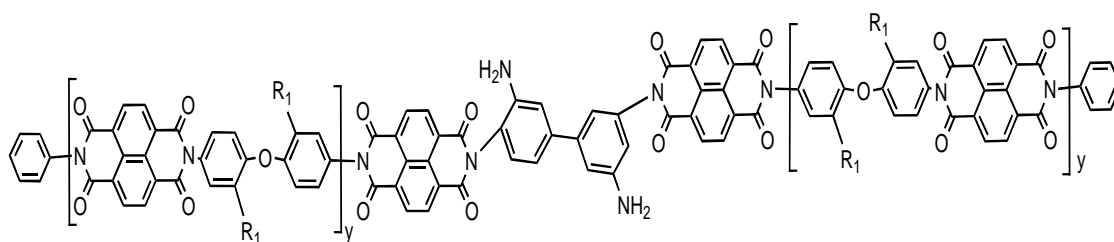
2,2'-dibromo-4,4'-diaminodiphenyl ether monomer



intermediated-polyimide 1 (S-B1)



intermediated-polyimide 2 (S-B2)



intermediated-polyimide 3 (S-B3)

**Figure 4-4 Structure of all intermediated product that obtained from method B**

where  $y$  is repeating unit and  $R_1$  represents  $-P=O(OEt)_2$

#### 4.2.2.2 Method B – Direct copolymerization of phosphonated monomer

- **Step 1 : Synthesis of 2,2'-dibromo-4,4'diaminodiphenyl ether monomer**

The 2,2'-dibromo-4,4'-diaminodiphenyl ether monomer (See Figure 4-4 (A)) was prepared via bromination of 4,4'-diaminodiphenyl ether (4,4'-ODA). This bromination method was modified from the procedure reported and Teclechiel and co-workers. [86] Bromine (10 mL, 0.2 mol) was added to 4,4'-diaminodiphenyl ether (10 g, 0.05 mol) in glacial acetic acid (250 mL) at room temperature. The reaction solution was stirred at 35°C for 5 min and then poured into cold water (1000 mL). The precipitated product was recovered by filtration and purified by Soxhlet extraction with an n-hexane/ethyl acetate (6:1) mixture. The product was dried in a vacuum oven overnight (8.5 g, 85% yield).

- **Step 2 : Synthesis of intermediate-polyimide 1 (S-B1)**

The second step was a polycondensation reaction. To a 125 mL three-neck flask, equipped with a dean stark trap and a N<sub>2</sub> inlet and outlet, 2 g (10 mmol) of 2,2'-dibromo-4,4'-diaminodiphenyl ether (from step 1 of method B) and 30 mL of m-cresol were added. After the 2,2'-dibromo-4,4'-diaminodiphenyl ether had completely dissolved, 2.79 g (10.4 mmol) of NTDA, and 0.88 g (8.6 mol) of triethylamine were added and the solution was stirred at 80°C for 2 h. Then 0.02 g (0.2 mmol) of aniline was added and the solution was stirred for another 2 h. The polymer was imidized at high temperature by heating the reaction mixture to 180°C for 16 h and then 200°C for 4 h. The 30 ml of toluene was added during the thermal imidization step. When the reaction was complete, the polymer was precipitated with 2-propanol (100 mL), filtered, washed with acetone and dried overnight at 80°C in a vacuum oven. The polyimide product (S-B1) was a brown powder (4.53 g, 95% yield) and its structure was shown in Figure 4-4 (B).

- **Step 3 : Synthesis of intermediate-polyimide 2 (S-B2)**

S-B1 chains were extended by using 3, 3'-diaminobenzidine, which has 4 reactive amine groups to selectively react with the one group of anhydride end-group of the S-B1, to produce S-B2 (Figure 4-4 (C)). The aniline provided the amine non-functional end-group to the S-B1, so that only a dimer needed to be formed. A stoichiometric molar ratio of 3,3'-diaminobenzidine to S-B1 and the steric hindrance of S-B1 would restrict the reaction to occur at only 2 amine groups of the 3,3'-diaminobenzidine. To a 100 mL three-neck flask, equipped with a N<sub>2</sub> inlet and outlet, 0.04 g (0.18 mmol) 3,3'-diaminobenzidine and 5 mL of m-cresol were added. After the diaminobenzidine was completely dissolved, 2 g (0.36 mmol) of S-B1 in 25 mL m-cresol was slowly dropped and stirred at 150°C for 6 h. When the reaction was completed, the product (S-B2) was precipitated with 2-propanol (100 mL), filtered, washed with acetone and dried overnight at 80°C in a vacuum oven. S-B2 was a dark brown powder (1.53 g, 75% yield).

- **Step 4 : Synthesis of intermediate-polyimide 3 (S-B3)**

S-B2 was phosphonated by using a 100 mL three-neck flask, equipped with a N<sub>2</sub> inlet and outlet. The 1% solution of S-B2 (1 g, 8.824 μmol) in THF was cooled to -78°C using a dry ice/2-propanol mixture. Desired amount of n-BuLi was slowly added and stirred for 30 min. Lithiations were expected to occur primarily at the brominated sites located on ortho positions to the ether linkages, because halogen-lithium exchange is favored over proton-lithium exchange at low temperature. Then, a 200% molar of excess amount of diethylchlorophosphate was quickly added and stirred for 3 h. The reaction was terminated with 2 mL of 2-propanol and the product (S-B3) was precipitated in 2-propanol (100 mL), filtered, washed with acetone and dried overnight at 80°C in a vacuum oven (0.67 g, 67% yield). The structure of S-B3 was presented in Figure 4-4 (D).

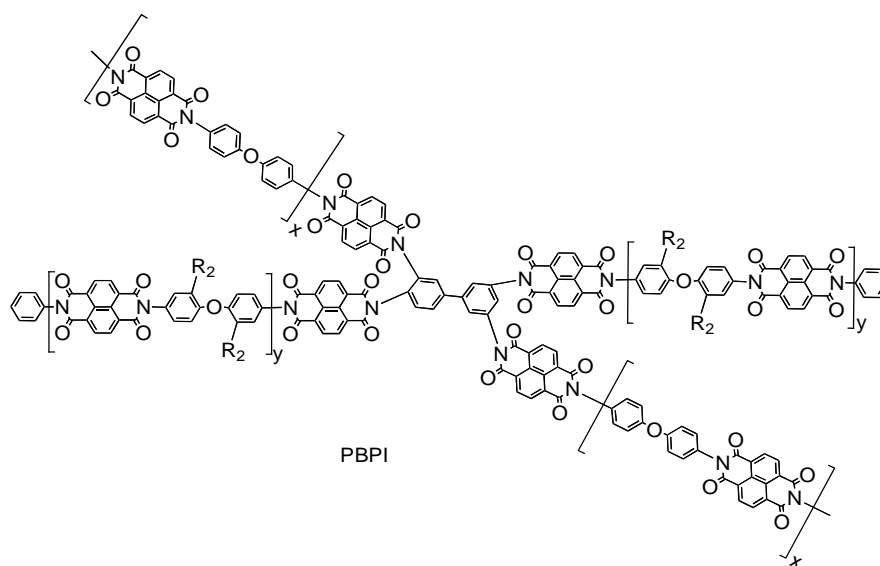
- **Step 5: Synthesis of phosphonated polyimide (final product)**

The S-B3 was converted to the phosphonic acid derivative by suspending it in THF (1 g/20 mL), adding a 5% excess of bromotrimethylsilane and then mixing the solution at room temperature for 24 h. The reaction mixture was then added to a 50% HCl solution in deionized (DI) water and stirred for 24 h. The hydrolyzed polyimide (S-B4) was then filtered, washed with DI water and dried at 50°C in a vacuum oven overnight. The structure of final product (paPI) was presented in Figure 4-2 as mention earlier.

#### 4.2.3 Synthesis of the phosphonated graft copolyimide

To a 250 mL three-neck flask, equipped with a N<sub>2</sub> inlet and outlet was added an equimolar amount of **PI** solution (main-chain) and **paPI** solution (side-chain) in m-cresol and stirred at 150°C for 12 h. with the addition of 15 mL of m-cresol to dilute the viscous solution. The reactions between the two polymers occurred at the two amines that remained after the chain extension reaction of S-B1. When the reactions were complete, the product was precipitated with 2-propanol (100 mL), filtered, washed with acetone and dried overnight at 80°C in a vacuum oven. The resulting branched, phosphonated graft copolyimides, denoted as PBPI, were a dark brown powder with the structure shown in Figure 4-5 .





**Figure 4-5 Structure of phosphonated graft copolyimide (PBPI)**

where  $x, y$  is repeating unit in main-chain and side-chain respectively

and  $R_2$  represents  $-P=O(OH)_2$

The phosphonated graft copolyimide with various phosphonation level and side chain length were prepared by varying the amount of phosphonic acid unit and degree of polymerization of paPI. The differences in the amount of phosphonic acid and side chain lengths of paPI-C were shown in Table 4-1. Consequently, PBPI-1, PBPI-2, PBPI-3, PBPI-4 and PBPI-5 were obtained from paPI-1, paPI-2, paPI-3, paPI-4 and paPI-5 respectively.

**Table 4-1 The degree of polymerization (DP) and % phosphonation of phosphonate polyimide; paPI samples**

Polymer	Degree of polymerization (DP)	% phosphonation
paPI-1	49	30
paPI-2	99	42
paPI-3	199	55
paPI-4	99	30

### 4.3 FILM PREPARATION

The blends of PBPI and pure polyimide based on NTDA-ODA with 4:1 w/w was completely dissolved in *m*-cresol at 120°C and casted in the clean petri-dishes, and then dried in oven at 80°C until the films completely dried, yield the fPBPI membranes. Then the films were peeled from petri dishes by immersing in clean water, the average of 160-180 μm thickness films were obtained and dried in over at 60°C overnight.

Then, the film surface was hot-pressed at 60°C for 3-5 min to smooth the films with Carver compression press (Institute of polymer science and polymer engineering in University of Akron, USA) before use in MEA fabrication step.



Figure 4-6 Carver compression press

## 4.4 CHARACTERIZATION AND PROPERTIES

### 4.4.1 Fourier Transform Infrared

All functional groups in polyimide structure were investigated by using Fourier transform infrared spectroscopy. The spectra were obtained with a Nicolet 380 FT/IR

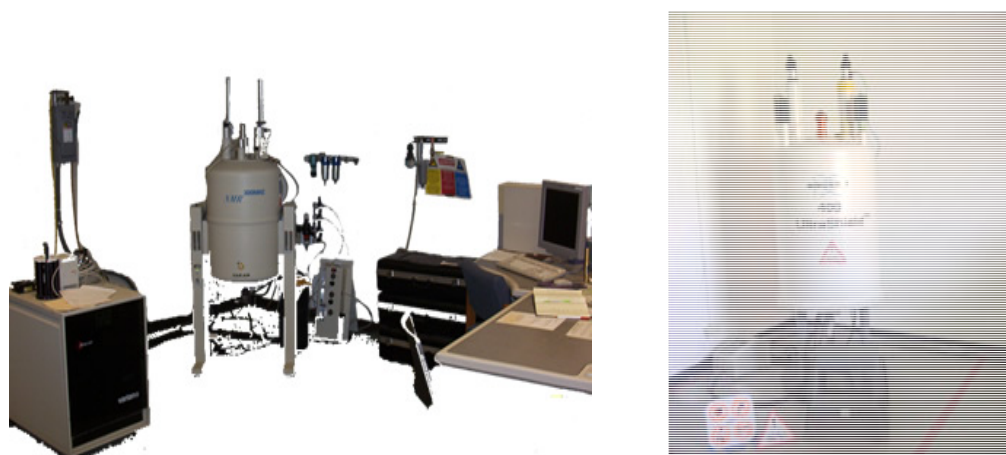
Spectrophotometer using the attenuated total reflectance (ATR) mode and the scanning a spectral range of  $400\text{-}4000\text{ cm}^{-1}$ .



**Figure 4-7 Nicolet 380 Fourier transform infrared**

#### 4.4.2 Nuclear Magnetic Resonance

The polymer structures were determined by using Nuclear magnetic resonance techniques. The  $^1\text{H}$ -NMR and  $^{31}\text{P}$ -NMR spectra were recorded by Varion Mercury-300 spectrometers (300 MHz) and Bruker Biospin DPX400 spectrometers (400 MHz). The NMR deuterated solvents such as deuterated dimethylsulfoxide ( $\text{DMSO-d}_6$ ) and chloroform ( $\text{CDCl}_3$ ) were used as reference. The presence of phosphonic acid was confirmed by  $^{31}\text{P}$ -NMR and % phosphonation was calculated from  $^1\text{H}$ -NMR.



(A) Varion Mercury-300 spectrometers

(B) Bruker Biospin DPX400  
spectrometers**Figure 4-8 Nuclear Magnetic Resonance Spectrometers****4.4.3 Thermal properties**

The thermal properties of all polyimide samples were measured by using Thermogravimetric analyzer (TA Instruments, TGA 2950) and Differential scanning calorimetry (TA Instruments, DSC 2920). For TGA, the polymer samples were measured at a temperature range of 30–800°C under a nitrogen atmosphere with heating rate of 20°C/min to investigate degradation temperature ( $T_d$ ). For DSC, the polymer were measured at a temperature range of 50–400°C under a nitrogen atmosphere with various heating rate, starting from 10°C/min to 50°C/min to investigate the glass transition temperature ( $T_g$ ). All samples were dried in a vacuum oven at 80°C for 24 h before the measurement.



**Thermogravimetric analyzer**  
(TA Instruments, TGA 2950)



**Differential scanning calorimetry**  
(TA Instruments, DSC 2920)

**4.4.4 Solubility**

The solubility of all polyimide samples was tested qualitatively by using 10 mg sample in 1 mL of various organic solvents such as *m*-cresol, NMP, DMSO, DMAC, DMF, Chloroform and

Acetone. The solubility test was performed at room temperature and elevated temperature (depending on boiling point of solvents).

#### 4.4.5 Intrinsic Viscosity

Intrinsic viscosity measurements were conducted with a Ubbelohde viscometer at 45°C in m-cresol

#### 4.4.6 Ion exchange capacity measurement

Ion exchange capacity (IEC) of the phosphonated polymers is determined by back-titration. The hydrolyzed polymer in the acid form was dried under vacuum at 60°C overnight, and then a known mass of polymer was neutralized to the sodium salt by soaking it in a saturated aqueous sodium chloride solution overnight. The neutralization reaction produces  $H_3O^+$ , and the exchanged solution was then back titrated with a 0.001 N NaOH using phenolphthalein as an indicator. The IEC was calculated from Eq. 4-1 and reported as the average value from measurements of three samples.

$$IEC \text{ (meq/g)} = \frac{V_{NaOH} \times N_{NaOH}}{M_{polymer}} \quad \text{Equation 4-1}$$

where  $V_{NaOH}$  and  $N_{NaOH}$  are the volume and normality of the NaOH solution and  $m_{polymer}$  is the mass of polymer used.

#### 4.4.7 Water Uptake and Swelling Ratio

Water uptake of the fully hydrated membrane samples was measured by immersing membrane samples (about 100 mg) into water at room temperature for 3–5 h, and then the samples were taken out, wiped with tissue paper swiftly, and weighed them. Water uptake (WU) of the film was calculated from Eq. 4-2:

$$WU = \frac{(W_s - W_d)}{W_d} \times 100\% \quad \text{Equation 4-2}$$

Where  $W_d$  and  $W_s$  are the weights of dry and corresponding water-swollen samples, respectively. The swelling of membranes were measured by the thickness changes, which was characterized by the following Eq. 4-3.

$$t_c = \frac{(t-t_s)}{t_s} \times 100\% \quad \text{Equation 4-3}$$

Where  $t_s$  is the thickness of dry membrane;  $t$  refers to thickness of the swollen membrane in water.

#### 4.4.8 Methanol Permeability

Methanol permeability measurement was carried out using a diffusion cell. Initially one compartment B of the cell was filled with only deionized water. The other compartment A was filled with 15 wt.% methanol solution in deionized water. The membrane that had the diffusion area of  $4 \text{ cm}^2$  was sandwiched by O-ring shaped Teflon on purpose of sealing and clamped between the two compartments tightly. This diffusion cell was kept stirring slowly during experiment. Methanol concentration in compartment A was kept unchanged by feeding from a reservoir filled with 15 wt.% of methanol solution. The concentration of methanol diffused from compartment A to B across the membrane was sampling every 10 min for 5 hours. The diffused methanol in sampling solution was detected using refractive index detector.

#### 4.4.9 Proton conductivity

Proton conductivity was measured using a galvanostatic four-point-probe ac Electrochemical impedance spectroscopy (EIS) technique, a conductivity cell was made up of two platinum wires carrying the current and two platinum wires sensing the potential drop, which was apart 1 cm. The fully hydrated membrane with deionized water during 24 h was cut in 1 cm wide, 4 cm long prior to mounting on the cell. After mounting sample onto two platinum foils on the lower compartment, upper compartment was covered, and then four bolts and nuts clamped the upper and lower compartment tightly. The impedance analyzer (PGSTAT, Autolab) was worked

in galvanostatic mode with ac current amplitude of 0.01 mA over frequency range from 8 MHz to 10 MHz by Nyquist method.

The conductance of the sample was obtained from the alternating-current potential difference between the two inner electrodes. The conductivity was calculated with the following equation:

$$\sigma = l/RS \quad \text{Equation 4-4}$$

Where  $\sigma$  is the proton conductivity (S/cm), R is the bulk resistance of the membrane, S is the cross-sectional area of the membrane (cm<sup>2</sup>), and l is the distance between the counter electrode and the working electrode (cm).



**Figure 4-9 PGSTAT, Autolab**

#### **4.5 Fabrication of membrane electrode assembly (MEA) and measurements of Fuel cell performance**

##### **4.5.1 Preparation of Pt/C catalyst /Nafion™ solution (Electrode solution)**

The electrode solution was prepared as following steps; Small amount of water was added to 0.5 g of the 40% (w/w) Pt/C catalyst until catalyst surface was wet to prevent the catalytic oxidation reaction of methanol. The 6-7 ml of methanol was slowly and carefully

dropped into catalyst since the combustion reaction possibly occurred in this step. The suspended Pt/C catalyst solution was sonicated for 45 min and then 2-3 drop of Nafion solution was added and sonicated again for 45-60 min.

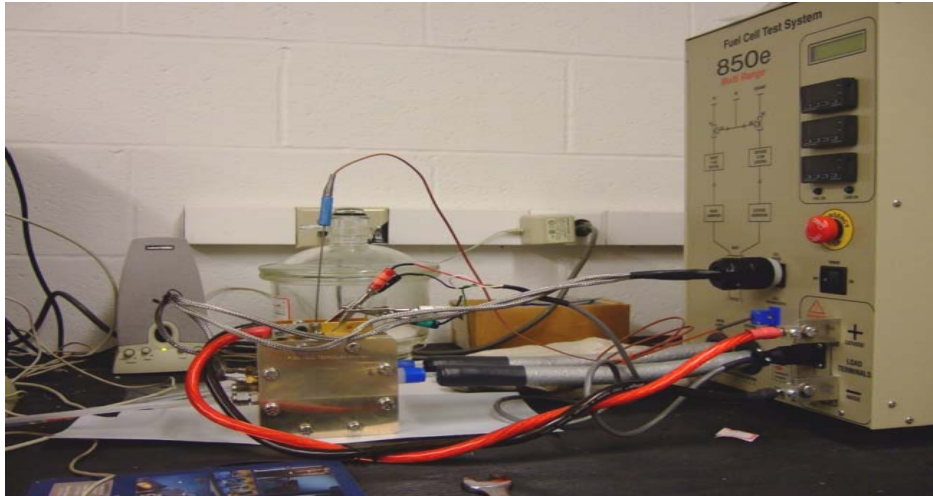
#### **4.5.2 Preparation of Membrane electrode assemblies (MEAs)**

Membrane electrode assemblies (MEAs) were prepared as follows; a 40%(w/w) Pt/C catalyst/Nafion™ solution from Alfa Aersa was used for preparation of the electrodes and graphite media (Sigracet®) from Ion Power were used for the gas-diffusion layers. The Pt/C catalyst concentration at the anode and cathode were 0.4 and 0.2 mg Pt/cm<sup>2</sup>, respectively. The two 5 cm<sup>2</sup> catalysts were air-brushed and then hot-pressed onto the membrane by compression press at 120°C, 1000 psi for 10 s.

#### **4.5.3 Measurement of proton conductivity**

The MEA was kept to controlled condition in a humidifier for 24 h at room temperature and then the proton conductivities were determined with a Scribner 850e Fuel Cell Station. The 0.2 L/min of H<sub>2</sub> and air were fed to anode and cathode respectively. Due to short ohmic period in polarization curve of phosphonated membrane samples, the constant current at 0.2 A was applied for all membrane samples including Nafion®117. The Impedance spectra were recorded at 10<sup>-1</sup> to 10<sup>4</sup> Hz in the range between 40 and 100°C and at desired humidity (33%, 54%, 74% and 100% RH). The proton conductivity was defined as the ratio of thickness to resistance, which determined from the complex plane or Nyquist plot, and reported in units of S/cm.





**Figure 4-10 Scribner 850e Fuel Cell Station**

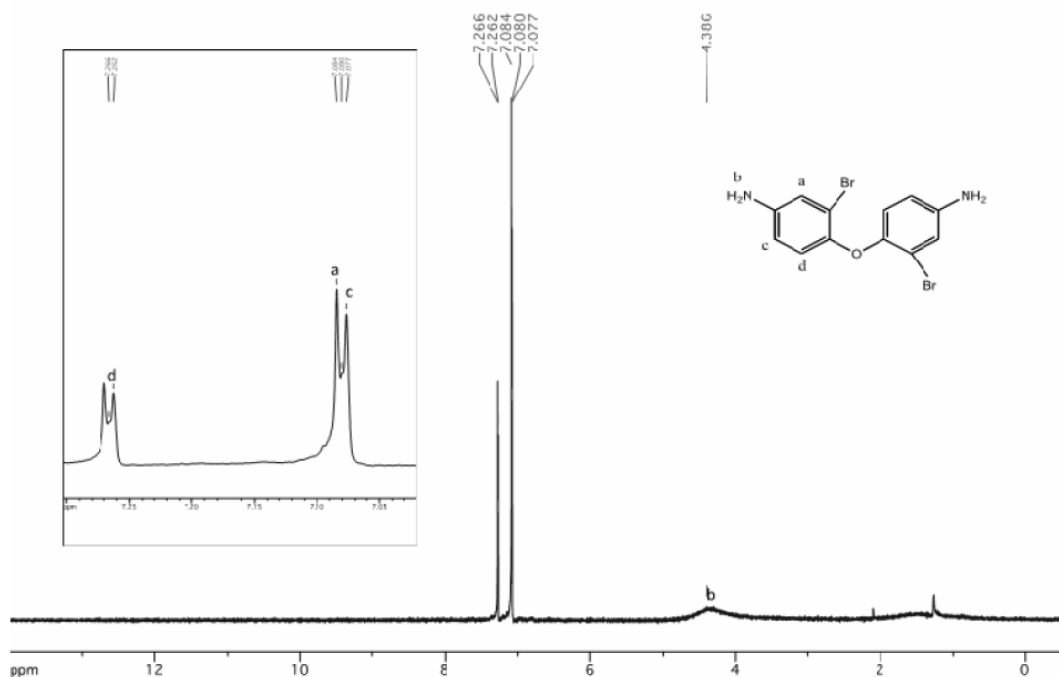
## CHAPTER V

### RESULTS AND DISCUSSION

This chapter will discuss on all experimental results starting from characterization of synthesized polyimide series throughout general properties and especially, investigated and compare various phosphonated graft copolyimide films' properties i.e. ion exchange capacity, water uptake and proton conductivity etc.

#### 5.1 THE CHARACTERIZATION RESULT OF 2,2'-DIBROMO-4,4'-DIAMINO-PHENYL ETHER MONOMER

The 2,2'-dibromo-4,4'-diaminophenyl ether monomer was prepared by direct bromination of 4,4'-diaminophenyl ether in the polar solvent such as glacial acetic acid. The structure of this monomer was investigated by <sup>1</sup>H-NMR technique. There were four different protons which presented at chemical shift of  $\delta = 7.264$  (d, 1.2 Hz, 2H) ppm, 7.082 (d, 1.2 Hz, 2H) ppm, 7.077 (s, 1H), 4.38 (s, 4H) ppm and its spectrum was shown in Figure 5-1.



**Figure 5-1** The  $^1\text{H-NMR}$  spectrum of 2,2'-dibromo-4,4'-diaminophenyl ether in  $\text{CDCl}_3$  solvent

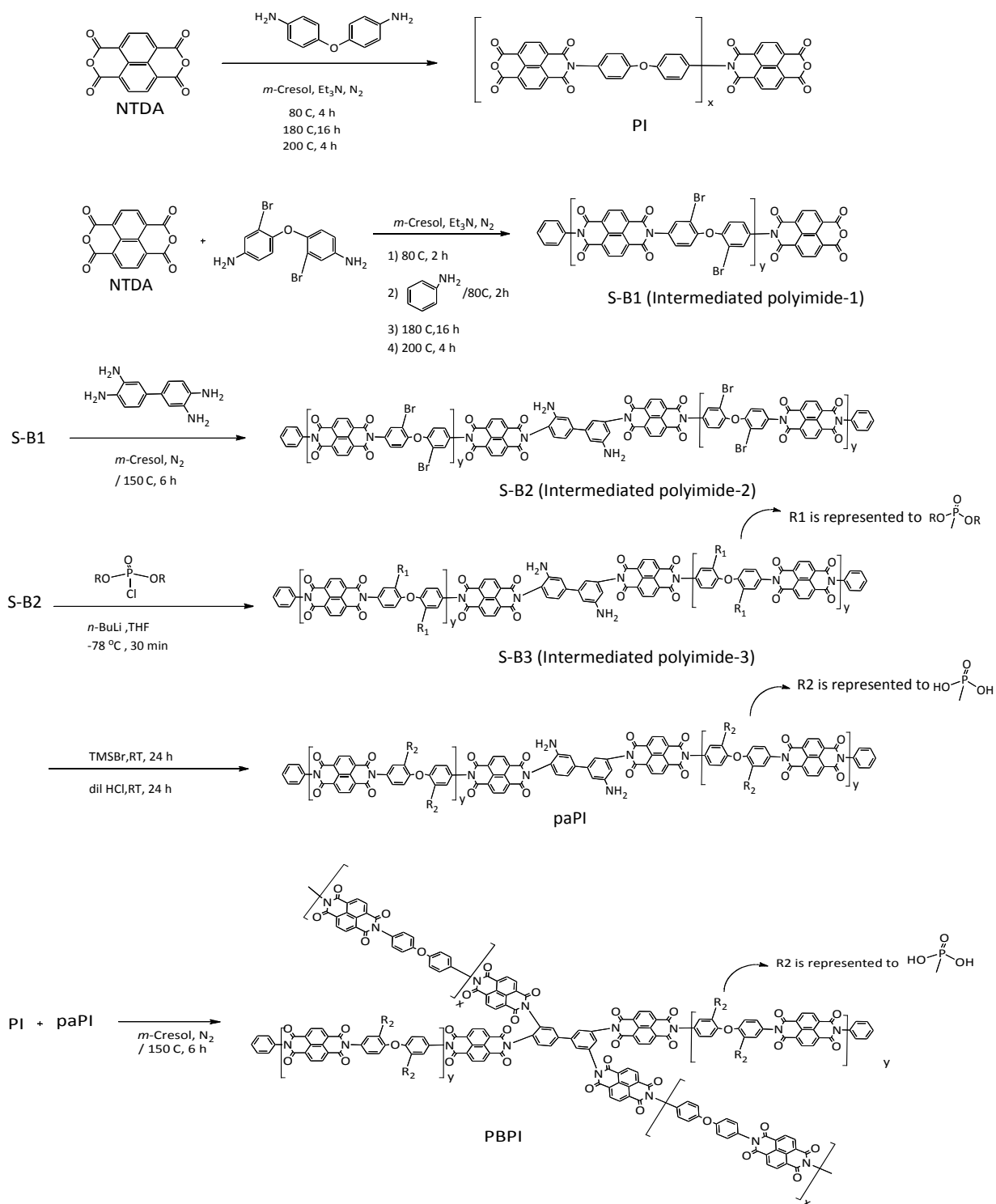
The bromination of 4,4'-diaminophenyl ether occurred readily in the presence of liquid bromine. The electrophilic aromatic substitution reaction of the bromination led to the substitution of the aromatic ring to the electrophile (bromine) at the *ortho*- position in order to generate the most stable carbocation. The carbocation was stabilized by the resonance structure where the ether substituent acted as an electron donating group to help the stabilization of the intermediate carbocation. The mono-substitution of bromine on each benzene ring was occurred due to the controlled molar ratio between 4,4'-diaminophenyl ether and bromine.

## 5.2 THE CHARACTERIZATION RESULTS OF OBTAINED POLYIMIDE SAMPLES

Regarding to different synthetic pathways that described in Chapter 4; the direct copolymerization of phosphonated monomer method (method B) were applied to prepare phosphonated polyimide side-chain polymer (paPI).

The preliminary results of  $^1\text{H-NMR}$  showed that the desired phosphonated polyimide structure was only obtained from method B. The direct lithiation of polyimide with organolithium reagent i.e. *n*-BuLi was not succeeded as same as previous reports on introduction of sulfonic acid to ortho-position of sulfone or ketone group. [6]The self-coupling between lithiated site and other site in polymer chain was possibly occurred since the intra-molecular reaction is generally more favor than inter-molecular reaction.

In this study, phosphonated graft copolyimide samples were synthesized via method B as shown in Scheme 5-1.



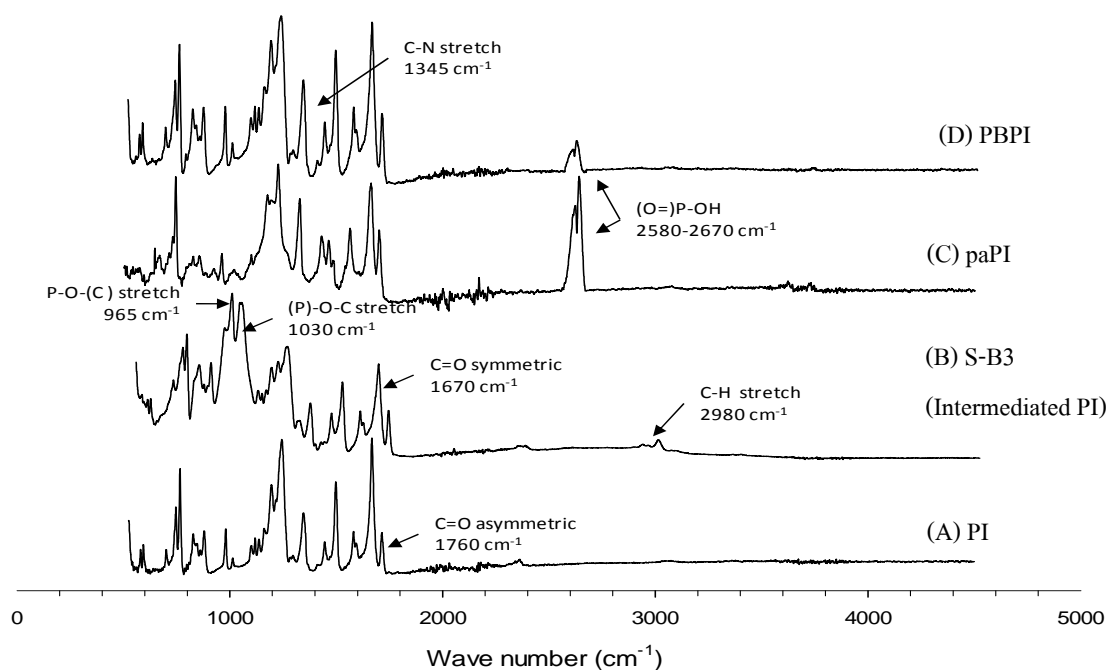
**Scheme 5-1** The synthetic pathway of phosphonated graft copolyimide

The functional group and structure of polyimide samples, which obtained from synthesis pathway in scheme 5-1 were studied by FTIR and NMR technique respectively and their results could be described as following;

## 5.2.1 THE POLYMER STRUCTURE

### 5.2.1.1 The FTIR Characterization

All polyimide products were purified by acetone soxhlet extraction to remove *m*-cresol solvent and impurities. The functional groups of polyimide samples were investigated by using FTIR technique with ATR mode. In this IR measurement, the band around 2300–2400  $\text{cm}^{-1}$ , which corresponded to the uncompensated background  $\text{CO}_2$  was not presented. [32]



**Figure 5-2 FTIR spectra of polyimide (A) PI, (B) S-B3 (Intermediated PI), (C) paPI and (D) PBPI samples**

As shown in Figure 5-2, the completion of the imidization step of all polyimide samples (PI, paPI, PBPI and intermediated S-B3 samples) were confirmed by the absence of carbonyl peak of anhydride unit in the regions around  $1670 \text{ cm}^{-1}$  and  $1740 \text{ cm}^{-1}$  and the presence of

carbonyl absorptions at at  $1710\text{ cm}^{-1}$  (asymmetric) and  $1780\text{ cm}^{-1}$  (symmetric) in imide unit. In addition, the C-N-C stretching absorption was observed around  $1345\text{ cm}^{-1}$ .

The S-B3 sample showed three new peaks at  $2980\text{ cm}^{-1}$ ,  $1030\text{ cm}^{-1}$  and  $965\text{ cm}^{-1}$ , which was attributed to C-H stretching of the ethyl groups, (P)-O-C stretching and P-O-(C) vibration of phosphonate ester respectively. [14] To avoid ester formation during hydrolysis step, the bromotrimethylsilane was used under mild condition instead of hydrochloric acid. The phosphonate ester  $((\text{CH}_3\text{CH}_2\text{O})_2\text{-P=O})$  unit was converted to phosphonic acid  $((\text{HO})_2\text{P=O})$  unit, this success could be confirmed by the disappearance of the phosphonate ester absorption band ( $2980\text{ cm}^{-1}$ ,  $1030\text{ cm}^{-1}$  and  $965\text{ cm}^{-1}$ ) and the arise of the new bands between  $2580\text{-}2670\text{ cm}^{-1}$  which corresponding to  $-\text{P(O)(OH)}$  unit. [22]

#### 5.2.1.2 The $^1\text{H-NMR}$ and $^{31}\text{P-NMR}$ Characterization

Figure 5-3 presented the comparison of  $^1\text{H-NMR}$  spectra of the polyimide (PI), s-B3 (Intermediate polyimide-3), phosphonated polyimide, (paPI), and the phosphonated graft copolyimide (PBPI). Unluckily, the polyimide samples in this study had poor solubility, which will be described in more details in next section. Due to their poor solubility in  $\text{DMSO-d}_6$  solvent, broad peaks with low intensity were observed. In addition, the NMR peaks are broadening because of the overlapping of same proton groups in various locations of the polymer chain. As a result, the coupling and splitting of  $^1\text{H-NMR}$  peaks wasnot observed, as generally found in normal macromolecule or polymer.

However, the formation of naphthalimide was confirmed by the chemical shifts at 8.7-8.8 ppm, which corresponded to the naphthalene protons. To extend the chain length and to add the free amine group into S-B1 (Intermediate polyimide-1), the 3,3'-diaminobenzidine which has 4 reactive amino groups was used. As mentioned earlier, A stoichiometric molar ratio of 3,3'-diaminobenzidine to S-B1 and the steric hindrance of S-B1 would restrict the reaction to occur at only 2 amine groups of the 3,3'-diaminobenzidine, this resulted in the presence of two unreacted

$\text{-NH}_2$  groups in S-B3 (Intermediate polyimide-3) and paPI Samples at 6.5 ppm and the resonances at 7.4-7.8 ppm was corresponding to the aromatic protons in 3,3'-diaminobenzidine. In addition, the success in grafting PI-A to paPI-C was confirmed by the disappearance of the  $\text{-NH}_2$  resonance at 6.5 ppm as shown in PBPI spectra.

Evidence for the complete hydrolysis of S-B3 was also obtained by  $^1\text{H-NMR}$ . The chemical shifts of the methyl proton and ethyl proton in phosphonate ester ( $\text{CH}_3\text{CH}_2\text{O-}$ ) at 1.29 ppm and 4.1 ppm [87] respectively, were observed in S-B3 spectrum and then disappeared after hydrolysis reaction, so both peaks were not presented in paPI-C spectrum as shown in Figure 5-3 (B) and Figure 5-3 (C).



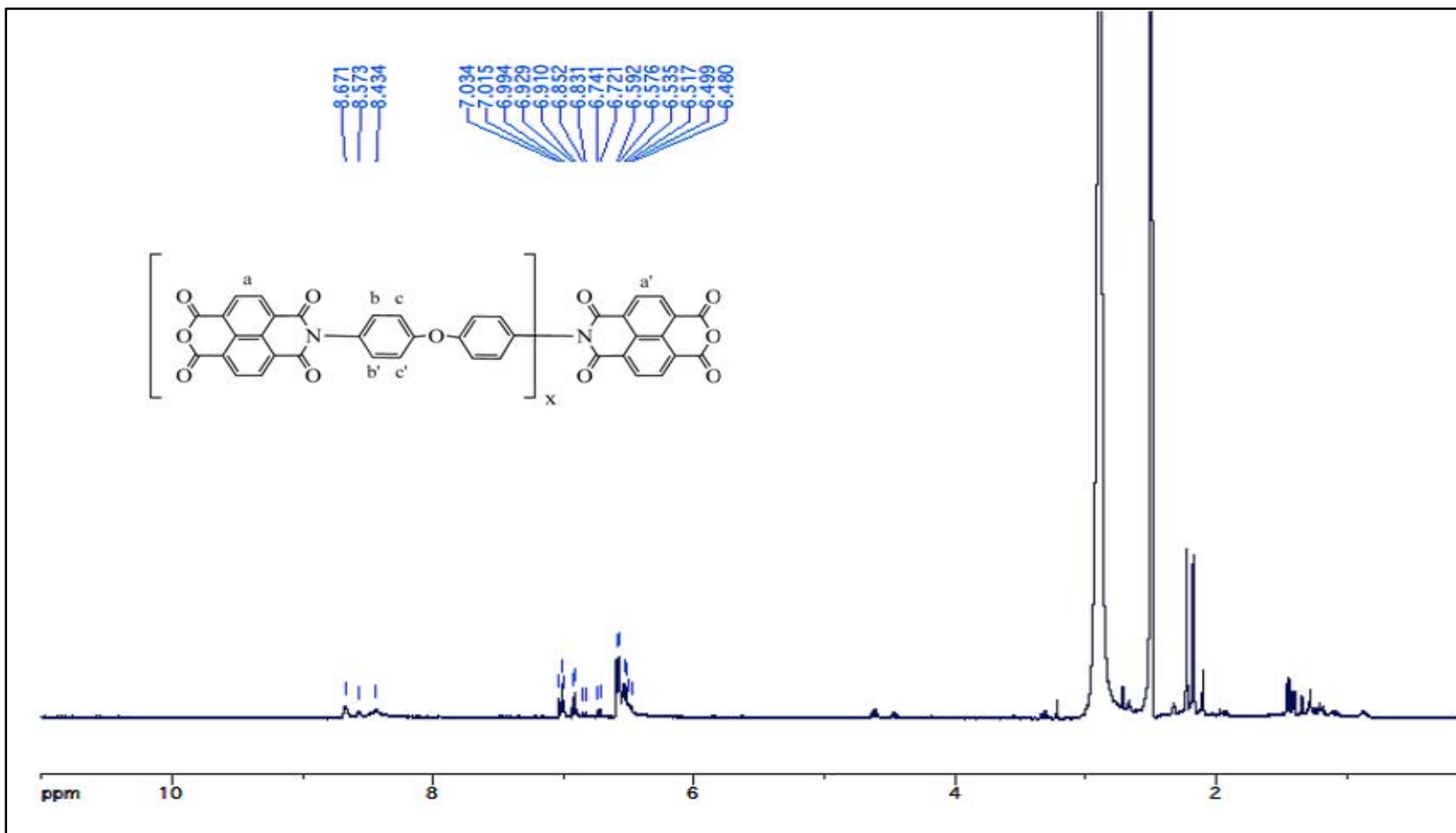


Figure 5-3 (A)  $^1\text{H-NMR}$  spectrum and chemical structure of polyimide, PI

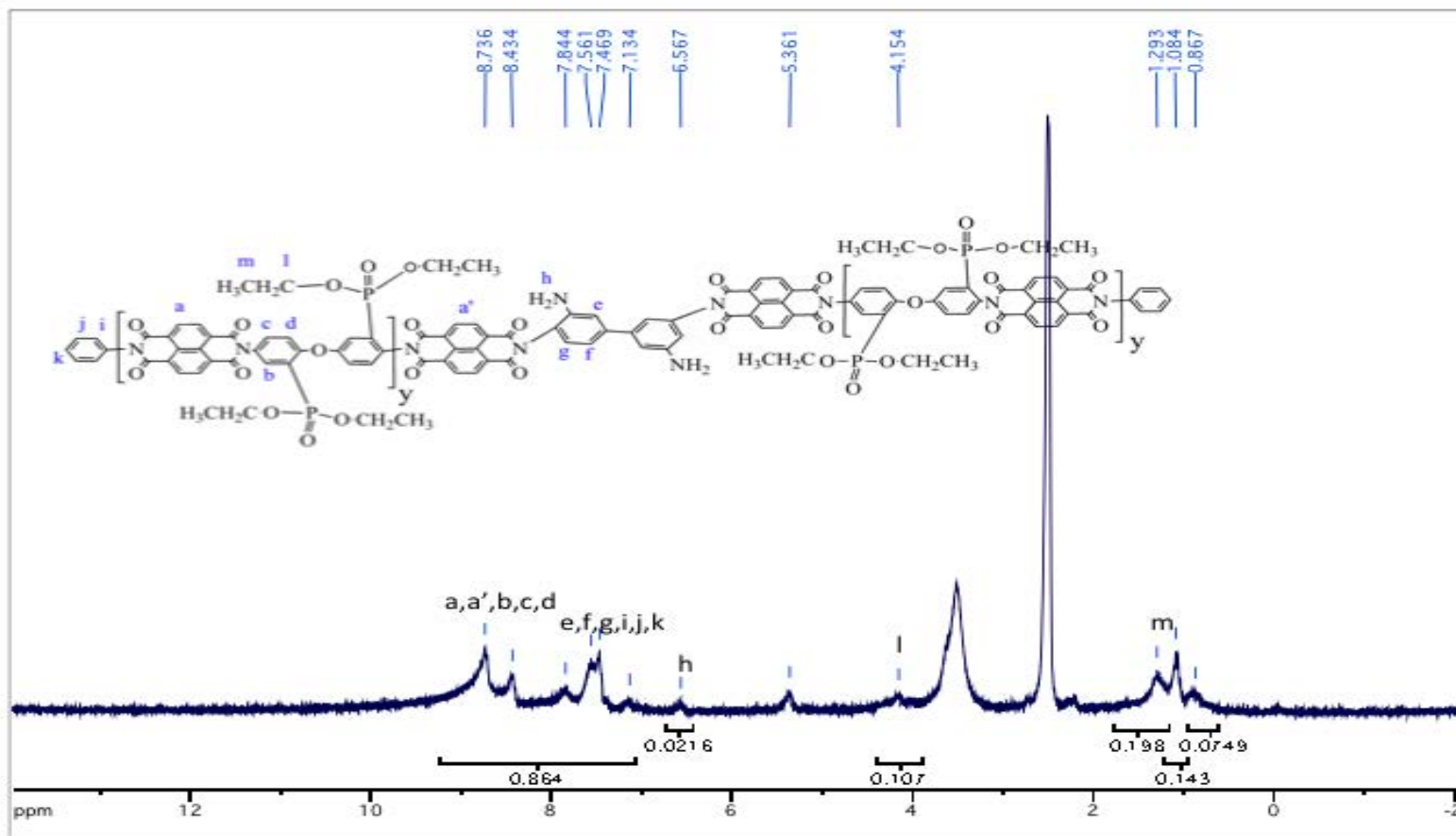


Figure 5-3 (B)  $^1\text{H-NMR}$  spectrum and chemical structure of polyimide S-B3 (Intermediate PI-3)

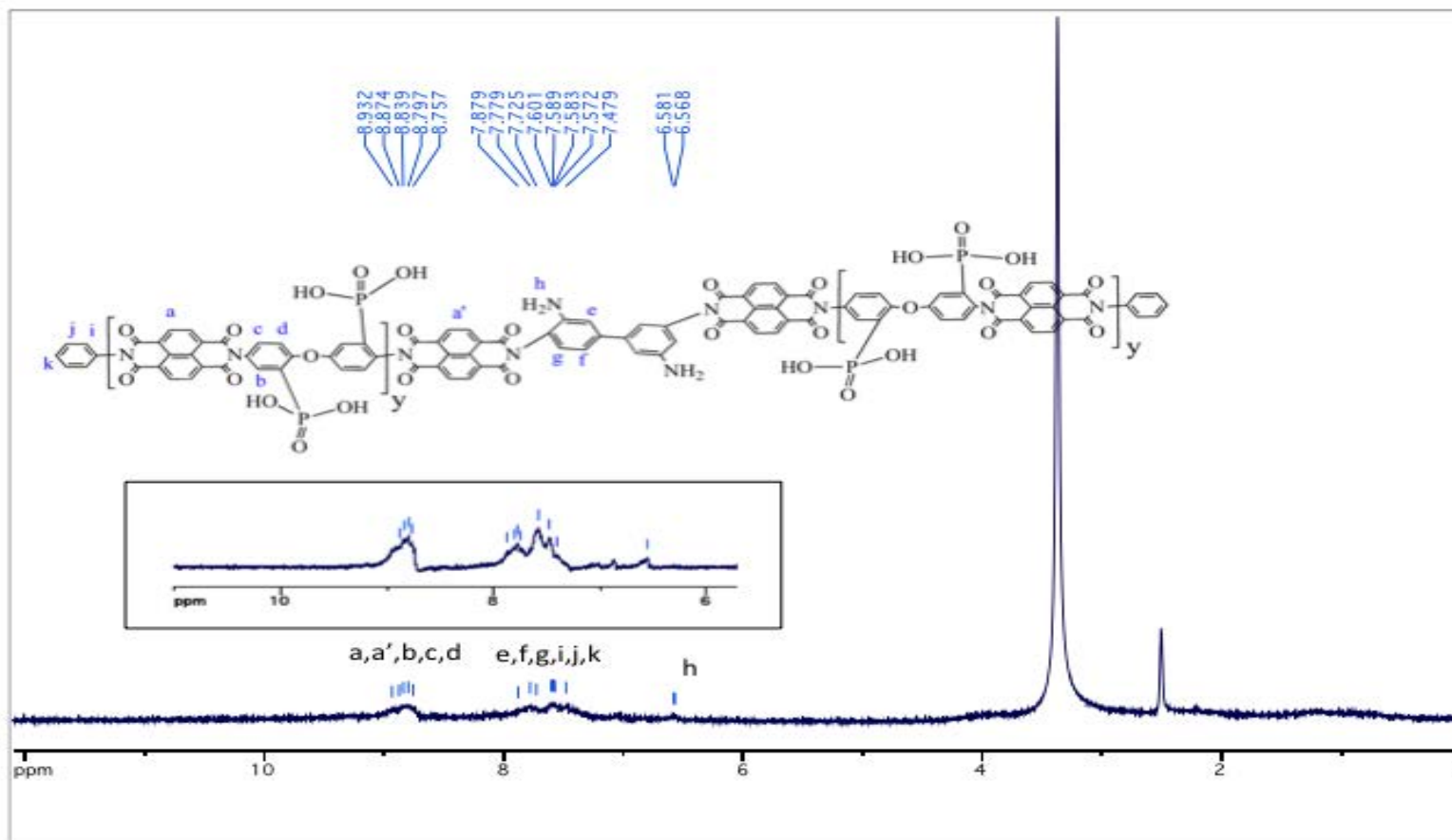


Figure 5-3 (C)  $^1\text{H-NMR}$  spectrum and chemical structure of phosphonated polyimide, paPI

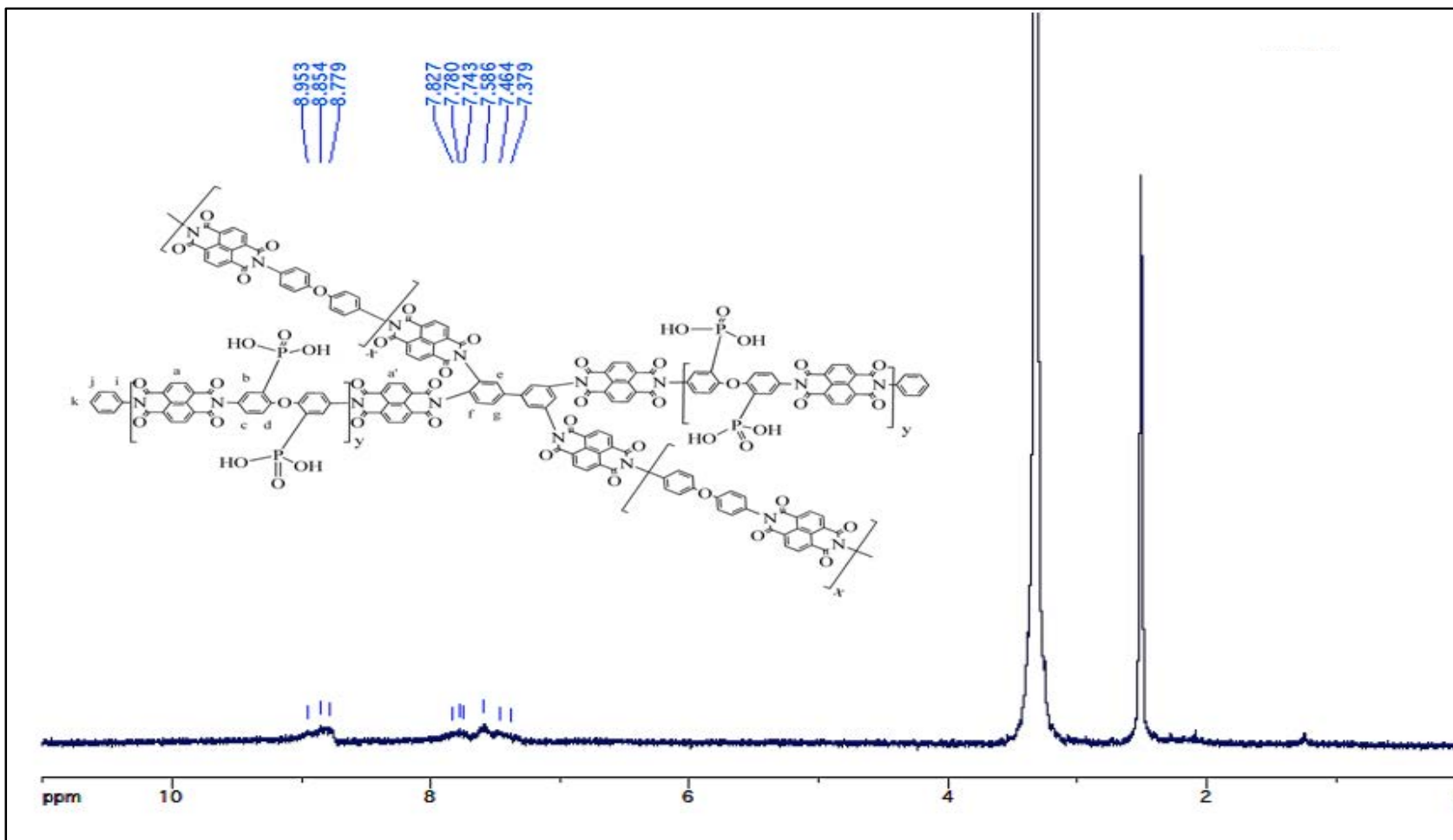
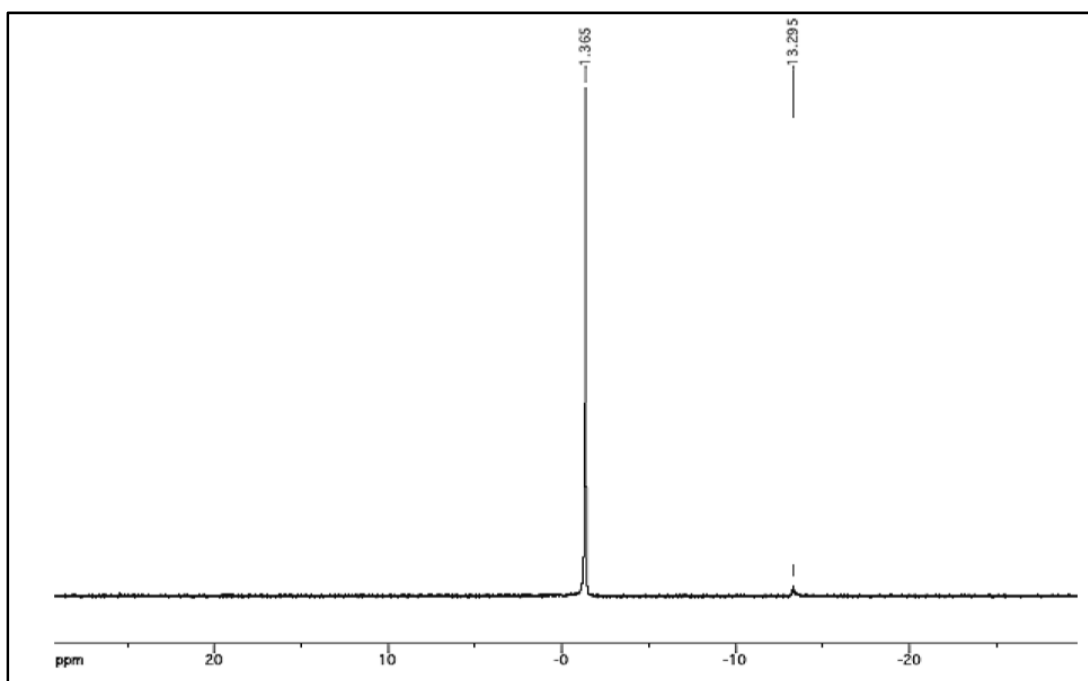


Figure 5-3 (D)  $^1\text{H-NMR}$  spectrum and chemical structure phosphonated graft copolyimide, PBPI

The accomplishment of phosphonation reaction was then confirmed again by  $^{31}\text{P}$ -NMR spectroscopy as shown in Figure 5-4. The phosphonic acid group in the phosphonated graft copolyimide; PBPI sample were found at -1.57 ppm while the remaining phosphonate ester groups were found at -13.29 ppm. Typically the organophosphonic acids,  $\text{C}-\text{P}(\text{O})(\text{OH})_2$ , show a chemical shift between -5 to 25 ppm, depending on adjacent atom and solvent [88]. According to  $^{31}\text{P}$ -NMR, the hydrolysis conversion, which calculated from the ratio between the peak intensity at -1.57 ppm and the sum of the peak intensities at -1.57 and -13.29 ppm, was approximately 98%.



**Figure 5-4**  $^{31}\text{P}$ -NMR spectra of phosphonated graft copolyimide; PBPI samples

To summarize, the characterization results confirmed that novel phosphonated graft copolyimide based on NTDA and ODA monomer was prepared. While the phosphonated polyimide side chain was obtained from the series of bromination and lithiation reaction, the graft structure was achieved by use of 3,3'-diaminobenzidine monomer with 4 reactive amine group.

### 5.2.2 THE SOLUBILITY MEASUREMENT

The solubility of polyimide, the phosphonated polyimide and phosphonated graft copolyimide samples were tested in various solvents such as *m*-cresol, NMP, DMSO, DMAc, DMF, chloroform and acetone etc., and their results were shown in Table 5-1. The measurement was conducted at both room temperature and elevated temperature, up to 120 °C. It was found that polyimide samples could be dissolved completely at elevated temperature in *m*-cresol with maximum concentration of 30%. Comparing between PI-A, paPI-C and PBPI samples, the paPI-C samples had better solubility in aprotic solvent than PBPI and PI-A samples due to their higher polarity of phosphonic acid group.[23] In addition, all polyimide samples were insoluble in chloroform and acetone.

**Table 5-1 Solubility of the polyimide samples**

Polymer	Solvents <sup>a</sup>						
	<i>m</i> -Cresol	NMP	DMSO	DMAc	DMF	Chloroform	Acetone
PI	s	ps	ps	ps	i	i	i
paPI-1 (DP=49)	s	s	ps	ps	ps	i	i
PBPI-1	s	s	ps	ps	ps	i	i

<sup>a</sup> s = soluble at elevated temperature, ps = partially soluble at elevated temperature, i = insoluble

### 5.2.3 THE VISCOSITY MEASUREMENT

To confirm the achievement of grafting process, the molecular weight of polyimide samples were determined. As described in previous section, because of the poor solubility of the polymers in any solvent other than *m*-cresol, the GPC method was not possible to determine their molecular weight. Due to their different arrangement and flexibility of polymer chain between standard polystyrene and phosphonated graft polyimide, the viscosity average molecular weights could not be determined by Mark-Houwink equation. In order to get an idea whether the phosphonated graft copolyimide, PBPI, successfully was obtained or not, the intrinsic viscosities of the polymers in *m*-cresol at 45°C were compared with the theoretical molecular weight calculated for 100% conversion of the reactions shown in Schemes 5-1.

**Table 5-2 Comparison of intrinsic viscosity and theoretical molecular weights of the polyimides**

Sample	Degree of polymerization	Theoretical $M_n^a$ (g/mol)	Intrinsic Viscosity [ $\eta$ ] (g/dL)
PI	149	33,000	9.30
paPI	49	22,000	8.16
PBPI	-	55,000	12.48

<sup>a</sup>The molecular weight is calculated assuming 100% conversion of monomers

Although the results in Table 5-2 did not identify the exact molecular weight of PBPI, the viscosity trend could imply their success in grafting process. With increasing of intrinsic viscosity of PBPI, the results were consistent to their theoretical  $M_n$  results.

#### 5.2.4 THE ION EXCHANGE CAPACITY (IEC)

As described in experimental section, the five difference in preparation side chain length of phosphonated polyimides samples; namely paPI-1 to paPI-5, were synthesized for studying the effect of phosphonation level and side chain length. To avoid any confusion, PBPI-1 samples were obtained from grafting PI-A to paPI-1 sample and PBPI-2 samples were obtained from grafting PI-A to paPI-2 sample and so on. The degree of polymerization and phosphonation level of paPI series were designed and shown in Table 4-1.

In this study, the IEC values were obtained from two methods; (A) NMR calculation ( $IEC_{NMR}$ ) and (B) Titration method ( $IEC_{Titration}$ ). The  $IEC_{NMR}$  was calculated from the sum of integrated area of protons of ethyl groups at 4.1 ppm and the methyl groups at 1.29 ppm divided by the integrated area of aromatic proton between 7.1 to 8.7 ppm in  $^1H$ -NMR spectra of phosphonate ester derivative polyimide (before hydrolysis). Then the degree of polymerization was obtained from Equation 5-1.

$$\% \text{ Phosphonation} = \frac{40X}{24 + 20X} \quad \text{Equation (1)}$$

Where X is degree of polymerization.

Table 5-3 shows the IEC values of all synthesized phosphonated polyimide samples. All  $IEC_{\text{Titration}}$  values of paPI-C samples were agreeing well with the  $IEC_{\text{NMR}}$  value. However, the  $IEC_{\text{NMR}}$  of PBPI samples couldnot be determined due to their too poor solubility in DMSO- $d_6$ . Comparing among paPI-1, paPI-4 and paPI-5 samples (with same 30% phosphonation), IEC values obtained from both methods showed similar trend. These values were not different although they have different side chain length because the amount of phosphonic acid and degree of polymerization were stoichiometric controlled during synthesis step.

**Table 5-3 Comparison of IEC values between NMR calculation and Titration method**

Polymer	% Phosphonation	$IEC_{\text{NMR}}$ (meq/g)	$IEC_{\text{Titration}}$ (meq/g)
paPI-1 (DP=49)	32	1.48	1.45
paPI-2 (DP=99)	42	2.10	1.98
paPI-3 (DP=199)	55	2.72	2.68
paPI-4 (DP=99)	30	1.50	1.47
paPI-5 (DP=199)	30	1.52	1.48
PBPI-1	-	-	1.02
PBPI-2	-	-	1.38
PBPI-3	-	-	1.67
PBPI-4	-	-	1.05
PBPI-5	-	-	1.03

Comparing between paPI and PBPI samples, all phosphonated graft copolyimide (PBPI) samples had lower IEC than phosphonate polyimide (paPI-C) samples. The decreases in the IEC of PBPI versus paPI-C were consistent with the dilution of the phosphonic acid groups due to the grafting of unphosphonated polyimide (PI) to the phosphonated polyimide paPI.



### 5.2.5 THERMAL PROPERTIES

A comparison of the thermal stability of PI, paPI and PBPI system can be shown in Figure 5-5. All polymer samples were stable up to at least 450°C. PI was stable up to ~590°C, where degradation of the imide bond occurred. For both paPI and PBPI, they showed two degradation stages, the first mass loss around 475°C, was likely due to the degradation of the phosphonic acid groups, and a second mass loss above 570°C, was due to the degradation of the polyimide.

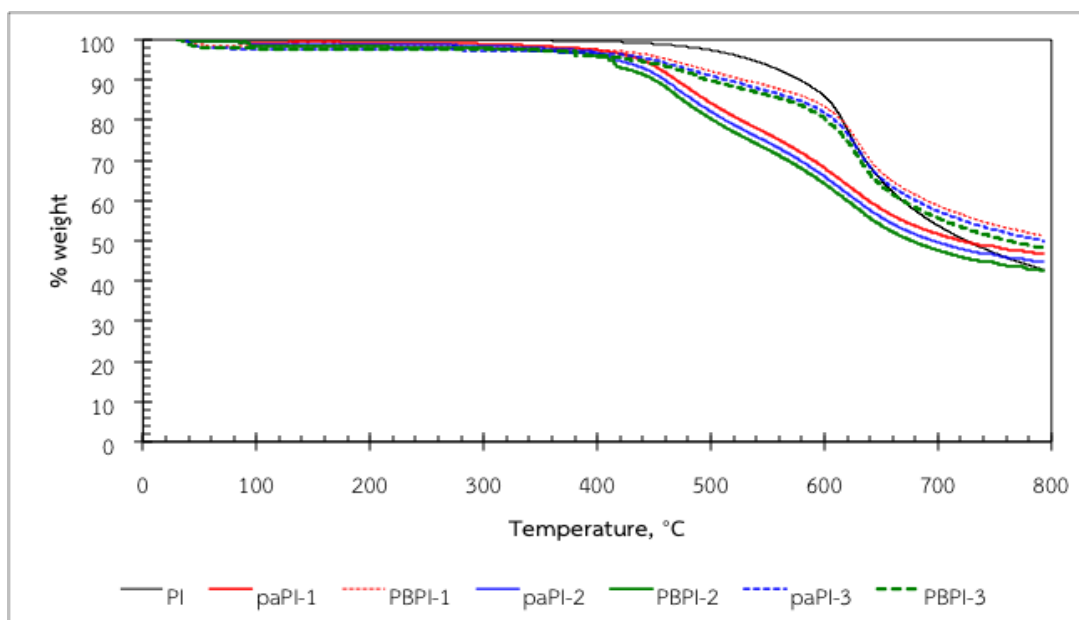


Figure 5-5 The example of TGA results of PI, paPI and PBPI samples

### 5.3 THE PROPERTIES OF PHOSPONATED GRAFT COPOLYIMIDE MEMBRANES

The fPBPI films were casted from mixture solution of pure polyimide and PBPI samples with ratio 1:4 (PI:PBPI) in *m*-cresol at 120°C. The membranes were dried in oven at 80°C for several days to evaporate the solvent. At this point, the membranes still have some residual *m*-cresol, so the membranes were washed in acetone several times to eliminate any remaining solvent and impurity. Their membranes were named as fPBPI samples, consequently, the fPBPI-1 means this membrane was prepared from PBPI-1 sample and so on.

### 5.3.1 THE RELATION BETWEEN ION EXCHANGE CAPACITY, WATER UPTAKE AND SWELLING PROPERTIES

Table 5-4 showed the properties of phosphonated graft copolyimide membranes and Nafion®117 membrane. The measurement of  $IEC_{\text{Titration}}$ , water uptake and degree of swelling of polymer membrane were conducted at room temperature.

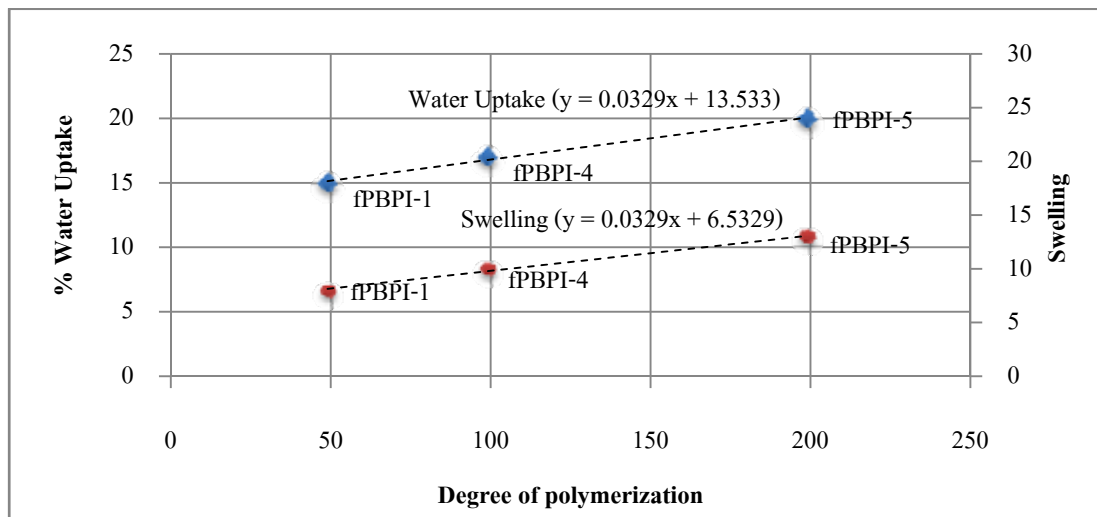
**Table 5-4 Comparison of phosphonate grafted copolyimide membrane and Nafion®117 properties.**

Polymer	$IEC_{\text{Titration}}$ (meq/g)	%Water Uptake	% Swelling
fPBPI-1	0.92	15	8
fPBPI-2	1.24	18	10
fPBPI-3	1.43	24	16
fPBPI-4	0.94	17	10
fPBPI-5	0.93	20	13
Nafion®117	0.91	32	18

\* All fPBPI membrane were prepared by blending with 20% PI-A in *m*-cresol

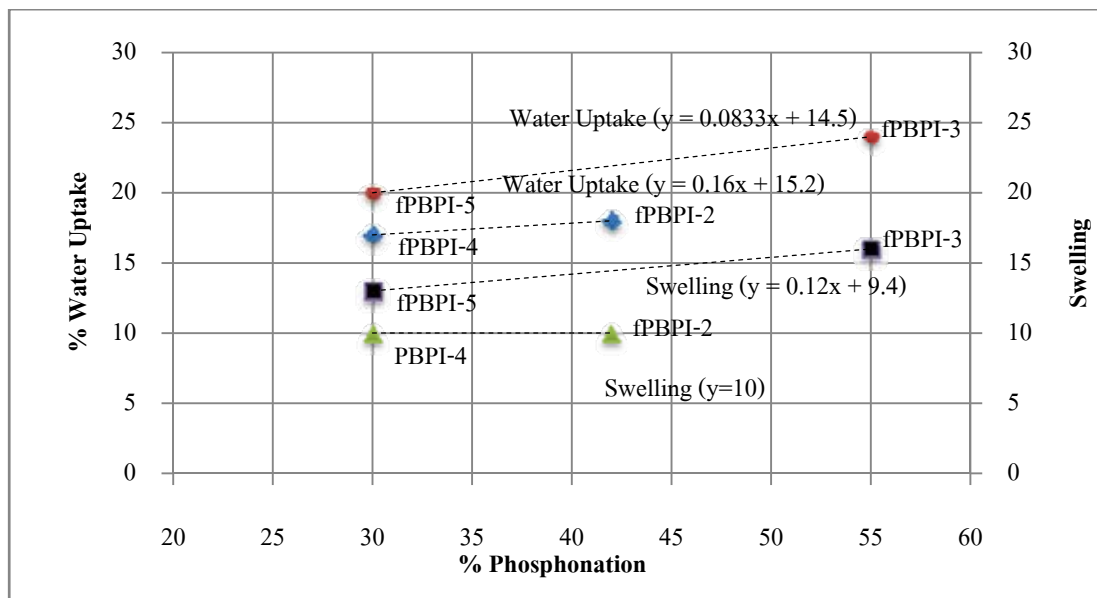
The amount of phosphoric acid trends of fPBPI membranes can be estimated from the IEC values by titration technique; it implied that fPBPI-3 membrane had the highest phosphonic acid contents among other fPBPI membrane. The IEC value between the phosphonated graft copolyimide (PBPI) powder (Table 5-2) and their membranes (fPBPI) in (Table 5-3) were compared and it was shown that the IEC values of all membranes (fPBPI-1 to fPBPI-5) were lower than the starting PBPI samples. This was due to the dilution of the phosphonic acid by blending the unphosphonated polyimide during film preparation step and resulted in lower water uptake and swelling ratio. Contrary to the IEC results, most fPBPI membranes had lower water uptake and swelling than Nafion. This could be explained by the differences in acidity and property between sulfonic acid and phosphonic acid. Nafion®117 had extremely high hydrophilicity of sulfonic acid group while the fPBPI membrane had lower hydrophobicity of

polyimide backbone and less acidity of phosphonic acid. Moreover, the fPBPI classes were generated by blending with normal polyimide (PI), which had no conductivity.



Remark : The degree of polymerization was from phosphonated polyimide (paPI) samples that identified in Table 5-3.

**Figure 5-6 The relation between side chain length and water uptake and swelling properties**



Remark : The %phosphonation was from phosphonated polyimide (paPI) samples that identified in Table 5-3.

**Figure 5-7 The relation between % phosphonation and water uptake and swelling properties**

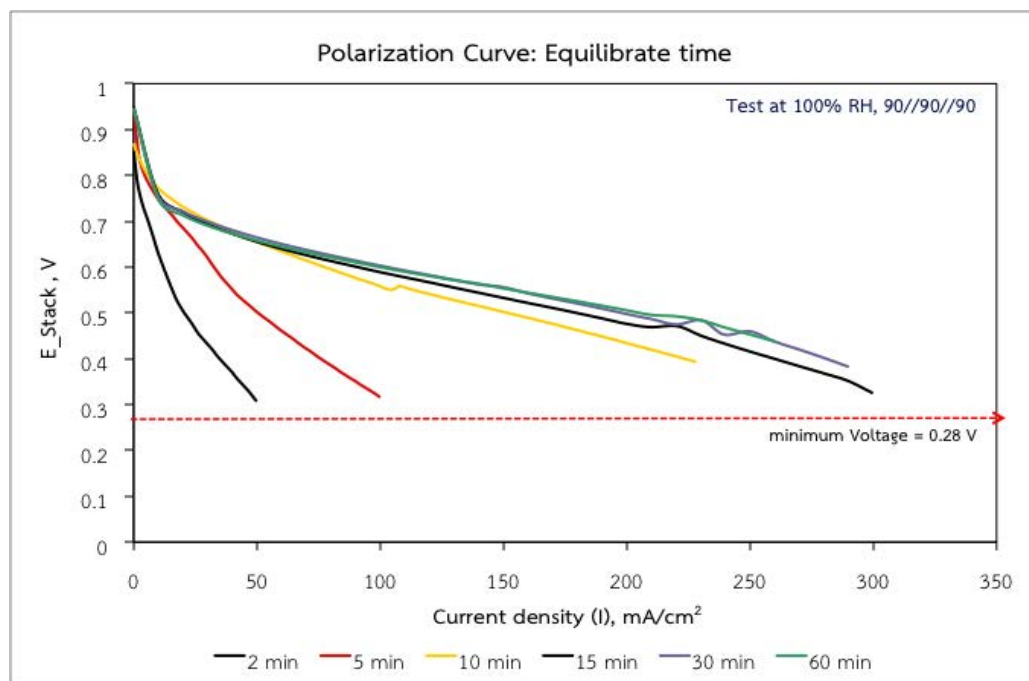
The effect of the side chain length and phosphonation level to water uptake and swelling ratio were investigated as shown in Figure 5-6 and Figure 5-7 respectively. As shown in Figure 5-5, the fPBPI-1, -4 and -5 membrane that prepared from 30-32% phosphonation of paPI-C polymer showed the slightly increasing trend of swelling and water uptake, however, their results didn't show much differences due to the addition of hydrophobic polyimide during film preparation process. As previously reported, the branch-like structure could uptake more water than the linear structure due to their wider inter-chain spacing [72,89] In addition, the distinct ionic domain structures possibly found in branched or block copolymers systems may lead a different relationship between IEC, water content, and proton conductivity, when compared to their random or linear copolymer. [45]

When comparing between the fPBPI system that prepared from similar side chain length of paPI samples; the fPBPI-2 and fPBPI-4 samples and the fPBPI-3 and fPBPI-5 samples, the fPBPI-5 (with 30% phosphonation level) had lower water uptake and swelling than fPBPI-3 (with 55% phosphonation level). However, this situation was not clearly observed in shorter side chain system. In addition, all membranes had lower water uptake due to the addition of hydrophobic unphosphonate part and agreed well with swelling results. As expected properties, the fPBPI-3 membrane which obtained from the highest phosphonation level of paPI-3 polymer, showed the highest of IEC about 1.43 meq/g, with swelling ratio at 16% and water uptake at 24%.

### 5.3.2 THE MEASUREMENT OF PEM FUEL CELL PERFORMANCE

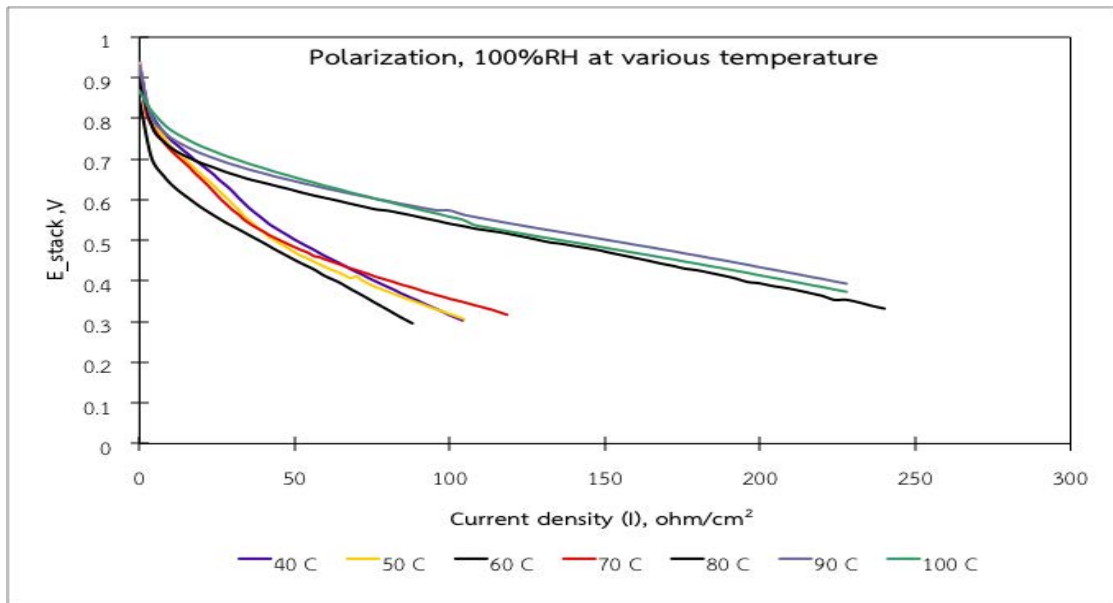
In this study, a single polymer electrolyte membrane fuel cell performance with an effective dimension  $5 \text{ cm}^2$  was fabricated. The 0.2 l/min of humidified  $\text{H}_2$  and air was fed to anode and cathode side respectively. Before started the measurement, the equilibrate time were examined at various operating condition. The fuel cell station was programmed to automatically terminate, if the voltage output was lower than 0.28 V. As shown in Figure 5-8, the power output (Integrated area of the curve) was rather similar if the system was left at 15, 30 or 60 minutes.

Therefore, before each measurement, the system was left running at least 15 minutes in order to ensure that system was reached its equilibrium.

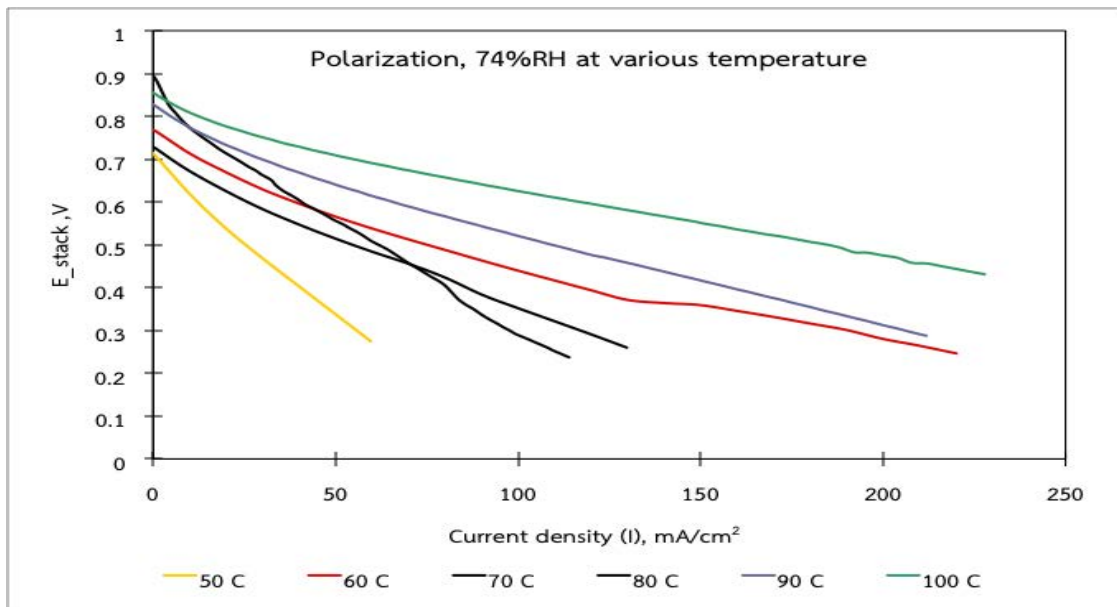


**Figure 5-8 The polarization curve of fPBPI-1 membrane at 90 °C and 100% RH under different equilibrate time.**

The voltage-current density relationship of membranes were investigated under various operating condition to find the maximum current load that membranes continually maintained their performance. The representative polarization curves of phosphonated graft copolyimide membrane for H<sub>2</sub>/Air PEM fuel cell under various relative humidity were shown in Figure 5-9 (A) to Figure 5-9 (D). The results showed that PEM fuel cell that used phosphonated graft polyimide membrane could not maintain their voltage output at relative humidity lower than 33% RH, so the proton conductivity was conducted at only 3 different relative humidities (100%, 74% and 54%) in this study.

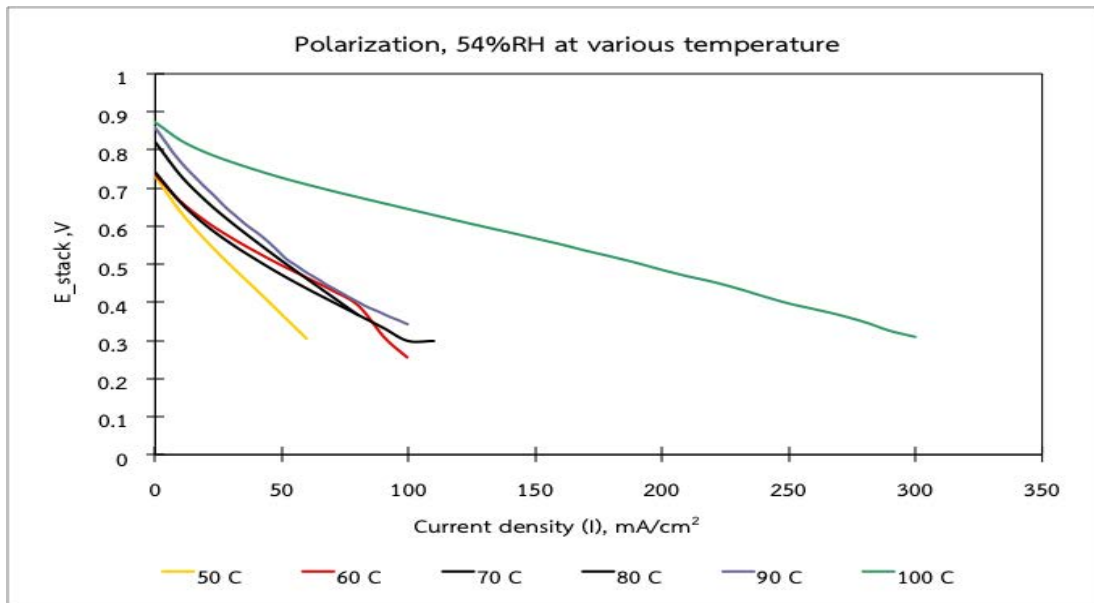


(A) The polarization curve of fPBPI-3 membrane at 100% RH (effective area is about 5 cm<sup>2</sup>, minimum voltage output at 0.28 V)

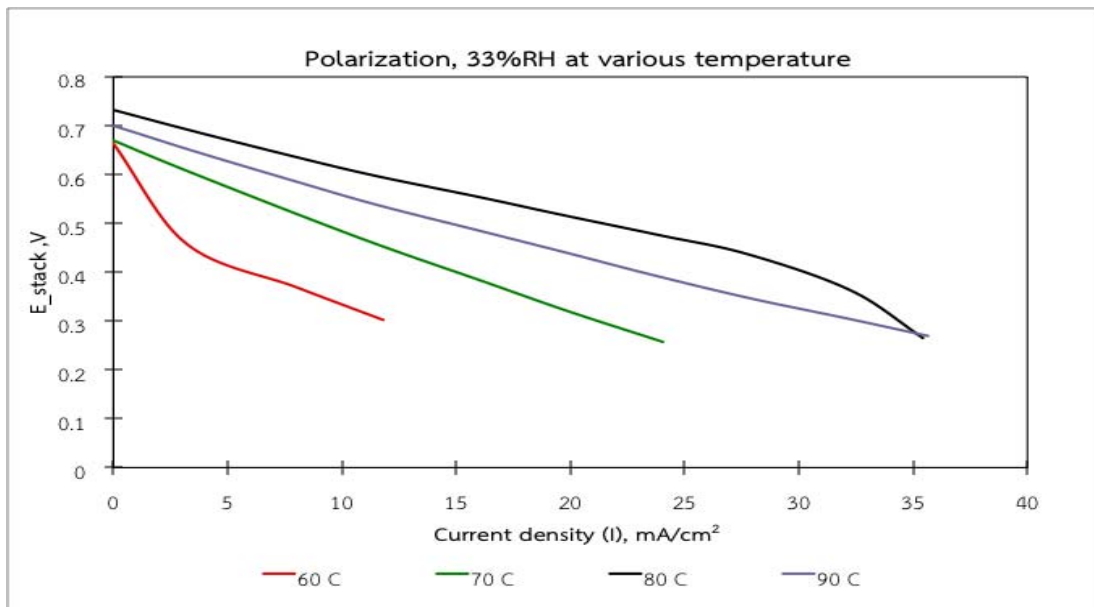


(B) The polarization curve of fPBPI-3 membrane at 74% RH (effective area is about 5 cm<sup>2</sup>, minimum voltage output at 0.28 V)

Figure 5-9 The study of suitable relative humidity range for proton conductivity measurements



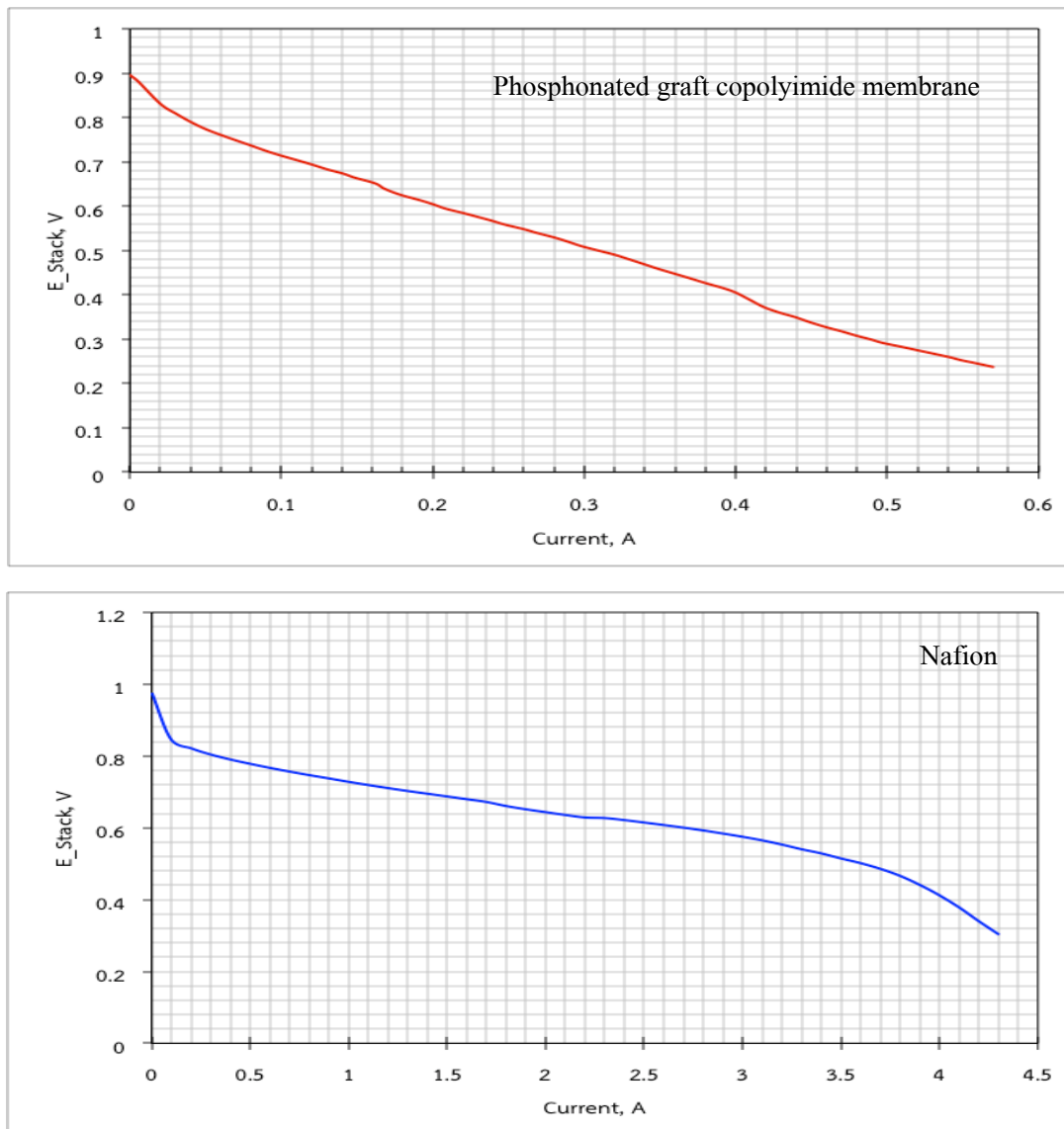
(C) The polarization curve of fPBPI-3 membrane at 54% RH (effective area is about 5 cm<sup>2</sup>, minimum voltage output at 0.28 V)



(D) The polarization curve of fPBPI-3 membrane at 33% RH (effective area is about 5 cm<sup>2</sup>, minimum voltage output at 0.28 V)

Figure 5-9 (Cont.) The study of suitable relative humidity range for proton conductivity measurement

Comparing between Nafion and phosphonated graft polyimide membranes, the Nafion membrane showed greater power output than phosphonated graft copolyimide membrane. The obtained maximum current of phosphonated graft copolyimide and nafion membranes were about 0.6 A and 2.5 A respectively.



**Figure 5-10 Comparison of polarization curve between phosphonated graft copolyimide (up) and Nafion membrane (down)**



However, the suitable current load was selected from the current value in ohmic period (middle range). Although Nafion show longer ohmic period than phosphonated graft copolyimide, only 0.2 A was applied to the samples for comparison reason as shown in Figure 5-10. This unexpected low current load might cause lower proton conductivity of Nafion membrane than previous or other studies. Actually, the proton conductivity was affected by many factors including operating condition i.e. temperature, relative humidity etc. and membrane property itself. In this study, the effect of phosphonation level, side chain length, operating condition were investigated and discussed as following;

#### **5.3.2.1 The effect of operating condition on proton conductivity**

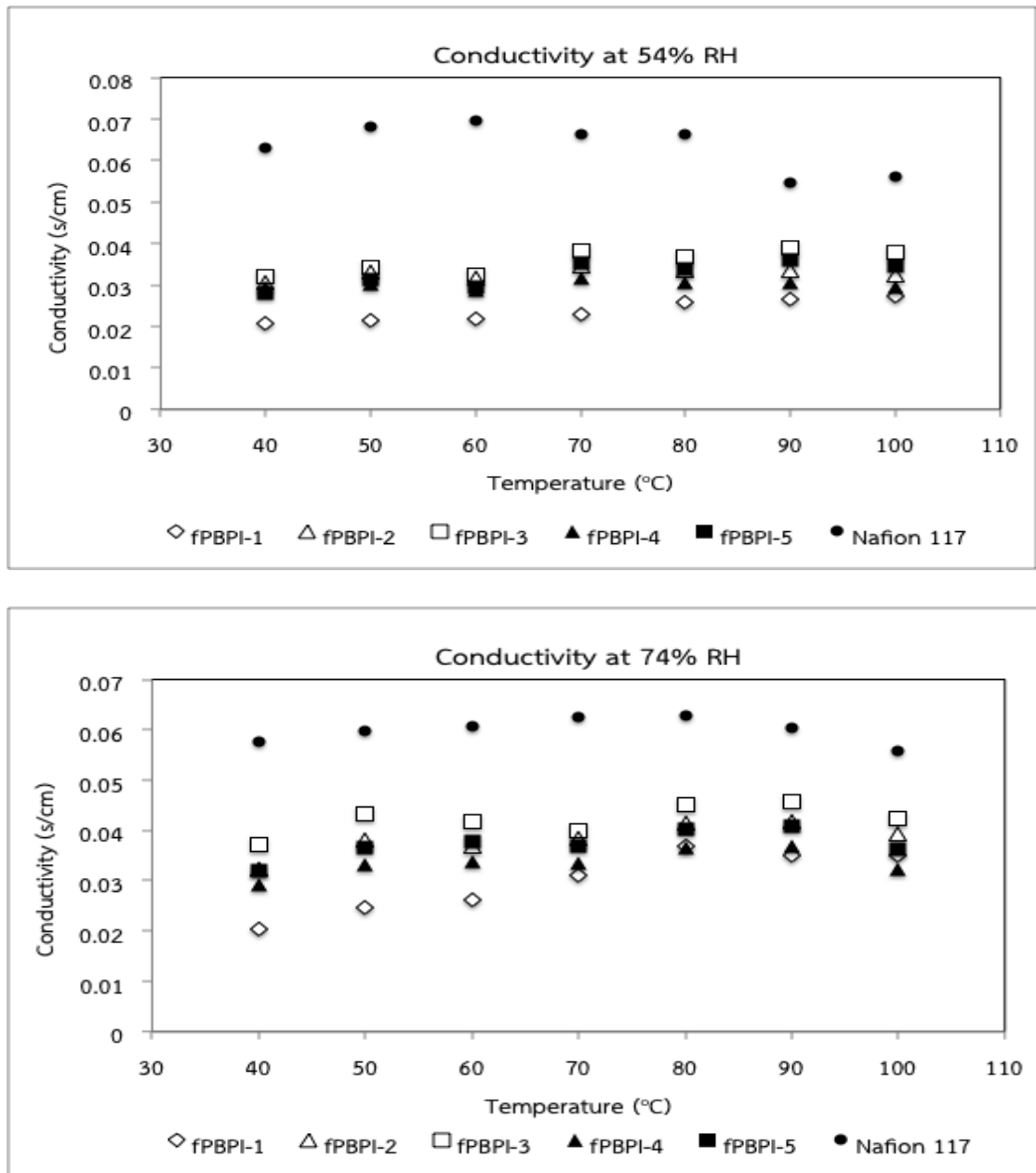
The proton conductivity of fPBPI membrane were measured at different temperatures starting from 40 °C to 100 °C, and various relative humidity at 54%, 74% and 100% respectively. In this experiment, the relative humidity was controlled by setting up the temperature of both electrodes and cell, example; if operating condition was desired at 80°C and 100%RH, the temperature would be set at 80//80//80 (Cathode//Cell//Anode). Moreover, the measurement procedure was importantly noted since it effected to the proton conductivity results. Differences in the measured proton conductivity value conducted during heating and cooling were observed. For example, the measured proton conductivity value at 80°C and 100%RH during heating from 40 °C to 80 °C were different from the value during cooling from 100 °C to 80 °C.

The results showed that the proton conductivity of fPBPI membranes was slightly increased with increasing of temperature as shown in Figure 5-11. Among the fPBPI membranes, the fPBPI-3 showed the highest proton conductivity at 90°C and 74% RH. For comparison, the proton conductivity of Nafion®117 were measured at the same conditions. The Nafion®117 membranes were used in this experiment without any treatment.

Comparing to Nafion®117, the proton conductivity of fPBPI membrane was lower than Nafion throughout temperature range. The proton conductivity of Nafion®117 was reduced

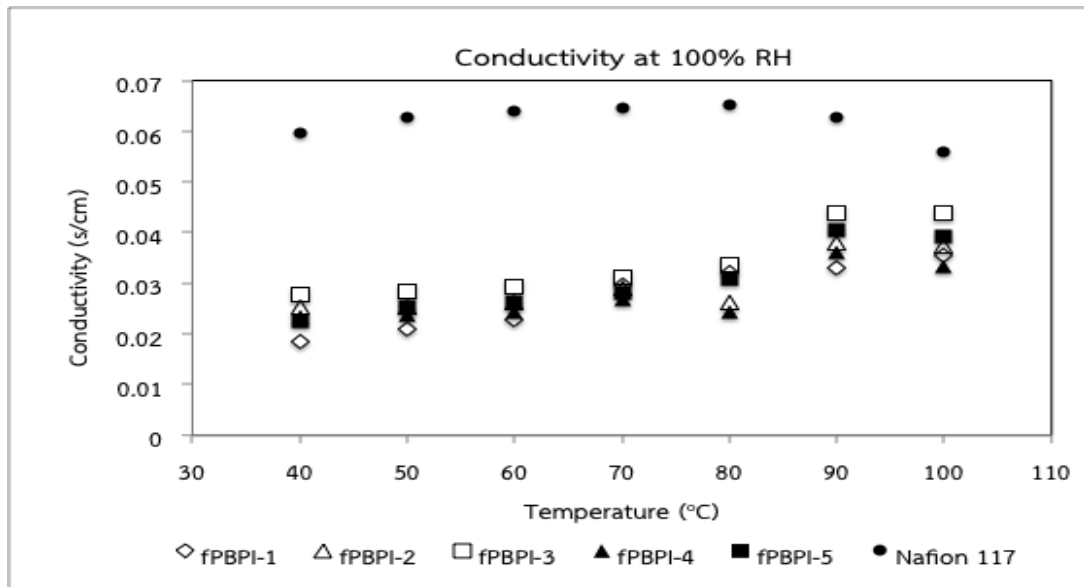
significantly at high temperature around 100°C and low relative humidity level due to the loss of water molecule, while fPBPI membranes showed the slightly decrease in proton conductivity at same condition. Presumably, the bulky structure of fPBPI can force polymer chain apart and increase inter-chain spacing, which water molecules could be trapped in and would not be easily evaporated at high temperatures. [72] However, polymer blend technique was used for preparation of fPBPI films, so if the pure PBPI were made as the membranes instead of blending, the higher proton conductivity would be attained. The film forming ability could also be adjusted using longer main chain length, which will increase the tensile and plastic properties beside blending with nascent polyimide to form a free standing film.

The proton conductivity results at 90°C were selected to investigate the relative humidity effect since the maximum proton conductivity of fPBPI-3 was obtained at this point. As shown in Figure 5-12, the proton conductivity of fPBPI membranes at 90°C showed relative humidity-dependency.



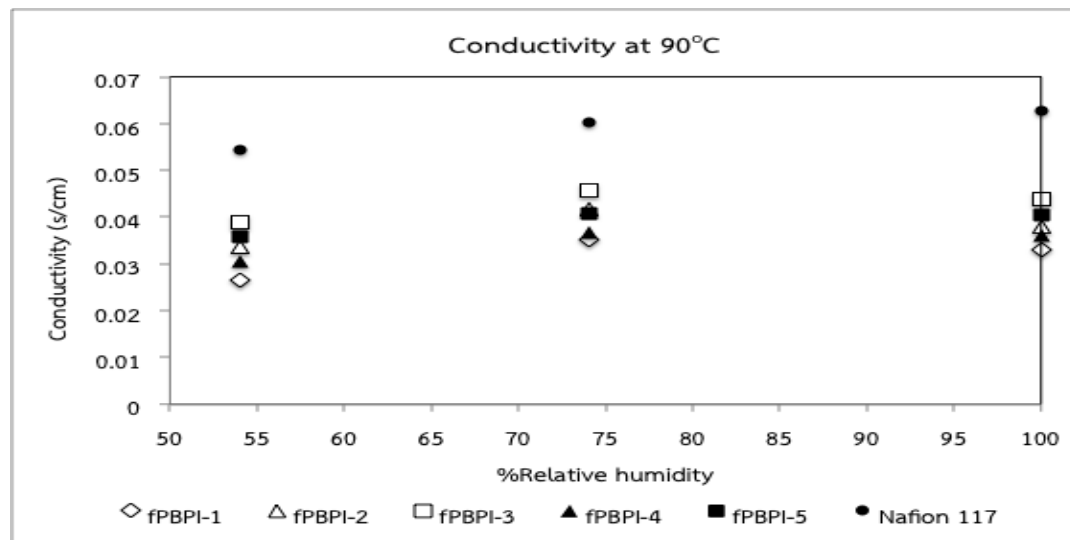
**Figure 5-11 Comparison of proton conductivity between phosphonated graft copolyimide membrane (blended with 20% PI) and Nafion®117 at 54%, 74% and 100% RH**

(Remark: At 100% RH and 100 C, the temperature of fuel cell test system was set at 98//100//98)



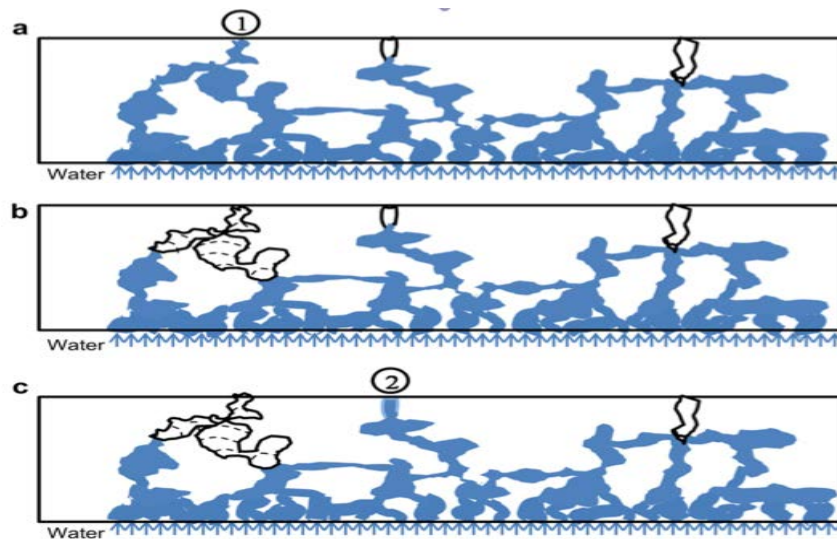
**Figure 5-11 (cont.) Comparison of proton conductivity between phosphonated graft copolyimide membrane (blended with 20% PI) and Nafion®117 at 54%, 74% and 100% RH**

(Remark: At 100% RH and 100 C, the temperature of fuel cell test system was set at 98//100//98)



**Figure 5-12 Comparison of proton conductivity between phosphonated graft copolyimide membrane and Nafion®117 at 90°C**

The trend of proton conductivity between Nafion®117 and fPBPI membranes was different. With increasing of relative humidity, the proton conductivity of Nafion®117 increased, while the proton conductivity of fPBPI membrane started to decrease at 100% RH. This probably affected from hydrophobic structure in fPBPI itself. As previous report, the water management problem could be occurred at high relative humidity i.e. saturation problem of water channel in membrane, water breakthrough at membrane surface or gas diffusion layer (GDL). [90] Lu et al. investigated the water management in PEM fuel cell and they reported capillary model system to explain how the water molecule emerges from gas diffusion layer as shown in Figure 5-13.



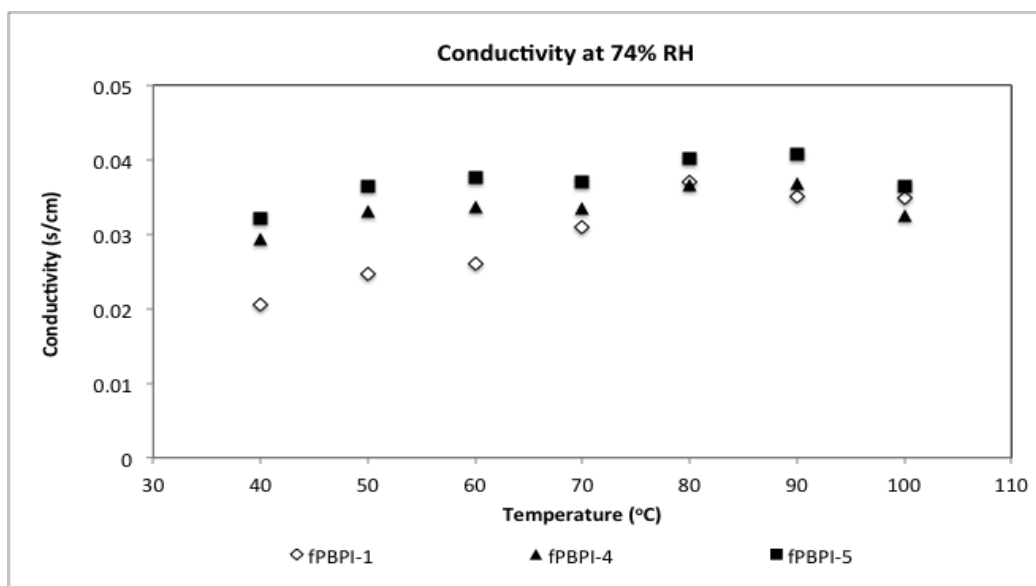
**Figure 5-13 A schematic of water drainage process of a model capillary system as water emerges from GDL surface.[90]**

(Noted : 1<sup>st</sup> water breakthrough at a preferential location; The ‘choke-off’ leaves empty pores in GDL and breaks down the water paths; Spontaneous redistribution of water occurs inside GDL, which may make breakthrough at 2<sup>nd</sup> location possible.)

The condensed water molecule at gas diffusion layer (GDL) or membrane surface possibly caused flooding problem in PEM fuel cell and this could block the gas flow channel and resulted in the decrease in proton conductivity. This situation was also observed in this study as well. During experiment, the water was observed at membrane surface and GDL when all part of membrane electrode assembly cell were taken apart after finish the measurement. Thus it was expected that fPBPI membrane that had high hydrophobicity could get more impact from this problem than Nafion®117 especially at high relative humidity. This observation agreed well with the water uptake results. In addition, this implied that the water transport phenomena in phosphonated graft copolyimide membranes had affected from many factors and no single mechanism that could fully describe them generally.

#### **5.3.2.2 The effect of side chain length on proton conductivity**

Comparing among the fPBPI membranes that prepared from phosphonated copolyimide (paPI) having similar phosphonation level of 30-32%; the fPBPI-1, fPBPI-4 and fPBPI-5 membrane, the effect of side chain length on proton conductivity was studied. To clearly observation, the proton conductivity results at 74% RH were selected to compare as shown in Figure 5-14. The highest proton conductivity was obtained from fPBPI-5 (prepared from paPI-5 (DP=199)), followed by fPBPI-4 (prepared from paPI-4 (DP=99)), and fPBPI-1 (prepared from paPI-1 (DP=49)), respectively. This supported our expectation that polymer which had longer side chain possibly gave higher proton conductivity if the membrane can uptake and retain more water molecule in their structure. However, the proton conductivity was not significantly different and started to decrease at higher temperature. The loss of water at high temperature is well known reason but the other was possibly too such as from polymer chain rearrangement, which investigated by Holdcroft et al. They studied various block copolymer membrane systems such as PVC-co-PS, sulfonated polyimide etc. [39,91] It was reported that some blocked copolymers with the longer side chains possibly gave the lower proton conductivity at high temperature due to over water absorption, ionic cluster and channel rearrangement [92]

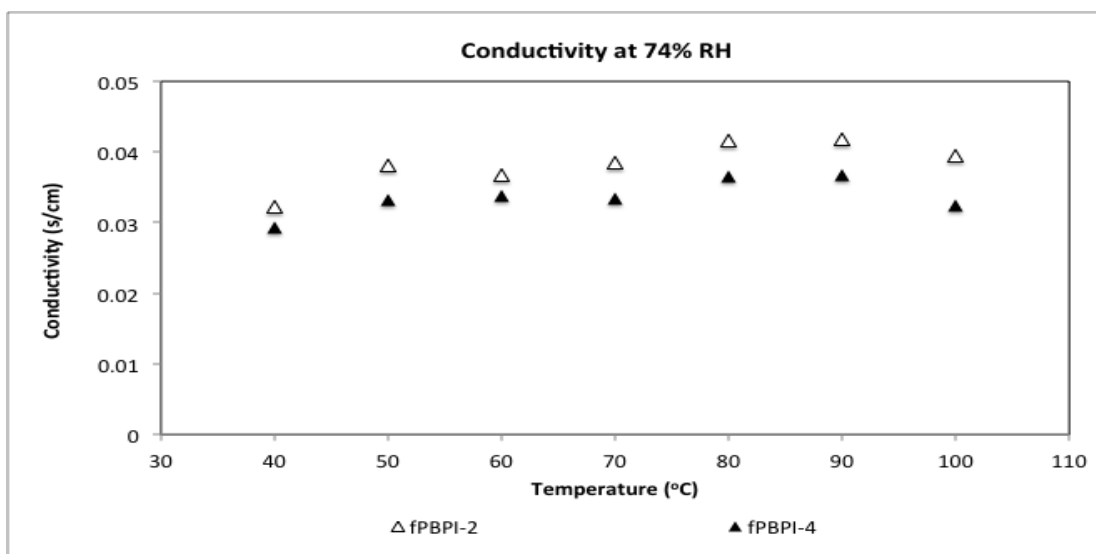


**Figure 5-14 The effect of side chain length on proton conductivity at 74% RH**

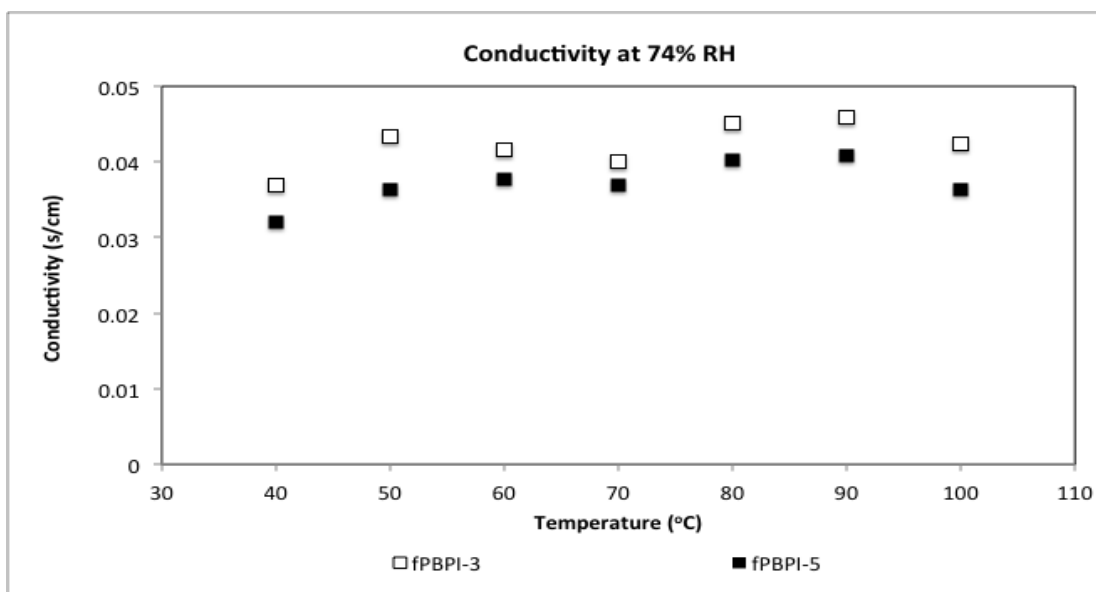
Remark: fPBPI-1 (prepared from paPI-1 with DP=49), fPBPI-2 (prepared from paPI-2 with DP=99) and fPBPI-5 (prepared from paPI-5 with DP=199)

### 5.3.2.3 The effect of phosphonation level on proton conductivity

Comparing among the fPBPI membranes that prepared from phosphonated copolyimide (paPI) having similar degree of polymerization; the fPBPI-2 and fPBPI-4 membrane system (prepared from paPI-2 and paPI-4 with DP=99) and the fPBPI-3 and fPBPI-5 membrane system (prepared from paPI-3 and paPI-5 with DP=199), the effect of phosphonation on proton conductivity was studied. To clarify the observation, the proton conductivity results at 74% RH were selected to compare as shown in Figure 5-15 as well.



(A) fPBPI-2 (prepared from paPI-2 with 42%phosphonation and fPBPI-4 (prepared from paPI-4 with 30% phosphonation)



(B) fPBPI-3 (prepared from paPI-3 with 55%phosphonation and fPBPI-5 (prepared from paPI-5 with 30% phosphonation)

Figure 5-15 The effect of phosphonation level on proton conductivity at 74% RH



Comparing between fPBPI-3 and fPBPI-5 system, the fPBPI-5 that had lower phosphonation level, showed the lower proton conductivity than fPBPI-3 regardless of their equal length. As mentioned before, the phosphonic acid unit played as a major role of proton transport in the fPBPI membrane in this study. With increasing of number of phosphonic acid, the proton conductivity was predictably increased. In this study, the amount of phosphonic acid site was desirably controlled by the 2,2'-dibromo-4,4'-diaminophenyl ether unit. It implied that the %phosphonation could relate to the distance between phosphonic acid sites. With lower amount of phosphonic acid, the distance between acid sites should be increased. [72] In my opinion, an optimal distance for promoting proton mobility in phosphonated graft copolyimide is existed, as same as what can be found in sulfonic acid containing polymer. This situation was also observed in proton transport mechanism in Nafion membrane via Grotthuss and vehicular mechanisms, that optimum distances between sulfonic acid groups will enhance higher proton conductivity. [45]

Moreover, these conductivity situations were also observed in the shorter chain length systems represented by fPBPI2 and fPBPI4. In addition, the fPBPI4 had lower proton conductivity than fPBPI5, this was similar to the cases, that the polymer with longer side chain possibly showed higher proton conductivity [73] However, it was previously suspected that phosphonic acid containing polymer might have different water absorption mechanisms from sulfonic acid containing polymer[93], so the optimum length of phosphonated polymer may be different from sulfonated polymer.

It can be concluded that the optimum distance of proton transfer group is one of major factor to enhance higher proton conductivity and our synthesis method can easily apply to adjust the distance of phosphonic acid unit to suit to the optimum length for better proton transportation.

### 5.3.3 THE PRELIMINARY STUDY OF PHOSPHONATED GRAFT COPOLYIMIDE IN DIRECT METHANOL FUEL CELL APPLICATION

In this study, the feasible property of phosphonated graft copolyimide for direct methanol fuel cell was preliminary investigated, thus only some membranes were sampled to do the methanol permeability measurement. The methanol permeability and proton conductivity of phosphonated graft copolyimide membranes and Nafion, which measured by four-points probe technique, of phosphonated graft copolyimide membranes and Nafion, were summarized in Table 5-5.

**Table 5-5 The methanol permeability and proton conductivity of phosphonate graft copolyimide membrane; fPBPI and Nafion®117**

Sample	Methanol permeability (cm <sup>2</sup> /s)	Proton conductivity (S/cm)
fPBPI-1*	$8.3 \times 10^{-8}$ (4%)	$3.42 \times 10^{-3}$ (4%)
fPBPI-2*	$2.6 \times 10^{-7}$ (12%)	$1.08 \times 10^{-2}$ (13%)
fPBPI-3*	$4.4 \times 10^{-7}$ (21%)	$2.42 \times 10^{-2}$ (30%)
Nafion®117	$2.1 \times 10^{-6}$ (100%)	$8.2 \times 10^{-2}$ (100%)

\* All membrane were prepared by blending with 20% PI in m-cresol

Methanol permeability was calculated by Equation 5-2;

$$C_B = \frac{A}{V_B} \frac{DK}{L} C_A (t - t_0) \quad \text{Equation 5-2}$$

Where  $C_B$  and  $C_A$  are the methanol concentration of permeated and feed side through the membrane, respectively.

$A$  are the effective area of membrane.

$L$  are the thickness of membrane.

$V_B$  are the volume of permeated compartment.

D are the methanol diffusivity.

K are the solubility, and

$t_0$  are the time lag.

The methanol permeability is specified as the product of diffusivity and solubility. The value of methanol permeability in this study for Nafion®117 is  $2.1 \times 10^{-6}$  cm<sup>2</sup>/s, which was comparable to value measured by Woo et al.[94] The methanol permeability of obtained PBPI membranes increased from  $8.3 \times 10^{-8}$  to  $4.4 \times 10^{-7}$  cm<sup>2</sup>/s with increasing of phosphonation level. It was noticed that the IECs of fPBPI membranes were closed to Nafion®117 (see Table 5-3) but the fPBPI membrane showed the lower methanol permeability by a magnitude. This reduction of methanol permeability was due to the addition of hydrophobic part during the membrane preparation and the difference in microstructure between these two polymers as mentioned before.

However, the Nafion®117 membrane displayed the three times higher proton conductivity than fPBPI-3 membrane, with regardless to five times higher methanol permeability than fPBPI-3. The proton conductivity of fPBPI membranes at room temperature and hydrated condition are investigated. At low phosphonation level of 30%, the fPBPI-1 exhibits poor proton conductivity only  $3.42 \times 10^{-7}$  s/cm. With increasing of phosphonation level, proton conductivity of fPBPI increased and reached the maximum at  $2.42 \times 10^{-7}$  s/cm. The fPBPI-3 with highest phosphonation level in this study displayed about one-third lower than Nafion®117 in spite of much higher IEC value. This different property of phosphonic acid group and sulfonic acid group should be further studied for understanding the proton transport in membranes. However the phosphonate graft polyimide displays low proton conductivity, their reduction of methanol crossover could increase feasibility in DMFC application.

## CHAPTER VI

### CONCLUSIONS AND RECOMMENDATIONS

#### 6.1 CONCLUSION

The novel phosphonated graft copolyimide based on NTDA and ODA monomer was synthesized. The phosphonated polyimide side chain, which played as major role of proton conducting polymer, was obtained from the combination of bromination and lithiation reaction while the graft structure was achieved by novel use of 3,3'-diaminobenzidine monomer with 4 reactive amine group. This synthesis route leads to relatively simple and easily adjustable of molecular weight, chain length of backbone (PI) or side chain (paPI) segment as well as phosphonation or sulfonation level, if preferred. The  $IEC_{NMR}$  and  $IEC_{Titration}$  values of obtained phosphonated polyimide series with range of 30-55% phosphonation were ranged from 1.48 to 2.72 meq/g and 1.45 to 2.68 meq/g respectively.

The phosphonated graft polyimide series (PBPIs) that synthesized in this study had better thermal property than Nafion®117, however, they had poor solubility and this became a main problem of this study because it was difficult to determine the exact molecular weight of obtained polyimide. Only *m*-cresol could dissolve phosphonated graft copolyimide sample at elevated temperature. The 160-180  $\mu\text{m}$  thickness of fPBPI membrane were prepared by solution casting of pure polyimide and PBPIs (1:4 w/w) mixture. All fPBPI membrane had lower  $IEC_{Titration}$  due to addition of hydrophobic pure PI. The effect of phosphonation level and side chain length of phosphonated polyimide side chain on water uptake and swelling properties were investigated. With increasing of side chain length, the water uptake and swelling slightly increased as shown in fPBPI-1, fPBPI-4 and fPBPI-5 membrane. However, the effect of phosphonation level to water uptake and swelling was not clearly observed especially in the shorter side chain system.

Based on spray technique using MEAs preparation, all phosphonated polymer membranes showed slightly lower proton conductivity than Nafion®117 at different temperatures and relative humidity. Moreover, it was found that the phosphonated graft copolyimide system with the longest side chain and the highest IEC had the highest proton conductivity while maintained their thermal and hydrolytic stability. As expected, the microstructure of polymer membrane should affect fuel cell performance due to different ionic clusters and water channels. The combination of graft structure and phosphonic acid site could affect the membrane properties and have some advantages in fuel cell operation especially at high humidity and temperature. However, their different mechanisms of water absorption and proton transport in phosphonated graft copolyimide membranes needed the further investigation and optimization. Moreover, it was found that the fPBPI3 membrane showed comparable proton conductivity with Nafion®117 at 90°C and 74%RH, moreover, this membrane also showed more stable proton conductivity at operating temperature of 80-100°C than Nafion®117.

In addition, the methanol permeability of fPBPI membrane was investigated. The Nafion®117 membrane displayed 3 times higher proton conductivity than fPBPI-3 membrane, with regardless to 5 times higher methanol permeability than fPBPI-3. With increasing of phosphonation level, proton conductivity of fPBPI increased and reached the maximum at  $2.42 \times 10^{-7}$  s/cm. Therefore, their reduction of methanol crossover could increase feasibility in DMFC application.

This novel structure of phosphonated graft copolyimide could increase the proton conductivity while maintaining the hydrolytic and thermal stability of membrane. Moreover, the easy adjustments in synthesis of chain length of both main chain and side chains, allowed flexibility to design the optimum requirement for PEMFC.

## 6.2 RECOMMENDATION

6.2.1 While preparing the membrane during fuel cell test period, the existing vacuum oven was not in fully functional condition, as a result, the pure PBPI films could not be obtained and the fPBPI films were used instead. The improvement of membrane preparation method can be done to obtain pure phosphonated graft copolyimide membrane. Without blending with hydrophobic pure polyimide, the increase in proton conductivity and Nafions comparable performance is expected.

6.2.2 The study of phosphonated graft copolyimide membrane morphology can help to understand the arrangement of hydrophilic ionic domain and hydrophobic domain in membrane with more details explanation of water absorption related to proton conductivity.

6.2.3 The addition of sulfonic acid to phosphonated graft copolyimide would increase solubility and proton conductivity of graft copolyimide sample.

6.2.4 Optimum in both chain length and main chain length should be investigated. Together with higher temperature experiment which this copolyimide can rival Nafion with cheaper cost of preparation and proton conductivity ability, especially with no halogen in molecules, less toxic when degraded will attain.

## REFERENCES

- [1] Zaidi, S.M.J., and Rauf, M.A. Fuel Cell Fundamentals. In Zaidi, S.M.J., and T. Matsuura (ed.) Polymer Membranes for Fuel Cells : Springer, 2009.
- [2] Cooper, K.R., Ramani, V., Fenton, J.M., and Kunz, H.R. Experimental Methods and Data Analyses for Polymer Electrolyte Fuel Cells : Scribner Associates, Inc., 2005.
- [3] Barbir, F. PEM Fuel Cells: Theory and Practices, New York: Elsevier, 2005.
- [4] Venkateshwaran, L.N., Tant, M.R. Wilkes, G.L. Charlier, P. and Jerome, R. Structure-property comparison of sulfonated and carboxylated telechelic ionomers based on polyisoprene. Macromolecules 25 (1992) : 3996-4001.
- [5] Kotov, S.V., Pedersen, S.D., Qiu, W., Qiu, Z.M., and Burton, D.J. Preparation of perfluorocarbon polymers containing phosphonic acid groups. Journal of Fluorine Chemistry 82 (1997) : 13-19.
- [6] Lafitte, B., and Jannasch, P. Polysulfone ionomers functionalized with benzoyl(difluoromethylenephosphonic acid) side chains for proton-conducting fuel-cell membranes. Journal of Polymer Science Part A: Polymer Chemistry 45 (2007) : 269-283.
- [7] Lafitte, B., and Jannasch, P. On the Prospects for Phosphonated Polymers as Proton-Exchange Fuel Cell Membranes, In Advance in Fuel cells, pp. 119-185 : Elsevier 2007
- [8] Lafitte, B., and Jannasch, P. Phosphonation of polysulfones via lithiation and reaction with chlorophosphonic acid esters. Journal of Polymer Science Part A: Polymer Chemistry 43 (2005) : 273-286.
- [9] Rusanov, A. Kostoglodov, P. Abadie, M.M., Voytekunas, V. and Likhachev, D. Proton-Conducting Polymers and Membranes Carrying Phosphonic Acid Groups, In: G. Scherer (ed.) Fuel Cells II, pp. 125-155. Berlin Heidelberg : Springer 2008.

- [10] Abouzari-Lotf, E., Ghassemi, H., Shockravi, A., Zawodzinski, T., and Schiraldi, D. Phosphonated poly(arylene ether)s as potential high temperature proton conducting materials. Polymer 52 (2011) : 4709-4717.
- [11] Ingratta, M., Elomaa, M., and Jannasch, P. Grafting poly(phenylene oxide) with poly(vinylphosphonic acid) for fuel cell membranes. Polymer Chemistry 1 (2010) : 739-746.
- [12] Tayouo, R., David, G., Améduri, B., Rozière, J., and Roualdès, S.P. New Fluorinated Polymers Bearing Pendant Phosphonic Acid Groups. Proton Conducting Membranes for Fuel Cell. Macromolecules 43 (2010) : 5269-5276.
- [13] Allcock, H.R. and Wood, R.M. Design and synthesis of ion-conductive polyphosphazenes for fuel cell applications: Review. Journal of Polymer Science Part B: Polymer Physics 44 (2006) : 2358-2368.
- [14] Miyatake K., and Hay, A.S. New poly(arylene ether)s with pendant phosphonic acid groups. Journal of Polymer Science Part A: Polymer Chemistry 39 (2001) : 3770-3779.
- [15] Allcock, H.R., Hofmann, M.A. and Wood, R.M. Phosphonation of Aryloxy-phosphazenes. Macromolecules. 34 (2001) : 6915-6921.
- [16] Schroeder, J.P., and Sopchak, W.P. The reaction of phosphorus trichloride and oxygen with polymers. Journal of Polymer Science 47 (1960) : 417-433.
- [17] Phillips, P.J., and MacKnight, W.J. Mechanical and thermal properties of phosphorylated polyethylene. Journal of Polymer Science Part B: Polymer Letters 8 (1970) : 87-94.
- [18] Phillips, P.J., Emerson, F.A. and MacKnight, W.J. Structure and Properties of Polyethylene Modified with Phosphonic Acid Side Groups. I. Mechanical and Thermal Studies. Macromolecules 3 (1970) : 767-771.
- [19] Phillips, P.J., Emerson, F.A. and MacKnight, W.J. Structure and Properties of



- Polyethylene Modified with Phosphonic Acid Side Groups. II. Dielectric Properties. Macromolecules 3 (1970) : 771-777.
- [20] Weiss, R.A., Lenz, R.W. and MacKnight, W.J. Properties of polyethylene modified with phosphonate side groups. I. Thermal and mechanical properties. Journal of Polymer Science: Polymer Physics Edition 15 (1977) : 1409-1425.
- [21] Johnson, R.G.L., Delf, B.W. and MacKnight, W.J. Structure of some ethylene–phosphonic acid copolymers. Journal of Polymer Science: Polymer Physics Edition 11 (1973) : 571-585.
- [22] Souzy, R., Ameduri, B., Boutevin, B., and Virieux, D. Synthesis of new aromatic perfluorovinyl ether monomers containing phosphonic acid functionality. Journal of Fluorine Chemistry 125 (2004) : 1317-1324.
- [23] Allcock, H.R., Hofmann, M.A., Ambler, C.M. and Morford, R.V. Phenylphosphonic Acid Functionalized Poly[aryloxyphosphazenes]. Macromolecules 35 (2002) : 3484-3489.
- [24] Wu, Q., and Weiss, R.A. Synthesis and characterization of poly (styrene-co-vinyl phosphonate) ionomers. Journal of Polymer Science Part B: Polymer Physics 42 (2004) : 3628-3641.
- [25] Elabd, Y.A., and Hickner, M.A. Block Copolymers for Fuel Cells. Macromolecules. 44 (2010) 1-11.
- [26] Hickner, M.A., Ghassemi, H., Kim, Y.S., Einsla, B.R., and McGrath, J.E. Alternative Polymer Systems for Proton Exchange Membranes (PEMs). Chemical Reviews 104 (2004) : 4587-4612.
- [27] Ding, J., Chuy, C., and Holdcroft, S. Enhanced Conductivity in Morphologically Controlled Proton Exchange Membranes: Synthesis of Macromonomers by SFRP and Their Incorporation into Graft Polymers. Macromolecules 35 (2002) : 1348-1355.

- [28] Lee, C.H., Park, C.H., and Lee, Y.M. Sulfonated polyimide membranes grafted with sulfoalkylated side chains for proton exchange membrane fuel cell (PEMFC) applications. Journal of Membrane Science 313 (2008) : 199-206.
- [29] Chen, X., Yin, Y., Chen, P., Kita, H., and Okamoto K.I. Synthesis and properties of novel sulfonated polyimides derived from naphthalenic dianhydride for fuel cell application. Journal of Membrane Science 313 (2008) : 106-119.
- [30] Takekoshi, T. Polyimide-Fundamentals and Applications, New York : Marcel Dekker, Inc., 1996.
- [31] Gunduz, N. Synthesis and Characterization of Sulfonated Polyimides as Proton Exchange Membranes for Fuel Cells. Doctoral dissertation, Virginia Tech, 2001.
- [32] Socrates, G. Infrared and Raman Characteristic Group Frequencies Table and Chart, England : John Wiley & Sons Ltd, 2001.
- [33] Russel, B. High Temperature Polymers for Proton Exchange Membrane Fuel Cells. Doctoral dissertation, Virginia Tech, 2005.
- [34] O'Hayre, R., Cha, S.W., Colella, W., and Prinz, FB., Fuel Cell Fundamentals : Wiley, 2008.
- [35] William, M.V., Fenton, J.M., and Kunz, H.R. Analysis of polarization curves to evaluate polarization sources in Hydrogen/Air PEM fuel cells. Journal of Electrochemical Society 152 (2005) : 635-644.
- [36] Yuan, X.Z., Song, C., Wang, H., and Zhang, J. Electrochemical Impedance Spectroscopy in PEM Fuel Cells: Fundamentals and Applications, London : Springer, 2010.
- [37] Meng, Y.Z., Tjong, S.C., Hay, A.S., and Wang, S.J. Proton-exchange membrane electrolytes derived from phosphonic acid containing poly(arylene ether)s. European Polymer Journal 39 (2003) : 627-631.
- [38] Agmon, N. The Grotthuss Mechanism. Chemical Physics Letters 244 (1995) : 456-462.
- [39] Peckham, T.J., Schmeisser, J., Rodgersab, M., and Holdcroft, S. Main-chain, statistically

- sulfonated proton exchange membranes: the relationships of acid concentration and proton mobility to water content and their effect upon proton conductivity. Journal of Materials Chemistry 17 (2007) : 3255-3268.
- [40] Doyle, M., Lewittes, M.E., and Roelofs, M.G. Ionic Conductivity of Nonaqueous Solvent-Swollen Ionomer Membranes Based on Fluorosulfonate Fluorocarboxylate, and Sulfonate Fixed Ion Groups. Journal of Physic Chemistry B 105 (2001) : 9387-9394.
- [41] Kreuer, K.D. On the development of proton conducting polymer membranes for hydrogen and methanol fuel cells. Journal of Membrane Science 185 (2001) : 29-39.
- [42] Kima, J., Kima, B., and Jung, B. Proton conductivities and methanol permeabilities of membranes made from partially sulfonated polystyrene-block-poly(ethylene-ran-butylene)-block-polystyrene copolymers. Journal of Membrane Science 207 (2002) : 129-137.
- [43] Kim, Y.S., and Piovvar, B.S. Polymer Electrolyte Membrane for Direct Methanol Fuel cells. In Advance in Fuel cells, pp. 187-226 : Elsevier, 2007.
- [44] Mauritz, K.A., Moore, R.B. State of Understanding of Nafion. Chemical Reviews. 104 (2004) : 4535-4585.
- [45] Rikukawa, M., and Sanui, K. Proton-conducting polymer electrolyte membranes based on hydrocarbon polymers. Progress in Polymer Science. 25 (2000) : 1463-1502.
- [46] Perrot, C., Gondon, L., Marestin, C., and Gebel, G. Hydrolytic degradation of sulfonated polyimide membranes for fuel cells. Journal of Membrane Science 379 (2011) : 207-214.
- [47] Gebel, G. Structural evolution of water swollen perfluorosulfonated ionomers from dry membrane to solution. Polymer 41 (2000) : 5829-5838.
- [48] Herz, H.G., Kreuer, K.D., Maier, J., Scharfenberger, G., Schuster M.F.H., and Meyer

- W.H. New fully polymeric proton solvents with high proton mobility.  
Electrochimica Acta 48 (2003) : 2165-2171.
- [49] Kreuer, K.D., Paddison, S.J., Spohr, E., and Schuster, M. Transport in Proton Conductors for Fuel-Cell Applications: Simulations, Elementary Reactions, and Phenomenology. Chemical Reviews 104 (2004) : 4637–4678
- [50] Adjemian, K.T., Srinivasan, S., Benziger, J., and Bocarsly, A.B. Investigation of PEMFC operation above 100 °C employing perfluorosulfonic acid silicon oxide composite membranes. Journal of Power Sources 109 (2002) : 356-364.
- [51] Antonucci, P.L., Aricò, A.S., Cretì, P., Ramunni, E., and Antonucci V. Investigation of a direct methanol fuel cell based on a composite Nafion®-silica electrolyte for high temperature operation. Solid State Ionics 125 (1999) : 431-437.
- [52] Li, Y. et al. Synthesis and characterization of novel sulfonated polyimides from 1,4-bis(4-aminophenoxy)-naphthyl-2,7-disulfonic acid. Polymer 48 (2007) : 2280-2287.
- [53] Zaidi, S.M.J., Mikhailenko, S.D., Robertson, G.P., Guiver, M.D., and Kaliaguine, S. Proton conducting composite membranes from polyether ether ketone and heteropolyacids for fuel cell applications. Journal of Membrane Science 173 (2000) : 17-34.
- [54] Kobayashi, T., Rikukawa, M., Sanui, K., and Ogata, N. Proton-conducting polymers derived from poly(ether-etherketone) and poly(4-phenoxybenzoyl-1,4-phenylene). Solid State Ionics 106 (1998) : 219-225.
- [55] Kreuer, K.D. Proton Conduction in Fuel Cells In Hydrogen-Transfer Reactions, pp. 709–736 : Wiley-VCH, 2010.
- [56] Gasa, J.V., Boob, S., Weiss, R.A., and Shaw, M.T. Proton-exchange membranes

- composed of slightly sulfonated poly(ether ketone ketone) and highly sulfonated crosslinked polystyrene particles. Journal of Membrane Science 269 (2006) : 177-186.
- [57] Swier, S., Shaw, M.T., and Weiss, R.A. Morphology control of sulfonated poly(ether ketone ketone) poly(ether imide) blends and their use in proton-exchange membranes. Journal of Membrane Science, 270 (2006) : 22-31.
- [58] Beihoffer, T.W., and Glass, J.E. Hydrophilic modification of engineering polymers. Polymer 27 (1986) : 1626-1632.
- [59] Guiver, M.D., Black, P., Tam, C.M., and Deslandes, Y. Functionalized polysulfone membranes by heterogeneous lithiation. Journal of Applied Polymer Science 48 (1993) : 1597-1606.
- [60] Sumner, M.J. et al. Novel proton conducting sulfonated poly(arylene ether) copolymers containing aromatic nitriles. Journal of Membrane Science 29 (2004) : 199-211.
- [61] Wang, F., Hickner, M., Kim, Y.S., Zawodzinski, T.A., and McGrath, J.E., Direct polymerization of sulfonated poly(arylene ether sulfone) random (statistical) copolymers: candidates for new proton exchange membranes. Journal of Membrane Science 197 (2002) : 231-242.
- [62] Dai, H., Zhang, H., Luo, Q., Zhang, Y., and Bi, C. Properties and fuel cell performance of proton exchange membranes prepared from disulfonated poly(sulfide sulfone) Journal of Power Sources 185 (2008) : 19-25.
- [63] Woo, Y., Oh, S.Y., Kang, Y.S., and Jung, B. Synthesis and characterization of sulfonated polyimide membranes for direct methanol fuel cell. Journal of Membrane Science 220 (2003) : 31-45.
- [64] Einsla, B.R., Hong, Y.T., Kim, S.Y., Wang, F., Gunduz, N., and McGrath, J.E.

- Sulfonated naphthalene dianhydride based polyimide copolymers for proton-exchange-membrane fuel cells. I. Monomer and copolymer synthesis. Journal of Polymer Science Part A: Polymer Chemistry 42 (2004) : 862-874.
- [65] Einsla, B.R. et al. Sulfonated naphthalene dianhydride based polyimide copolymers for proton-exchange-membrane fuel cells: II. Membrane properties and fuel cell performance. Journal of Membrane Science 255 (2005) : 141-148.
- [66] Fang, J. et al. Novel Sulfonated Polyimides as Polyelectrolytes for Fuel Cell Application. 1. Synthesis, Proton Conductivity, and Water Stability of Polyimides from 4,4'-Diaminodiphenyl Ether-2,2'-disulfonic Acid. Macromolecules 35 (2002) : 9022–9028.
- [67] Guo, X., Fang, J., Watari, T., Tanaka, K., Kita, H., and Okamoto, K.I. Novel Sulfonated Polyimides as Polyelectrolytes for Fuel Cell Application. 2. Synthesis and Proton Conductivity of Polyimides from 9,9'-Bis(4-aminophenyl)fluorene-2,7-disulfonic Acid. Macromolecules 35 (2002) : 6707-6713.
- [68] Genies, C. et al. Stability study of sulfonated phthalic and naphthalenic polyimide structures in aqueous medium. Polymer 42 (2001) : 5097-5105.
- [69] Genies, C., Merciera, R., Silliona, B., Cornet, N., Gebel, G., and Pineri, M. Soluble sulfonated naphthalenic polyimides as materials for proton exchange membranes. Polymer 42 (2011) : 359–373.
- [70] Ye, X., Bai, H., and Ho, W.S. Synthesis and characterization of new sulfonated polyimides as proton-exchange membranes for fuel cells. Journal of Membrane Science 279 (2006) : 570-577.
- [71] Ken, I., and Okamoto, Y. Methanol permeability and proton conductivity of sulfonated copolyimide membranes. Journal of membrane science 258 (2005) : 115-122.
- [72] Saito, M., Arimura, N., Hayamizu K., and Okada, T. Mechanisms of Ion and Water

- Transport in Perfluorosulfonated Ionomer Membranes for Fuel Cells. The Journal of Physical Chemistry B 108 (2004) : 16064-16070.
- [73] Peron, J. et al. Fuel cell catalyst layers containing short-side-chain perfluorosulfonic acid ionomers. Journal of Power Sources 196 (2011) : 179-181.
- [74] Parcero, E., Fernández-Carretero, F.J., Compañ, V., Herrera, R., del Castillo, L.F., and Riande, E. Electrochemical Properties of Cation-Exchange Membranes Based on Polysulfones. Journal of The Electrochemical Society 155 (2008) : F245-F252.
- [75] Pu, H., and Wang, D. Studies on proton conductivity of polyimide/H<sub>3</sub>PO<sub>4</sub>/imidazole blends. Electrochimica Acta 51 (2006) : 5612-5617.
- [76] Abu-Thabit, N.Y., Ali, S.A., and Zaidi, S.M.J. New highly phosphonated polysulfone membranes for PEM fuel cells. Journal of Membrane Science 360 (2010) : 26–33.
- [77] Pu, H. A new anhydrous proton conducting material based on phosphoric acid doped polyimide. European polymer Journal 41 (2005) : 2505-2510.
- [78] Sander, M., and Steininger, E., Phosphorylation of polymer, Journal of Macromolecular Science part C, 2 (1968) : 57-72.
- [79] Stone, C., Daynard, T.S., Hu, L.Q., Mah, C., and Steck, A.E. Phosphonic acid functionalized proton exchange membranes for PEM fuel cells. Journa of New Materials Electrochemical System (2000) : 43-50.
- [80] Souzy, R., and Ameduri, B. Functional fluoropolymers for fuel cell membranes. Progress in Polymer Science 30 (2005) : 644-687.
- [81] Yanagimachi, S., Kaneko, K., Takeoka, Y., and Rikukawa M. Synthesis and evaluation of phosphonated poly(4-phenoxybenzoyl-1,4-phenylene). Synthetic Metals 135-136 (2003) : 69-70.
- [82] Jakoby, K., Nunes, S.P., and Peinemann, K. Proton conductive membrane for electrochemical applications. Patent CA2412310 (2004).

- [83] Jakoby, K., Peinemann, K.V., and Nunes, S.P. Palladium-catalyzed phosphonation of polyphenylsulfone. Macromolecular Chemistry and Physics 204 (2003) : 61-67.
- [84] Cabasso, I., Jagur-Grodzinski, J., and Vofsi, D. Synthesis and characterization of polymers with pendent phosphonate groups. Journal of Applied Polymer Science 18 (1974) : 1969–1986.
- [85] Xu, X., and Cabasso, I. Preliminary study of phosphonate ion exchange membranes for PEM fuel cells. Journal of Polymer Material Science (1993) : 68.
- [86] Teclechiel, D., Christiansson, A., Bergman, Å., and Marsh, G. Synthesis of Octabrominated Diphenyl Ethers from Aminodiphenyl Ethers. Environmental Science & Technology 41 (2007) : 7459-7463.
- [87] Parcerro, E., Herrera, R., and Nunes, S.P. Phosphonated and sulfonated polyphenylsulfone membranes for fuel cell application. Journal of Membrane Science 285 (2006) : 206-213.
- [88] Kühn, O. Phosphorus-<sup>31</sup>P-NMR Spectroscopy: Springer, 2008.
- [89] Erdmenger, T., Vitz, J., Wiesbrock, F., Schubert, U.S. Influence of different branched alkyl side chains on the properties of imidazolium-based ionic liquids. Journal of Materials Chemistry 18 (2008) : 5267-5273.
- [90] Lu, Z., Daino, M.M., Rath, C., Kandlikar, S.G., Water management studies in PEM fuel cells, part III: Dynamic breakthrough and intermittent drainage characteristics from GDLs with and without MPLs. International journal of hydrogen energy 35 (2010) : 4222–4233.
- [91] Peckham, T.J., and Holdcroft, S. Structure-Morphology-Property Relationships of Non-Perfluorinated Proton-Conducting Membranes. Advanced Materials, 22 (2010) : 4667-4690.
- [92] Ding, J., Chuy, C., and Holdcroft, S., Enhanced Conductivity in Morphologically



- Controlled Proton Exchange Membranes: Synthesis of Macromonomers by SFRP and Their Incorporation into Graft Polymers. Macromolecules 35 (2002) : 1348-1355.
- [93] Brandell, D., Karo, J., Liivat, A., and Thomas, J. Molecular dynamics studies of the Nafion®, Dow® and Aciplex® fuel-cell polymer membrane systems. Journal of Molecular Modeling 13 (2007) : 1039-1046.
- [94] Woo, Y.T., Oh, S.Y., and Kang, Y.S. Synthesis and characterization of sulfonated polyimide membranes for direct methanol fuel cell. Journal of Membrane Science 220 (2003) 31-45.

## VITA

Miss Nathinee Srinate was born on December 10, 1982 in Bangkok, Thailand. After graduating from Triamudom Suksa School in 2000, she spent 6 years at Chulalongkorn University and eventually received Bachelor's Degree of Science in Chemical Technology at Department of Science in 2004, and Master's Degree of Engineering in Chemical Engineering at the Department of Chemical Engineering in 2006. After the M.Eng graduation, she has received the Royal Golden Jubilee Ph.D. program, Thailand Research Fund to study the Doctoral Degree of Engineering in Chemical Engineering at Chulalongkorn University in July, 2008. She had spent one-year research at Department of Polymer Engineering, The University of Akron, USA during her Ph.D. Program.